ISSN 2348-0637
VOLUME 6, 2019

RÜSIE

A JOURNAL OF CONTEMPORARY SCIENTIFIC ACADEMIC AND SOCIAL ISSUES

KOHIMA SCIENCE COLLEGE, JOTSOMA
(An Autonomous Government P. G. College)
NAAC Accredited "A" Grade (1st Cycle, 2011)
NAAC Re-Accredited "A" Grade (2nd Cycle, 2017)

ISSN 2348-0637

ISSN 2348-0637

CONTRIBUTORS

J. R. Yimchunger
Assistant Professor
Department of Mathematics
Kohima Science College (Autonomous)
Jotsoma- 797002, Nagaland, India
e-mail: janeroselineyim@gmail.com

Dr. S. K. Srivastava
Assistant Professor
Department of Geology
Nagaland University, Kohima Campus,
Meriema-797004, Nagaland, India
e-mail: sksrivatava@nagalanduniversity.ac.in

Abeni Odyuo
Assistant Professor
Department of Geology
Kohima Science College (Autonomous)
Jotsoma-797002, Nagaland, India
e-mail: abenikapfo@gmail.com

A. Moalong Kichu
Research Scholar
Department of Geology
Nagaland University, Kohima Campus,
Meriema-797004, Nagaland, India

Dr. Chetan Kachhara
Assistant Professor
Department of Physics
Kohima Science College (Autonomous)
Jotsoma-797002, Nagaland, India.
e-mail: chetankachhara@yahoo.co.in

Dr. Pallab Changkakoti
Assistant Professor
Department of Statistics
Kohima Science College (Autonomous)
Jotsoma-797002, Nagaland, India
e-mail: c.pallab@gmail.com

Thejakielie Meyase
Assistant Professor
Department of Geology
Kohima Science College (Autonomous)
Jotsoma-797002, Nagaland, India.
e-mail: thejakieliemeyase@gmail.com

Dr. Vethselo Doulo
Assistant Professor
Department of Zoology
Kohima Science College (Autonomous)
Jotsoma-797002, Nagaland, India
e-mail: vdoulo4@gmail.com

Keduolhoulie Belho
Assistant Professor
Department of Tenyidie
Kohima College, Kohima-797001
Nagaland, India
e-mail: keduobelho@gmail.com

Dziesevituo Angami
Associate Professor
Department of Zoology
Kohima Science College (Autonomous)
Jotsoma-797002, Nagaland, India

Kerheingunuo Shüya
Department of Zoology
Kohima Science College (Autonomous)
Jotsoma-797002, Nagaland, India

Dziesetuonuo Mepfhüo
Department of Physics
Kohima Science College (Autonomous)
Jotsoma-797002, Nagaland, India.

CONTRIBUTORS

Bendangkokba R Jamir
Department of Physics
Kohima Science College (Autonomous)
Jotsoma-797002, Nagaland, India

Dr. Petevino Chase
Assistant Professor
Ura College of Teachers Education,
Kohima-797001, Nagaland, India
e-mail: petechs@gmail.com

Dr. Neizo Puro
Assistant Professor
Department of Botany
Nagaland University, Lumami- 798627, Nagaland, India
e-mail: neizopuro@nagalanduniversity.ac.in

Wenyitso Kapfo
Assistant Professor
Department of Botany
Kohima Science College (Autonomous)
Jotsoma-797002, Nagaland, India
e-mail: wenitso@gmail.com

Dr. Kedovikho Yhoshü
Assistant Professor
Department of Geography
Nagaland University, Lumami-798627, Nagaland, India
e-mail: kedovikho@nagalanduniversity.ac.in

ISSN 2348-0637

CONTENTS Page

ISSN 2348-0637

MODULES INVARIANT UNDER ENDOMORPHISMS AND AUTOMORPHISMS OF THEIR INJECTIVE HULLS

Reviewed

J. R. Yimchunger
Department of Mathematics, Kohima Science College, Jotsoma-797002, Nagaland, India
e-mail: janeroselineyim@gmail.com

Abstract. A module invariant under endomorphisms of its injective hull is called an endomorphism-invariant module. Endomorphism-invariant modules are precisely the quasi-injective modules. A module invariant under automorphisms of its injective hull is called an automorphism-invariant module. Automorphism-invariant modules, which generalize the notion of quasi-injective modules, are precisely the pseudo-injective modules. A module invariant under idempotent endomorphisms of its injective hull is called an idempotent-invariant modules. Idempotent-invariant modules, which also generalize the notion of quasi-injective modules, are precisely the quasi-continuous modules. In this paper, some results of these classes of modules are established.

Keywords: Endomorphism-invariant module, automorphism-invariant module and idempotent-invariant module.

Introduction

Throughout, R will denote an associative ring with unity and all modules are unitary R-modules, unless otherwise stated. For a module M, $E(M)$, $End(M)$ and $Aut(M)$ will denote the injective hull, the endomorphism ring and the group of automorphisms of M, respectively. We write $N \subseteq M$ if N is a submodule of M, $N \subseteq^{ess} M$ if N is an essential submodule of M and $N \subseteq^{\oplus} M$ if N is a direct summand of M.

Automorphism-invariant modules, introduced by Lee and Zhou (2013) has been extensively studied and used to characterize various modules and rings, in recent times.

A module which is invariant under endomorphisms of its injective hull is called an *endomorphism-invariant module*, i.e., M is an endomorphism-invariant module if $f(M) \subseteq M$ for all $f \in End(E(M))$. Johnson and Wong (1961) proved that a module M is invariant under any endomorphism of its injective hull if and only if any homomorphism from a submodule of M to M can be extended to an endomorphism of M. A module which is invariant under automorphisms of its injective hull is called an *automorphism-invariant module*, i.e., M is an automorphism-invariant module if $f(M) \subseteq M$ for all $f \in Aut(E(M))$. Noyan Er *et. al* (2013) proved that a module is automorphism-invariant if and only if any monomorphism from a submodule of M to M can be extended to an endomorphism of M. A module which is invariant under idempotent endomorphisms of its injective hull is called an *idempotent-invariant module*, i.e., M is an idempotent-invariant module if $f(M) \subseteq M$ for all $f^2 = f \in End(E(M))$. Goel and Jain (1978) proved that idempotent-invariant modules are precisely the $\pi-$-injective modules which are the same as quasi-continuous modules defined by Jeremy (1974). A ring is said to be *clean* if each of its elements is the sum of a unit and an idempotent. A module is said to be *clean* if its endomorphism ring is clean. A right R-module M is said to satisfy the *exchange property* if for every right R-module A and any two direct sum decompositions $A = M_1 \oplus N = \oplus_{i \in I} A_i$ with M_1 ; M , there exist submodules B_i of A_i such that $A = M_1 \oplus (\oplus_{i \in I} B_i)$. If this holds only for $|I| < \infty$, then M is said to satisfy the finite exchange property. A module is called *square-free* if it contains no non-zero submodules isomorphic to a square $A \oplus A$. A sub-module N of a module M is said to be *essential* in M if for every non-zero submodule B of M, $B \cap N \neq 0$. A module M is called *uniform* if and only if every non-zero submodule of M is essential in M.

In this paper, it is established that every endomorphism-invariant module is automorphism-invariant but the converse is

not true; also, every endomorphism-invariant module is idempotent-invariant but the converse does not hold. Certain conditions under which an automorphism-invariant module becomes endomorphism-invariant and under which an idempotent-invariant module becomes endomorphism-invariant are investigated. Various implications of these classes of modules are established and several counter-examples are provided to justify why certain classes of these modules are not contained in the other class.

Endomorphism-invariant modules and automorphism-invariant modules

For an *R*-module *M*, consider the following conditions:
(C1) Every submodule of *M* is essential in a direct summand of *M*.
(C2) Every submodule of *M* that is isomorphic to a direct summand of *M* is itself a direct summand of *M*.
(C3) If *A* and *B* are direct summands of *M* with $A \cap B = 0$ then $A \oplus B$ is also a direct summand of *M*.
M is called a C_1- or a *CS* (or an *extending*) *module* if it satisfies (C1); *M* is called a *continuous module* if it satisfies (C1) and (C2); *M* is called a *quasi-continuous module* if it satisfies (C1) and (C3).

A module which is invariant under endomorphisms of its injective hull is called an endomorphism-invariant module, i.e., *M* is called an endomorphism-invariant module if $f(M) \subseteq M$ for all $f \in End(E(M))$.
A module which is invariant under automorphisms of its injective hull is called an automorphism-invariant module, i.e., *M* is called an automorphism-invariant module if $f(M) \subseteq M$ for all $f \in Aut(E(M))$.
Endomorphism-invariant modules are automorphism-invariant but the converse is not true, in general.

Theorem 1.1. *Every endomorphism-invariant module M is automorphism-invariant.*

Proof. Let *M* be an endomorphism-invariant module. Then $f(M) \subseteq M$ for all $f \in End(E(M))$. In particular, $f(M) \subseteq M$ for all $f \in Aut(E(M))$.Thus *M* is an automorphism-invariant module.
In general, the converse of the above theorem is not true.

Example. If *R* is the ring of all eventually constant sequences $(x_n)_{n\in N}$ of elements in $\mathbf{Z}_2$, then $E(R_R) = \prod_{n\in N} \mathbf{Z}_2$ has only one automorphism, namely the identity automorphism. Thus R_R is an automorphism-invariant module but R_R cannot be endomorphism-invariant as R_R does not satisfy (C1).

Theorem 1.2. *Every endomorphism-invariant module is clean.*

Proof. Let *M* be an endomorphism-invariant module. Then $f(M) \subseteq M$ for all $f \in End(E(M))$. Since every endomorphism-invariant module satisfies (C1) and (C2), *M* is continuous and continuous modules are clean (Goel and Jain, 1978).

Theorem 1.3. *Every* C_1 *automorphism-invariant module is endomorphism-invariant.*

Proof. Let *M* be a C_1 automorphism-invariant module. Since automorphism-invariant modules satisfy (C3) (Lee and Zhou, 2013), *M* is idempotent-invariant i.e. $f(M) \subseteq M$ for all $f^2 = f \in End(E(M))$. Also *M* being automorphism-invariant, $f(M) \subseteq M$ for all $f \in Aut(E(M))$. As $E(M)$ is an injective module, it is clean and so any $f \in End(E(M))$ is a sum of an automorphism and an idempotent endomorphism. Thus $f(M) \subseteq M$ for all $f \in End(E(M))$ and so *M* is an endomorphism-invariant module.

Theorem 1.4. *A uniform automorphism-invariant module is endomorphism-invariant.*

Proof. Let *M* be a uniform automorphism-invariant module. Since *M* is uniform, every non-zero submodule *N* of *M* is such that $N \subseteq^{ess} M$ and so *M* is a C_1-module. Thus *M* is endomorphism-invariant by Theorem 1.3.

A summand of an endomorphism-invariant module is endomorphism-invariant but a direct sum of endomorphism-invariant modules need not be endomorphism-invariant, as illustrated by the following example:
The $\mathbf{Z}-$module ¤ $\oplus \mathbf{Z}_p$ is not endomorphism-invariant even though ¤ being injective as a $\mathbf{Z}-$module, is endomorphism-

ISSN 2348-0637

invariant and $\mathbf{Z}_p$ being simple as a $\mathbf{Z}-$ module, is endomorphism-invariant.

Theorem 1.5. (Guil and Srivastava, 2013) *Every automorphism-invariant module has the finite exchange property and also the full exchange property.*

Proof. Let M be an automorphism-invariant module. Let $S = End(M)$ and let $J(S)$ denote the Jacobson radical of *S*. Then $S/J(S)$ is a von Neumann regular ring and idempotents lift modulo $J(S)$ (Guil and Srivastava, 2013) and such a ring is an exchange ring (Nicholson, 1977). Thus $S = End(M)$ is an exchange ring and so M has the finite exchange property.

Since M is automorphism-invariant, $M = A \oplus B$, where A is endomorphism-invariant and *B* is a square-free module Er *et. al* (2013). Since $B \subset^{\oplus} M$, and M has the finite exchange property, *B* also has the finite exchange property and for square free modules, the finite exchange property implies the full exchange property (Nielsen, 2010). *A* being endomorphism-invariant has the full exchange property. As *M* is a direct sum of *A* and *B*, both having the full exchange property, M also has the full exchange property.

Theorem 1.6. (Guil and Srivastava, 2013) *Every automorphism-invariant module is clean.*

Proof. Let M be an automorphism-invariant module. Then $M = A \oplus B$,where A is endomorphism-invariant and *B* is a square-free module. By Theorem 1.2, *A* is clean. $End(B)$ is an exchange ring as *B* has the finite exchange property as seen in Theorem 1.5. Also, idempotents in $End(B)/J(End(B)$ are central (Mohamed and Müller, 1990). Thus $End(B)/J(End(B)$ is a clean ring as $End(B)/J(End(B)$ is an exchange ring with all idempotents central. Since idempotents lift modulo $J(End(B)$, $End(B)$ is a clean ring and so *B* is a clean module. M being a direct sum of two clean modules, is also a clean module.

Endomorphism-invariant modules and idempotent-invariant modules

Theorem 2.1. *Every endomorphism-invariant module M is idempotent-invariant.*

Proof. Let *M* be an endomorphism-invariant module. Then $f(M) \subseteq M$ for all $f \in End(E(M))$. In particular, $f(M) \subseteq M$ for all $f^2 = f \in End(E(M))$. Thus *M* being invariant under all idempotent endomorphisms of its injective hull, is an idempotent-invariant module.

The converse of the above theorem does not hold, in general as illustrated by the following example:

The $¢ -$module $¢$ is idempotent-invariant but not endomorphism-invariant.

We thus have the following implications:

Endomorphism-invariant $\Rightarrow$ Automorphism-invariant and

Endomorphism-invariant $\Rightarrow$ idempotent-invariant although the converse in both implications are not true.

It is note-worthy to mention that the classes of automorphism-invariant modules and idempotent-invariant modules are not contained in one another as shown by the following example:

Example . If $\mathbf{Z}$, ¤ denote the ring of integers and rational numbers respectively, $\mathbf{Z}_{\mathbf{Z}}$ is an idempotent-invariant module which is not automorphism-invariant because the injective hull ¤ $_{\mathbf{Z}}$ of $\mathbf{Z}_{\mathbf{Z}}$ has the automorphism $\alpha : ¤ \to ¤$ defined by $\alpha(x) = \frac{x}{2}$ but $\alpha(\mathbf{Z}) \subset \mathbf{Z}$.

Endomorphism-invariant modules and automorphism-invariant modules are clean but idempotent-invariant modules are not clean, in general.

For any *R*-module *M*, a monomorphism $\theta \in End(M)$ is called an *essential monomorphism* if $Im(\theta)$ is an essential submodule of *M*. A module *M* is called *essentially co-Hopfian* if every essential monomorphism in *End(M)* is an automorphism.

Theorem 2.2. *Every essentially co-Hopfian idempotent-invariant module is clean.*

Proof. Let *M* be an essentially co-Hopfian idempotent-invariant module. Since *M* is idempotent-invariant, every $\theta \in End(M)$ is such that $\theta = g + h$, where $g = g^2 \in End(M)$ and h is an essential

monomorphism and so $\mathrm{Im}(h) \subseteq^{ess} M$. As M is essentially co-Hopfian, $h \in Aut(E(M))$. Thus every $\theta \in End(M)$ being the sum of an idempotent and an automorphism, $End(M)$ is a clean ring and so M is a clean module.

Although the classes of automorphism-invariant and idempotent-invariant modules are not contained in one another, the following theorem shows that uniform automorphism-invariant modules are idempotent-invariant.

Theorem 2.3. *Every uniform automorphism-invariant module is idempotent-invariant.*

Proof. Let M be a uniform automorphism-invariant module. Since M is uniform, it satisfies (C1) and M being automorphism-invariant, satisfies (C3) (Lee and Zhou, 2013). Thus M is an idempotent-invariant module.

Corollary 2.4. Every extending automorphism-invariant module is an idempotent-invariant module.

Proof. The proof follows from the fact that a module is extending if and only if it is uniform.

As is the case in endomorphism-invariant modules, a direct sum of idempotent-invariant modules need not be idempotent-invariant as illustrated in the following example:

Example . Let $R = \begin{pmatrix} \mathrm{F} & \mathrm{F} \\ 0 & \mathrm{F} \end{pmatrix}$ where F is any field and let $P = \begin{pmatrix} \mathrm{F} & \mathrm{F} \\ 0 & 0 \end{pmatrix}$ and $Q = \begin{pmatrix} 0 & 0 \\ 0 & \mathrm{F} \end{pmatrix}$.

Here, P and Q are idempotent-invariant as R-modules. However, $R = P \oplus Q$ is not idempotent-invariant as R_R satisfies (C1) but does not satisfy (C3).

Although endomorphism-invariant modules as well as automorphism-invariant modules are clean and they also satisfy the exchange property, it is not so for idempotent-invariant modules.

For example, $\mathbf{Z}_{\mathbf{Z}}$ is an idempotent-invariant module but $\mathbf{Z}$ is not a clean ring. It has been proved that every clean ring is an exchange ring. In fact, $\mathbf{Z}$ is not even an exchange ring.

Acknowledgement: The author is thankful to Prof. Ashish Srivastava, Saint Louis University, U.S.A. and Prof. Pedro A. Guil Asensio, University of Murcia, Spain for their suggestions while the author visited HRI, Allahabad in 2018.

References

Camillo, V. P., Khurana, D., Lam, T. Y., Nicholson, W. K. and Zhou, Y. (2006). Continuous modules are clean. *J. Algebra*. **304**; 94–111.

Dinh H. Q. (2005). A note on pseudo-injective modules, Comm. *Algebra*. **33**: 361–369.

Dung, N. V., Huynh, D. V., Smith, P. F. and Wisbauer, R. (1994). Extending Modules, Pitman Research Notes in Mathematics series. *Longman Scientific and Technical, Harlow*.

Er, N., Singh, S. and Srivastava, A. K. (2013). Rings and modules which are stable under automorphisms of their injective hulls. *J. Algebra*. **379**: 223–229.

Goel, V. K. and Jain, S. K. (1978). $\pi-$ injective modules and rings whose cyclic are $\pi-$injective. *Comm. Algebra*. **6(1)**: 59–73.

Guil Asensio, P. A. and Srivastava, A. K. (2013). Automorphism-invariant modules satisfy the exchange property. *J. Algebra*. **388**: 101–106.

Jeremy, L. (1974). Modules et anneaux quasi-continus. *Canad. Math. Bull*. **17**; 217–228.

Johnson, R. E. and Wong, E. T. (1961). Quasi-injective modules and irreducible rings. *J. Lond. Math. Soc.* **36**: 260-268.

Lee, T. K. and Zhou, Y. (2013). Modules which are invariant under automorphisms of their injective hulls. *J. Algebra Appl.* **12(2)**: 1250159, 9.

Mohamed, S. H. and Müller, B. J. (1990). Continuous and Discrete Modules. *London Math. Soc. Lecture Note Ser*. Cambridge Univ. Press, Cambridge.

Nicholson, W. K. (1977). Lifting idempotents and exchange rings. *Trans. Amer. Math. Soc*. **229**: 269–278.

Nielsen, P. P. (2010). Square-free modules with the exchange property. *J. Algebra*. **323 (7)**:1993-2001.

ISSN 2348-0637

PROVENANCE OF THE SILICICLASTICS AT DISANG-BARAIL TRANSITION, NW OF KOHIMA: REFLECTIONS FROM GEOCHEMICAL ATTRIBUTES

Reviewed

*S. K. Srivastava, **Abeni Odyuo, ***A. Moalong Kichu
*&***Department of Geology, Nagaland University, Kohima Campus, Meriema-797004
**Department of Geology, Kohima Science College,Jotsoma-797002, Nagaland
*e-mail: sksrivatava@nagalanduniversity.ac.in

Abstract: In the present study Major Oxides, Trace and Rare Earth Elements compositions have been used to infer the source rock tectonics and the composition of the provenance of the siliciclastics at Disang-Barail Transition, North-West of Kohima town. Studied Tertiary sediments are fine to medium grained, ranging in composition from wacke to sublith arenite categories. Study suggests that the sediments for the siliciclastics at DBTS have been supplied by mixed provenance, with some contribution from igneous rocks having granitic and granodioratic composition. It also suggests an intense chemical weathering in the source area and an active /transitional tectonic set-up. Trace element analysis points towards some biogenic activities under marine depositional environment having good ventilation with no carbonate precipitation.

Keywords: Disang-Barail, rare earth elements.

Introduction

Geologically, Nagaland forms a part of the Assam-Arakan tectonic province. This includes Assam, Nagaland, Arunachal Pradesh, Manipur, Mizoram, Tripura, and extends south- eastwards into the Arakan coast of Myanmar.

Morpho-tectonically, the Assam-Arakan basin is divisible into three parts corresponding to the geological units. The eastern limit is defined by the Naga-Lushai-Patkai hill range which is described geologically under three different belts:

- Belt of Schuppen
- Inner Fold Belt
- Ophiolite Belt and Naga Metamorphics

Several workers, while following the pioneer work of Evans (1932), have attempted the stratigraphy, sedimentology, structure and tectonic framework of the region (Bhandari *et al.*, 1973; Dasikachar, 1974; Dasgupta, 1977; Banerjee, 1979; Ganju and Khar, 1985; Acharya, 1986, 1991; and Naik *et al.*, 1991). In recent years, attention has been paid towards the study of Northeast Indian sedimentary basin in the light of plate tectonic. Srivastava (2002) and Srivastava *et al*. (2004), identified a well- developed transition zone between Disang and Barail Groups named Disang- Barail Transitional Sequences (DBTS). Also, Srivastava (2015), Srivastava and Pandey (2011); Srivastava *et al.* (2015, 2017, 2018); Kichu and Srivastava (2018) and Kichu *et al*. (2018) have worked on various areas of IFB regarding provenance, tectonic setting, and the depositional environment.

Study area

The study area forms a part of Kohima Synclinorium within the Inner Fold Belt and lies towards north-west of Kohima town. The area under investigation is incorporated in the topographic sheet no. 83 K/2 of the Survey of India. The rocks that are exposed in the study area are of Disang-Barail Transition (DBTS, Srivastava, 2002; Figure 1). The study area exposes a mixed lithology of sand-silt and shale. Sandstones from the study area range between fine to medium sand fraction. Sedimentary structures observed in the study area include wave ripples, plane and fine cross laminations, hummocky cross stratification and channel. Biogenic structures recorded from the study area belong either to *Skolithos* or *Cruziana* assemblage suggesting a near shore-shallow marine depositional environment (Srivastava, 2002).

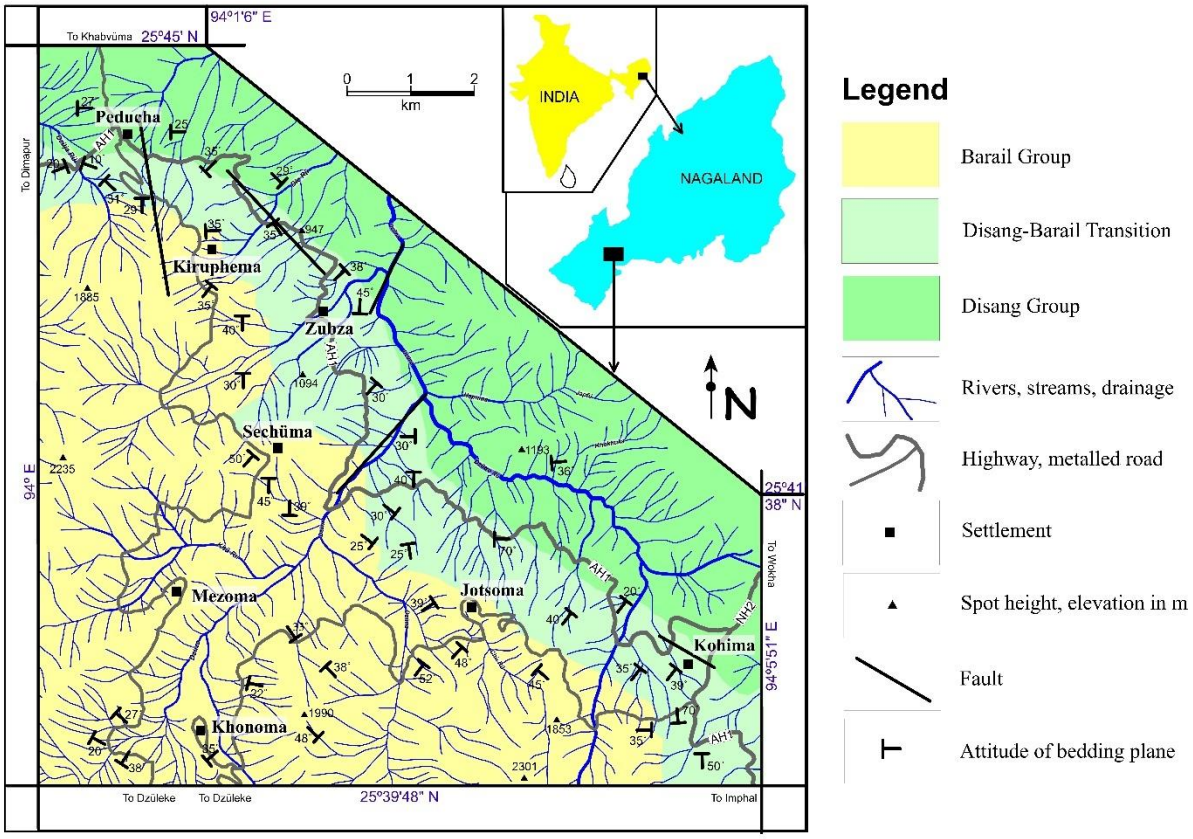

Fig. 1: Geological map of the study area (after Kichu *et al*., 2018)

In the present study, an attempt is made to reconstruct the provenance using geochemical properties of the siliciclastics at the DBTS. For the purpose, ten (10) sandstone samples were analyzed for their major, trace and rare earth concentrations. Major and trace elemental analysis were carried out at the ONGC laboratories, Dehradun using XRF; and REE was done at the RSIC, IIT, Bombay using ICP-MS. Results are shown in the following tables (Tables 1, 2 and 3).

Petrographic composition and framework analysis are useful in reconstruction of the tectonic settings and also to understand the source rock composition. Many publications on the subject also signify their importance. However, it may not give the true relationship between the detrital mode and tectonic settings (Mack, 1984) as the post depositional processes some time destroy the original composition of the detritus. In such cases, geochemical parameters can be used to understand the tectonic settings. Interplay of variables such as weathering, transportation, diagenesis, sorting and heavy mineral composition generally modifies the primary modes of the detritus. Nevertheless, by using geochemical composition of the sediments, provenance composition and tectonic settings can still be inferred (McLennan *et al*., 1993). Potter (1978), Dickinson and Valloni (1980), Valloni and Maynard (1981), Bhatia (1983) and Roser and Korch (1986), using modern sands of known tectonic settings, have shown that there is systematic variation in framework mineralogy and provenance type and tectonics.

Major Oxides

Major oxide composition of the siliciclastics have been used effectively by Bhatia (1983), Roser and Korch (1986), Suttner and Dutta (1986), Herron (1988), Condie (1976), Blatt *et al*. (1980), Siever (1987), LeMaitre (1976) and others for interpreting the nature of source rocks, tectonic settings and classifying the siliciclastic sediments. This is due to the fact that, specially in the fine-grained sediments, concentration of major elements are generally unaffected during the post depositional

ISSN 2348-0637

changes despite the large volumes of fluid that pass through the sedimentary pile (Wintesch and Kvale, 1994).

Chemical Maturity

Chemical maturity index (CMI) of clastic sediments can be shown as SiO_2 percent and SiO_2/Al_2O_3 ratio. SiO_2/Al_2O_3 ratio, which defines the chemical maturity of clastic sediments, can be also be used for classifying them. Sediments of the study area show a moderately higher SiO_2/Al_2O_3 ratio. Bivariate plot between SiO_2 and $Al_2O_3+K_2O+Na_2O$ (Suttner and Dutta, 1986) suggest moderate chemical maturity and semi humid-semi arid climate (Figure 2). This is further supported by low TiO_2/ Al_2O_3 ratios. Low K_2O/Al_2O_3 ratio points towards a sedimentary recycling (Bauluz *et al*., 2000). Srivastava *et al*. (2004), while working with sandstones from the same area, have suggested a recycling of the sediments based on their petrographic compositions. Degradation of feldspar, which is very sensitive to chemical weathering, increases the mobility of many elements through clays (Taylor and McLennan, 1985). Degree of weathering of the source rocks can be interpreted by the degree of feldspar, which is known as index of alteration and is expressed by the formula CIA= $100[Al_2O_3/(Al_2O_3+CaO+Na_2O+K_2O)]$ (Nesbitt and Young, 1982). In the present study, total CaO has been considered for determination of CIA as there is no method to differentiate between carbonate CaO and silicate CaO. Similar approach has been adopted by other workers (Roser *et al*., 1996; Al-Harbi and Khan, 2008; Sen *et al*., 2012). CIA values for most of the samples are high thus indicating an intense weathering in the source area.

Type of siliciclastic (rich, intermediate or poor) has been determined by using the plot suggested by Crook (1974) and a quartz rich siliciclastics have been interpreted (Figure 3).

Table 1: Major Oxide composition of the siliciclastics at Disang-Barail Transition, NW of Kohima town (in weight %).

Sample No	SiO_2%	Al_2O_3%	MgO%	Na_2O%	P_2O_5%	K_2O%	CaO%	TiO_2%	MnO%	Fe_2O_3%
R 98/198	60.37	24.03	0.00	0.55	0.19	2.74	0.16	1.32	0.15	7.30
R96/6	61.06	23.27	1.46	0.59	0.14	4.03	1.10	1.49	0.06	3.67
R96/36	64.38	20.59	1.20	0.57	0.14	2.90	0.98	1.75	0.04	4.31
R97/63	67.45	20.98	0.78	0.51	0.17	3.01	0.31	1.44	0.02	2.25
R97/114	68.02	19.79	0.70	0.55	0.15	3.26	0.25	1.40	0.02	2.77
R97/179	61.49	22.82	0.49	0.61	0.15	4.36	0.14	1.50	0.06	5.23
R 97/184	55.97	26.25	0.83	0.57	0.12	4.98	0.17	2.08	0.03	5.63
R97/171	49.34	30.38	0.75	0.58	0.13	4.91	0.22	2.56	0.04	6.55
R97/172	49.30	14.57	0.00	0.57	0.24	2.33	0.33	1.54	1.22	29.83
R97/55	55.89	25.65	1.48	0.59	0.15	4.46	1.11	2.02	0.04	7.99

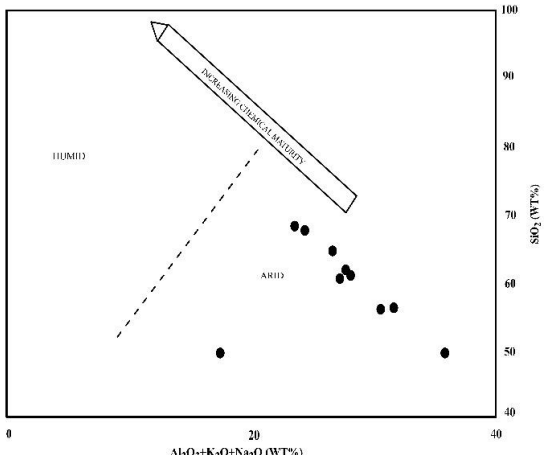

Fig. 2: Bivariate plot of SiO_2 vs $Al_2O_3+K_2O+Na_2O$ (after Suttner and Dutta, 1986)

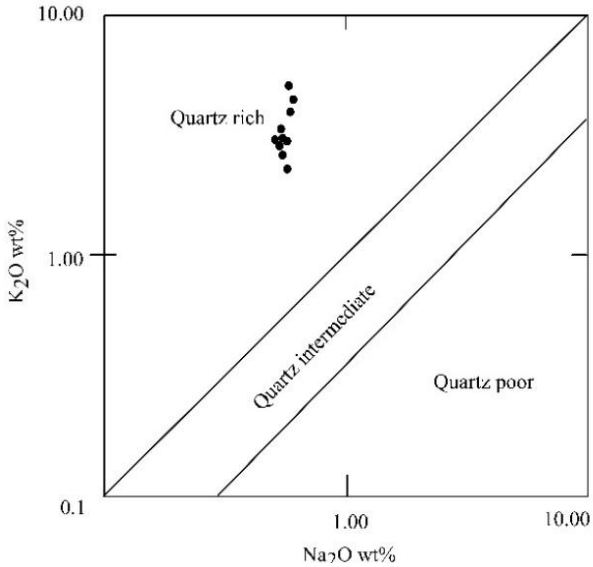

Fig. 3: Bivariate plot of K_2O vs Na_2O (after Crook, 1974)

Tectonic Setting

Relief features of the earth are basically controlled by the plate tectonics of the region. Many workers, including Middleton (1960), Crook (1974), Bhatia (1983) and Roser and Korsch (1986) basing on their works, have suggested that both source and basin set up can be interpreted from major element data. Major elements undergo some changes due to sedimentary processes where SiO_2 content increases and CaO and Na_2O decrease which can help in understanding the weathering conditions also as this is controlled by the tectonic setting as well. For provenance type and tectonic settings, plots suggested by Condie (1976), LeMaitre (1976), Bhatia (1983) and Roser and Korch (1986) have been used and a mixed provenance has been interpreted; where some sediment has also been supplied by the rocks of granitic/granodioritic composition (Figure 4 & 5). However, the plot suggested by Bhatia (1983) is inconclusive and does not show any affinity towards a particular field (Figure 6). Discriminatory plot suggested by Roser and Korch (1986) suggests a transitional tectonic setting for these sediments (Figure 7 & 8). Plot suggested by Herron (1988) has been used to classify the siliciclastics on the basis of its major oxide composition where it suggests a wacke category (Figure 9).

ISSN 2348-0637

Srivastava *et al.* (2004) have categorized these siliciclastics as lith and sub-lith arenite categories on the basis of petrographic composition. This shifting may be due to the presence of very fine sediments which are generally ignored in the petrographic analysis (Sen *et al.*, 2016). However, plot suggested by Crook (1974) suggests a quartz rich siliciclastics (Figure 3).

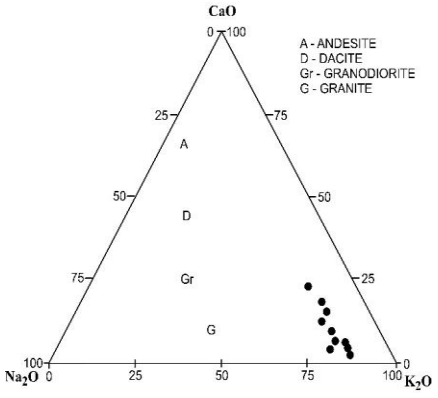

Fig. 4: Ternary plot of CaO-Na_2O-K_2O (after LeMaitre, 1976)

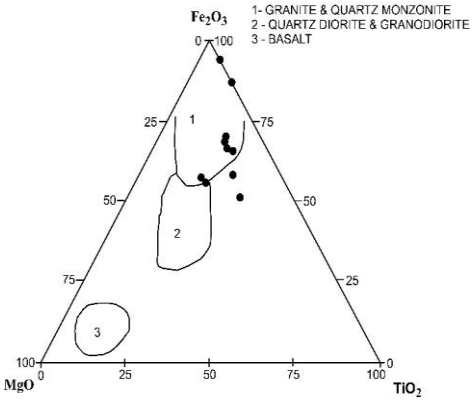

Fig. 5: Ternary plot of Fe_2O_3-MgO-TiO_2 (after Condie, 1967)

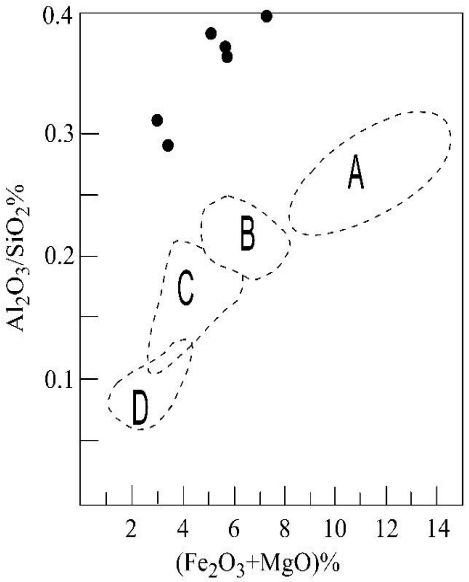

Fig. 6: Bivariate plot of Al_2O_3/SiO_2 vs Fe_2O_3+MgO (after Bhatia, 1983)

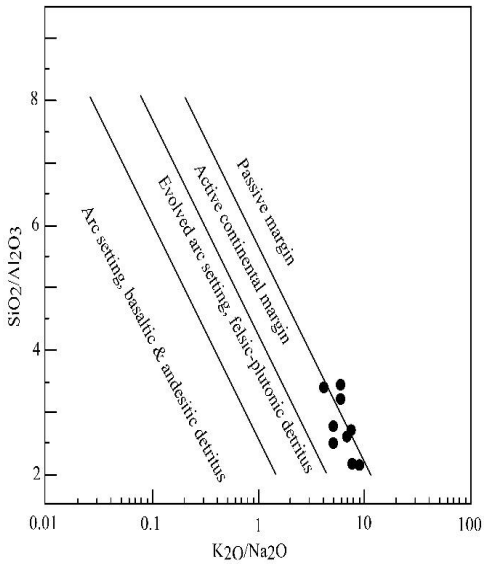

Fig. 7: Bivariate plot of $SiO2/Al_2O_3$ vs K_2O/Na_2O (after Roser and Korsch, 1986)

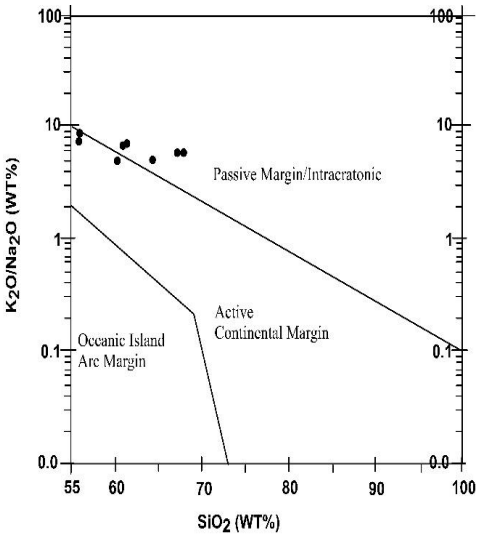

Fig. 8: Bivariate plot of K_2O/Na_2O vs SiO_2 (after Roser and Korsch, 1986)

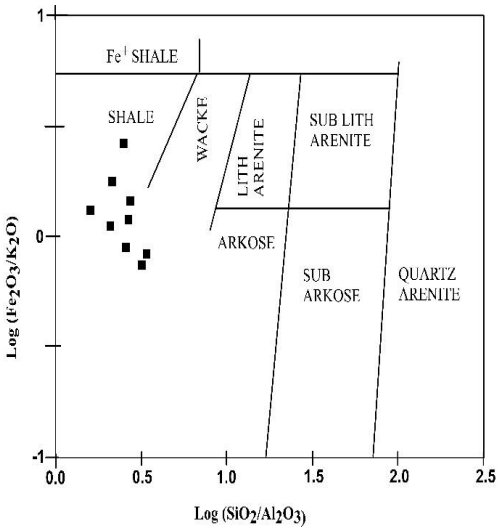

Fig. 9: Bivariate plot of log (Fe_2O_3/K_2O) vs log $(SiO_2/Al_2O_3$(after Herron,

Trace elements

The Trace elements composition of sandstones and shales from the DBTS of the study area exhibit substantial concentration of Barium (Ba) and subordinate Nickel (Ni), Vanadium (V) and Chromium (Cr). The concentrations of these elements together with Gallium (Ga) indicate the influence of marine environment. The content of Cr and V further indicate slightly to highly anaerobic conditions. The subordinate concentration of Nickel (Ni) has been attributed to the biogenic activities during deposition. A high value for Barium (Ba) relates to a deeper basinal condition. Nevertheless, the higher concentration of Barium (Ba) has also been attributed to the volcanogenic supply (Alexandrove, 1973) in contrast to low concentration of Sr which indicates a non-volcanogenic provenance. The overall trace element contents of the study area reveal a relatively deeper basinal condition supplemented in a sediment supply from a mixed provenance.

Table 2: Trace elemental composition of the siliciclastics at Disang-Barail Transition, NW of Kohima town (in ppm)

Sample No	V	Cr	Co	Ni	Ga	Rb	Sr	Ba	Zn
R 98/198	167	64	29	192	5	57	18	295	168
R96/6	17	59	18	153	6	64	11	318	360
R96/36	195	59	21	166	3	27	209	865	75
R97/63	25	53	14	147	1	22	185	847	162
R97/114	168	54	17	158	0	57	5	336	66
R97/179	177	59	23	183	3	69	19	347	359
R 97/184	208	64	19	183	3	69	19	359	276
R97/171	262	69	22	197	0	66	35	562	162
R97/172	172	67	68	193	0	31	250	547	511
R97/55	210	68	24	184	10	30	354	161	161

ISSN 2348-0637

Trace element geochemistry has been utilized by many workers (Nesbitt *et al*., 1980; Bhatia and Crook, 1986; Floyd and Leveridge, 1987; McLennan *et al*., 1990; and McLennan, 2001) for determination of source rock chemistry, depositional environment and palaeo-tectonic set up. Trace elements are suitable for provenance and tectonic setting of clastic sediments as they have low mobility and low residence time in sea water. Presence of Cr suggests some contribution from deep seated igneous rocks. Presence of Cr (53-69 ppm) in all the analyzed samples suggests a near shore environment. This also suggests there has been some contribution from metamorphic source too (Raghuwanshi, 2007). Zn is also present in all the samples which is generally found associated with sulfur and chloride as they have high affinity for these elements. Gallium (Ga) shows its presence in almost all the samples and show uniform distribution but does not have significant concentration. Generally, Ga is associated with clay mineral illite. Illite has been reported in all the samples analyzed indicating a deep burial condition (Srivastava and Pandey, 2001). High concentration of Barium (Ba) also suggests a near shore environment. This also suggests intense chemical weathering. Vanadium (Va) is generally derived from marine planktons and is preserved under low pH and high reducing conditions (Lewan and Maynard, 1982; Lewan, 1984). High concentration of Vanadium suggests organic derivation. V/Cr ratios of the sediments are good indicator of ventilation in the depositional environment (Dypiv, 1979). In the present study, in most of the samples, V/Cr ratio is more than 2, indicating good ventilation in the depositional environment.

Rare Earth Elements (REE)

Use of REE in evaluating the genesis of sedimentary rocks is more clearly understood since they are more resistant to removal by weathering and metamorphism. Further, it has also been clearly understood that REE pattern of average composition of upper continental crust is a suitable tool in interpreting the composition of source terrain. Major assumption behind equating the REE pattern of source rock is that the REE are transferred nearly quantitatively in the terrigenous components during erosion and sedimentation (McLennan, 1989).

In order to compare the relative abundance of the siliciclastics at the DBTS, data obtained from the analysis has been normalized. Such normalization is needed to neutralize odd-even effects caused by relative abundance of even atomic numbered REE as compare to odd ones. In the presence case, both chondrite (CI) as well as Post Archaean Australian shale (PAAS) normalized data were used and compared with the CI and PAAS patterns.

The REE patterns of the DBTS resemble with those of PAAS in possessing pronounced Eu depletion together with La_N /Yb_N ranging between 0.526 and 4.813 (La_N /Yb_N less than 15 for Post Archaean sedimentary rocks). The presence of pronounced negative Eu anomaly with respect to average CI and PAAS is very conspicuous feature of REE pattern of the sediments of the study area. Most of the earlier models on bulk crustal component have suggested that there is no significant depletion or enrichment of Eu in the REE pattern of average upper continental crust (Taylor and McLennan, 1985). Consequently, the presence of Eu depletion has been interpreted as reflecting shallow, intra-crustal differentiation leading to Eu depletion in the upper continental crust, associated with the production of granitic, ganodioritic rocks. Accordingly, the presence of negative Eu anomaly in these sediments appears to represent the similar Eu depletion in source terrain.

The REE patterns in the DBTS are spectacularly enriched with HREE thereby presenting a LREE depleted pattern in contrast to Post Archean sedimentary rocks with LREE enriched and HREE depleted pattern. The anomalous enrichment of HREE may be attributed to dominance of very fine to fine sand, silt and clay size fractions as well as exceptional concentration of Zircon in the heavy fractions (Cullers *et al*., 1987; 1988). Further, among the sand fractions, the coarser sizes tend to have lowest REE abundances and commonly display La/Yb ratio than finer grain sizes. For the rocks of the study area, La/Yb ratio may be considered as 4 for both sand and clay fractions. For framework grains in sandstones and siltstone, the REE chemistry of the various mineral grains depend on the

igneous/metamorphic history of the provenance (Hanson, 1980; 1989). Review of REE chemistry for the siliciclastics by Taylor and McLennan (1985) indicates that the mineral quartz contains very low abundances of REE, much of the content being present within inclusions. If carbonate minerals are precipitated in equilibrium with sea water, they typically possess negative Ce anomalies which may be reflected in the bulk REE patterns of the sediments (Piper, 1974; Palmer, 1985). REE pattern in the study area exhibit pronounced positive Cerium anomaly (Average Ce/Ce*=2.29). This feature may be attributed to the chemistry of sea water without carbonate precipitation during the deposition of DBTS. Absence of carbonate phase in the sediments of the study area further substantiate the above statement.

Gromet and Silver (1983, Figure 10) recorded that a large proportion of the compliment of REE in some granitic rocks is found within minor phases such zircon, sphene, allanite and monazite. In the sedimentary cycles, the minor phases of granite appear as heavy minerals and may be concentrated locally during sedimentary sorting processes. As stated earlier, almost all samples analyzed (Srivastava, 2002) are found to contain significant amount of zircon, a mineral with high REE abundances. This high zircon concentration may exhibit REE pattern significantly different from the REE pattern of the source rocks.

Table 3: REE composition of the siliciclastics at the DBTS.

Sample ➡ / Element ⬇	R96/13 FS	R7/110 VFS	R98/198 SH	R97/63 SH	R97/114 SH	R97/58 MS	R97/113 FS	R97/99 VFS	R97/101 VFS	R96/6 SH
La	1.04	3.79	ND	ND	1.89	5.49	ND	1.82	ND	17.51
Ce	9.48	9.57	ND	ND	44.45	13.16	21.56	38.05	ND	45.99
Pr	------	-------	-----	------	-------	------	-------	-------	------	-------
Nd	-------	-------	-----	------	--------	-------	-------	--------	------	-------
Sm	ND	ND	ND	ND	2.29	ND	0.84	0.81	ND	1.67
Eu	ND	ND	ND	ND	0.61	ND	0.38	0.50	ND	1.26
Gd	34.05	19.77	52.54	32.50	50.13	ND	30.18	34.79	33.06	65.87
Tb	ND	ND	ND	ND	ND	ND	ND	ND	ND	ND
Dy	------	------	-----	------	------	-----	-----	-------	------	-------
Ho	------	-------	-----	-------	------	-------	-------	--------	-------	-------
Er	2.82	ND	1.24	ND	4.13	ND	ND	ND	ND	ND
Tm	-----	------	-------	------	-------	-----	-------	-------	--------	------
Yb	0.56	0.59	1.42	6.27	1.74	0.62	1.11	1.88	0.93	2.57
Lu	0.76	0.14	1.39	1.61	0.87	0.34	0.64	0.69	0.99	0.17

FS: Fine sand, VFS: Very fine sand, MS: Medium sand, SH: Shale, ND: Non-determinable, -----Absent

ISSN 2348-0637

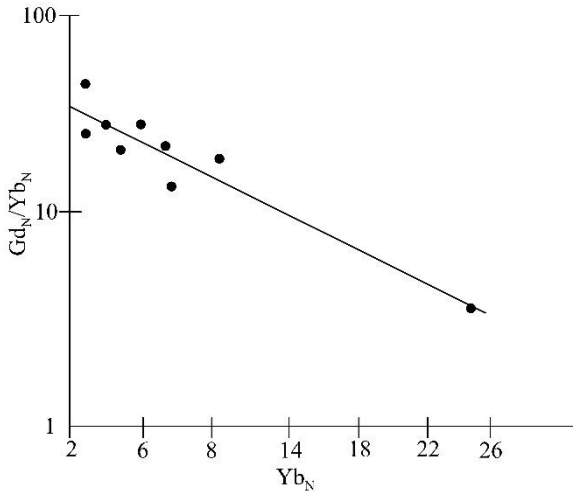

Fig. 10: Plot of Gd_N/Yb_N vs Yb_N (after Gromet and Silver, 1983)

Conclusions

Based on the geochemical attributes and their analysis following conclusions have been drawn in the present study:

1. Sediments for the siliciclastics at DBTS have been supplied by mixed provenance, dominated by a recycled orogen.
2. Contribution from granitic/granodioratic rocks alongwith some contribution from metamorphic sources also.
3. High CIA value indicates intense chemical weathering in the source area. This also suggests that sediments are chemically matured.
4. A transitional tectonic settings.
5. Studies also suggest modified composition during weathering under warm and humid climate.
6. Trace element analysis suggests a mixed provenance, biogenic activities, both volcano and non-volcanogenic supply under the influence of marine environment of deposition. This also points towards good ventilation during the deposition of these sediments.
7. REE analysis suggests a granitic/granodioratic source with some contributions from sedimentary source. REE pattern is influenced by exceptional concentration of zircon. REE analysis also suggests there were no carbonate precipitations during the deposition of these sediments.

Acknowledgements

Present work has been done at the Department of Geology, Nagaland University, Kohima Campus, Meriema. Authors thank the concerned authorities. SKS also thanks the ONGC and the RSIC, IIT Bombay for the geochemical analysis.

References

Acharya, S. K. (1986). Cenozoic plate motions creating eastern Himalayas and Indo-Burmese Range around the northeast corner of India. Ophiolites and Indian plate margin. *In Ghosh, N. C. and Vardarajan, S. (eds)*.143-161.

Acharya, S. K. (1991). Late Mesozoic-Early Tertiary basin evolution along the Indo-Burmese range and Andman Island arc. In Tondon, S. K.; Charu, C. P. and S. M. Casshyap (eds). *Proc. Sem. on sedimentary basins of India: Tectonic Context*. 105-130.

Alexandrove, E. A. (1973). The Precambrian Banded Iron Formation of the Soviet Union. *Econ. Geol*. **68**:1035-1062.

Al-Harbi, O. A. and Khan, M. M. (2008). Provenance, diagenesis, tectonic setting and Geochemistry of Twail sandstone (Lower Devonian) in Central Saudi Arabia. *Journal of Asian Earth Sciences*. 33: 278-287.

Banerjee, R. K. (1979). Disang shale, its stratigraphy, sedimentary history and basin

configuration in northeastern India and Burma. Q. *Jour. Geol. Min. Metal. Soc. India*. **51**: 144-152.

Bauluz, B., Mayaya, M. J., Fernandez-Nieto, C. and Gonzalez Lopez, J. M. (2000). Geochemistry of Precambrian and Palaeozoic siliciclastic rocks from the Iberian Range (NE Spain): implications for source area weathering, sorting, provenance and tectonic setting. *Chemical Geology*. **168(1)**: 135-150.

Bhandari, L. L., Fuloria, B. C. and Sastri, V. V. (1973). Stratigraphy of Assam Valley. *Bull. Am. Assoc. of Petrol. Geol.* **57(4)**: 642-654.

Bhatia, M. R. (1983). Plate Tectonics and Geochemical Composition of Sandstones. *The Journal of Geology*. **91(6)**: 611–627.

Bhatia, M. R. and Crook, K. A. W. (1986). Trace element characteristics of grawackes and tectonic setting discrimination of sedimentary basins. *Contrib. Mineral. Petrol*. **92**: 181-193.

Blatt, H., Middleton, G. and Murray, R. (1980). Origin of Sedimentary Rocks, *Prentice Hall Inc., Englewood Cliffs, New Jersey*. 782.

Condie, K. C. (1967). Geochemistry of early Precambrian Greywacke from Wyoming. *Geochim. Cosmochim. Acta*. **321**: 2136-2147.

Crook, K. A. W. (1974). Lithofacies and geotectonics: the significance of compositional variations in flysch arenites (graywackes). *In*: Modern and Ancient Geosynclinal Sedimentation (*Eds*. R.H. Dott and R.H. Shaver). *SEPM sepc. Pub*. **19**: 304-310.

Cullers, R. L., Chaudhry, S., Kilbane, N. and Korch, R. (1979). Rate earth element and size fraction and sedimentary rocks of Pennsylvanian-Permian age from the Mid Continent of the USA. *Geochem. Cosmochin. Acta*. **43**:1285-1305.

Cullers, R. L., Barrett, T., Carlson, R. and Robbinson, C. (1987). Rare earth elements and mineralogic changes in Holocene soil and stream sediments. A case study in wet mountains, Colorado, USA. *Chem. Geol*. **63**: 275-297.

Cullers, R. L., Basu, A. and Suttner, L. J. (1988). Geochemical signature of provenance in sand size material in soils and stream sediments near the Tobacco Root batholith, Montana, USA. *Chem. Geol*. **70**: 335-348.

Dasgupta, A. B. (1977). Geology of Assam-Arakan region, *Quart. Jour. Min. Met. Soc. India*. **49:** 1-50.

Desikachar, S. V. (1974). A review of the tectonic and geologic history of the Eastern India in terms of plate tectonic theory, *Jour. Geol. Soc. India*. **15(2):** 137-149.

Dickinson, W. R. and Valloni, R. (1980). Plate setting and provenance of sands in modern ocean basin, *Geology*. **8:** 82-86.

Dypivik, H. (1979). Mineralogy and Geochemistry of the Mesozoic sediments of Andsya, North Norway. *Sedimentary Geology*. **24**: 45-67.

Evans, P. (1932). Tertiary succession in Assam, *Trans. Min. Geol. Inst. India*. **37:** 155-260.

Floyd, P. A. and Leveridge, B. E. (1987). Tectonic environment of the Devonian Granscatho Basin, South Cornwall: Framework, mode and geochemical evidence from Turbiditic Sandstone. *Jour. Geol. Soc. Lon*. **144**: 531-542.

Ganju, J. L. and Khar, B. M. (1985). Structures, tectonics and hydrocarbon prospect of Naga Hills based on integrated remotely sensed data. *Petro. Asia Jour*. **8(2):** 142-151.

Gromet, P. and Silver, L. T. (1983). Rare earth element distribution among mineral in granodiorite and their petrographic implications. *Geochemica Cosmochemica Acta*. **47**: 925-935.

Hanson, G. N. (1980). Rare earth element in petrographic studies of igneous system. *Ann. Rev. Earth Planet Sci*. **8**: 371-400.

Hanson, G. N. (1989). An approach to trace element modeling using simple igneous system as an example. *Rev.Min*. **21**: 348.

Herron, M. M. (1988). Geochemical classification of terrigenous sands and shales from core or log data. *J. Sediment. Petrol*. **58:** 820–829.

Kichu, A. M. and Srivastava, S. K. (2018). Diagenetic environment of Barail sandstones in and around Jotsoma Village, Kohima district, Nagaland, India. *Journal of Geoscience Research*. **3(1)**: 31-35.

Kichu, A. M., Srivastava, S. K. and Khesoh, K. (2018). Trace fossils from Oligocene Barail sediments in and around Jotsoma, Kohima, Nagaland - implications for

ISSN 2348-0637

palaeoenvironment. *Jour. Palaeo. Soc. India*. **63(2)**: 197-202.

LeMaitre, R. W. (1976). The chemical variability of some common igneous rocks. *Jour. Petrol*. **17**: 589-637.

Lewan, M. D. and Maynard, J. B. (1982). Factors controlling the enrichment of vanadium and nickel in the bitumen of organic sedimentary rocks. *Geochemica cosmochemica Acta*. **46**: 2547-2560.

Lewan, M. D. (1984). Factors controlling the proportionality of the vanadium and nickel ratios in crude oils. *Geochemica cosmochemica Acta*. **48**: 2231-2238.

Mack, G. H. (1984). The sands and sandstones of Eastern Moray. *Edinburgh Geol. Soc. Trans*. **7:** 148-172.

McLennan, S. M. (1989). REE in sedimentary rocks – Influence of provenance and sedimentary processes. *In*: Geochemistry and Mineralogy of REE (*Eds*. B. R. Lipin and G. A. McKey). *Min. Soc. Am., Washington*. 348.

McLennan, S. M., Taylor, S. R., McCulloch, M. T. and Maynard, J. B. (1990). Geochemical and Nd-Sr isotopic composition of deep sea turbidites: crustal evolution and plate tectonic assosciations. *Geochemica cosmochemica Acta*. **54**: 2015-2050.

McLennan, S. M., Hemming, S., McDaniel, D. K. and Hanson, G. N. (1993). Geochemical approaches to sedimentation, provenance and tectonics. *Geol. Soc. Amer. Spl. Paper*. **284:** 21-40.

McLennan, S. M. (2001). Relationship between the trace element composition of sedimentary rocks and upper continental crust. *Geochemistry, geophysics and geo-system*. **2(4)**: 1-24.

Middleton, G. V. (1960). Chemical composition of sandstones. *Geol. Soc. Am. Bull*. **71**: 1011-1026.

Naik, G. C., Padhy, P. K. and Mishra, J. (1991). Hydrocarbon exploration and related geo-scientific problems in Northeast India. *Proc. Regional symposium on hydrocarbon deposits in northeast India, Gauhati, Assam*. 175-195.

Nesbitt, H. W., Morkovics, G. and Price, R. C. (1980). Chemical processes affecting alkalies and alkaline earths during continental weathering. *Geochemica cosmochemica Acta*. **44**: 1695-1666.

Nesbitt, H. W. and Young, G. M. (1982). Early Proterozoic climates and plate motions inferred from element chemistry of lutuites. *Nature*. **299**: 715-717.

Palmer, M. R. (1985). Rare earth elements in foraminifera test. Earth Planet. *Sci. Lett*.**73**: 205-298.

Piper, D. Z. (1974). Rare earth elements in the sedimentary cycle: Summery. *Chem. Geol*. **40**: 285-305.

Potter, P. E. (1978). Petrology and chemistry of modern big rivers. *Jour. Geol*. **86:** 423-449.

Raghuwanshi, R. S. (2007). Petrographic and geochemical characteristics of the Kanar sandstone Formation, NE of Barwah, Khargone District, Madhya Pradesh. *Jour. Geol. Soc. India*. **69(6)**: 1298-1304.

Roser, B. P. and Korsch, R. J. (1986). Determination of tectonic setting of sandstone-mudstone suites using SiO_2 content and Na_2O/K_2O ratio. *Jour. Geol*. **49**: 635-650.

Roser, B. P., Copper, R. A., Nathan, S. and Tulloch, A. J. (1996). Reconnaisance sandstone geochemistry, provenance and tectonic setting of the Lower Palaeozoic terrains of the West Coast and Nelson, New Zealand. *NZ Jour. Geol. Geophysics*. **39**: 1-16.

Sen, S., Das, P. K., Bhagaboty, B. and Singha, L. J. C. (2012). Geochemistry of shales of Barail Group occurring in and around Mandarlisa, North Cachar Hills, Assam: Its implications. *Int. Jour. Chem. and Applications*. **4(1)**: 25-37.

Sen, S., Baruah, H., Das, P. K. and Singh, L. J. C. (2016). Reflections from compositional attributes of the Mandarlisa Barail sandstones, NC Hills District, Assam. In S.K.Srivastava (ed), Recent trend in Earth Science Research with special reference to NE India. Today and Tomorrow Publisher, New Delhi, 314p. 31-64.

Siever, R. (1979). Plate tectonic controls on diagenesis. *Jour. Geol*. **87**: 127-155.

Srivastava, S. K. and Pandey, N. (2001). Palaeoenvironmental reconstruction of Palaeogene Disang-Barail Transitional Sequences, NW of Kohima, Nagaland, NE India (Abst.). *Seminar on Contribution to Himalayan Geology, Dehra Dun*. 7.

Srivastava, S. K. (2002). Facies architecture and depositional model for Palaeogene Disang-Barail Transition, North West of

Kohima, Nagaland, *Unpub. PhD thesis, Nagaland University, Kohima*.

Srivastava, S. K., Pandey, N. and Srivastava, V. (2004). Tectono-sedimentary evolution of Disang-Barail Transition, NW of Kohima, Nagaland, India, *Himalayan Geology*. **25(2)**: 121-128.

Srivastava, S. K. and Pandey, N. (2011). Search for provenance of Oligocene Barail sandstones in and around Jotsoma, Kohima, Nagaland, *Journal of the Geological Society of India*. **77:** 433-442.

Srivastava, S. K., Vadeo, K. and Kichu, A. M. (2015). Petrography and diagenesis of Palaeogene sandstones, South of Kohima Town, Nagaland, India. *Int. Jour. Earth Sci. Engineering*. **8(5)**: 2025-2032.

Srivastava, S. K., Liba, B. and Chuzo, V. (2017). Lithofaceis analysis of the Palaeogene sediments in parts of Kohima Synclinorium, Nagaland, India: Implications for the depositional environment. *Him. Geol*. **38(1)**: 30-37.

Srivastava, S. K., Laskar, J., Keditsu, V. and Awomi, L. (2018). Petrography and Major element Geochemistry of Palaeogene sandstones, South of Kohima Town, Nagaland. *Jour. Applied Geochemistry*. **20(1)**: 41-49.

Suttner, L. J. and Dutta, P. K. (1986). Alluvial sandstone composition and palaeoclimate framework mineralogy, *Jour. Sed. Petrol.* **56:** 329-345.

Taylor, S. R. and McLennan, S. M. (1985). The continental crust: Its composition and evolution. Blackwell, Oxford, UK, 349p.

Valloni, R and Maynard, J. B. (1981). Detrital modes of recent deep sea sand and their relation to tectonic setting: A first approximation. *Sedimentology*. **28**: 75-83.

Wintesch, R. P. and Kvale, C. M. (1994). Differential mobility of elements in burial diageneis of siliciclastic rocks. *Jour. Sed. Pet*. **64**: 349-361.

ISSN 2348-0637

COMPARING ANN AND GARCH MODELS FOR PREDICTING MONTHLY RAINFALL IN DIBRUGARH, ASSAM, INDIA

Reviewed

Pallab Changkakoti
Department of Statistics, Kohima Science College (Autonomous), Jotsoma -797002, Nagaland, India
e-mail: c.pallab@gmail.com

Abstract: To predict or forecast any given time series data, prediction models are necessary. Some of the available Time series data prediction models are ARIMA, GARCH, ANN, Fuzzy model, spectral model, Markov model etc. In this paper an attempt has been made to compare the forecasting ability of Artificial Neural Network (ANN) to Generalized Autoregressive Conditional heteroskedasticity (GARCH) model using 110 years of monthly rainfall time series data collected from India Meteorological Department, Govt. of India for Dibrugarh city in the state of Assam in India. Results show that for prediction of monthly rainfall in the said region ANN model is slightly more efficient than the GARCH model.

Keywords: ANN, GARCH, rainfall.

Introduction

Predicting the hydrological variables like rainfall, flood stream and runoff flow is one of the principal resources of water resource planning. Time series analysis of the occurrence of such variables have utmost importance in monitoring the hydrological behaviour of a region. The most vital factor in water resource management, irrigation scheduling and agriculture management is rainfall forecasting (Mimikou, 1983; Hamlin *et al*., 1987). Irrigation is not very common in wet and semi wet climate and the farmers have to rely on the rain water for crop water requirements. When rainfall is not enough the supplemental irrigation will be applied. Therefore modelling, monitoring, and forecasting of rainfall are very much important in agricultural activities (Geng *et. al*., 1986; Hoogenboom, 2000; Sentelhas *et. al*., 2001).

Rainfall is treated as one of the most complex and difficult events among other hydrological events. The rainfall data are multidimensional, nonlinear and dynamic. True quantitative forecasting of rain is a challenging and difficult job because of the complexity of atmospheric processes. Statistical forecasting methods such as ARIMA, Regression Model, Hidden Markov Model, Exponential Smoothing etc. and Artificial Intelligence (AI) methods such as Artificial Neural Network (ANN), adaptive network based Fuzzy Inference System (FIS), Genetic Algorithm (GA) have been proposed as forecasting techniques. The statistical techniques have developed for many years but have been proven to be incapable of handling nonlinear series (Kamruzzaman *et. al*., 2003; Kihoro *et. al*., 2000). Hence AI methods have been used successfully in series forecasting, where the only goal is to minimize the predictive error. Thus these methods have been applied in solving numerous forecasting problems (Jang, 1993; Charhate *et. al*., 2007; Banik *et. al*., 2007; Kumar *et. al*., 2007).

Empirical works (e.g. Whigham *et. al*., 2001; Navone *et. al*., 1994; Sen *et. al*., 2001; Lee *et. al*., 2006; Mondol *et. al*., 2004; Islam *et. al*., 2002; Wahid *et. al*., 1999 and many others) have been carried out to forecast rainfall in context of various countries.

Some time series data exhibits volatile nature, where the conditional variance varies continually with time. This type of time series data are said to exhibit risk, where risk is measured in terms of volatility. If the time series data is highly volatile the error series obtained from the model, will no longer be a Gaussian time series. In such cases, if the conditional variance of the time series data at a time t, is modelled in terms of previous variances, such a modeling on conditional variances may be used to predict the time series data. ARIMA–GARCH error models were developed to take into accounts both the mean and volatility of the daily rainfall series (Yusof et al., 2013). This type of modeling is the basic principle behind ARCH models. ARCH models are introduced by Engle (1982). Later, Bollerslev (1986) proposed a Generalized ARCH (GARCH) model, which is an equivalent version of higher order ARCH model. The term conditional implies the level

of association on the past sequence of observations and the autoregressive describes the feedback mechanism that incorporates past observations into the present (Laux *et. al*., 2011). So far few attempts have been reported on using GARCH models in hydrological literature series (Yusof *et. al.*, 2013).

The use of Artificial Neural Networks (ANN) in various domain of research have shown that ANNs have powerful pattern classification and pattern recognition capabilities. The ANN is inspired by the biological system of the brain particularly the ability to learn and generalize from experience. At present the ANN is being used in wide variety of tasks in the fields of business, industry, science etc. (Widrow *et. al*., 1994). One of the major application area of ANN is forecasting (Sharda, 1994).

Any forecasting model assumes that there is a relationship between the past values and the future of a time series or other relevant variable. ANN have a better ability to identify the functional relationship than traditional statistical forecasting models. Finally, ANN are non-linear. In most of the traditional statistical forecasting models such as the Box-Jenkins or ARIMA methods (Box and Jenkins, 1976; Pankratz, 1983) assume that the models are linear. But the models would be totally inappropriate if the system is non linear. In fact real world systems are often nonlinear. (Granger *et. al.*, 1993).

Since 1980, many different ANN models have been proposed. Some of the most influential are the multi layer perceptrons (MLP), Hopfield (1982) networks and Kohonen's (1982) self organizing networks.

In this paper an attempt is made to compare the prediction ability of GARCH and ANN models using monthly rainfall data over Dibrugarh in Assam, India.

Data

Dibrugarh city is the headquarters of the Dibrugarh district in the state of Assam in India. Dibrugarh has a humid subtropical climate with extremely wet summer and relatively dry winters. It receives an average rainfall of 2758 mm per year. For this study monthly total rainfall from 1901 to 2010 for 110 years have been obtained for Dibrugarh from India Meteorological Department (IMD), Government of India.

Methodology

In the present study, artificial neural networks (ANN) and Generalized Autoregressive Conditional Heteroskedasticity (GARCH) models were used for forecasting monthly rainfall at Dibrugarh, Assam in India individually. These models are explained as follows.

GARCH Modeling: According to Bollerslev's GARCH model, the present conditional variance is modeled as a function of past variances and past values of squared innovations or residuals. The GARCH modeled time series data, is shown in (3.1), where c stands for a constant term, and ε_t stands for residual time series, which is Gaussian distributed with zero mean and variance σ_t^2

$$y_t = c + \varepsilon_t \qquad (3.1)$$

In (3.1) $\varepsilon_t = \sigma_t z_t$ where $z_t = N(0,1)$ is the Gaussian random sequence with independent identically distributed (i.i.d) random variables of zero mean and unit variance. The variance σ_t^2 is modeled as in (3.2), for a GARCH (*p*,*q*) process.

$$\sigma_t^2 = \alpha_0 + \sum_{i=1}^{p} \alpha_i \sigma_{t-1}^2 + \sum_{j=1}^{q} \beta_j \varepsilon_{t-j}^2 \qquad (3.2)$$

From (3.2), it can be seen that present conditional variance is represented as a function of past variances and past values of squared innovations. If *p* and *q* are taken as 1, the model is the simplest one and is GARCH (1,1). If $p > 1$, $q > 1$, that means the present variance at time t, is a function of previous variances at time $t-1, t-2 \ldots, t-p$ and also a function of *q* previous squared residual values.
Prediction: After validation, the model can be used in the prediction of future volatility values. In GARCH after the parameter estimation step is complete, only the future conditional variances can be predicted but not the future values. To obtain the future forecasts, a gaussian i.i.d with zero mean and unit variance is simulated and correspondingly its variance is made σ_t^2 using $\varepsilon_t = \sigma_t z_t$. σ_t^2 is obtained by substituting the estimated

ISSN 2348-0637

parameters in (3.2). Using the parameter *c* and the simulated time series ε_t, the GARCH predictions y_t are obtained.

ANN Modeling : It is already mentioned that one of the major application area of ANN is forecasting. Some distinguished features of ANN that make it more appropriate in forecasting are as follows. Firstly, the assumptions about the ANN model are few. ANN are capable of learning the functional relationship among the data even if the underlying relationship are hard to describe. For a large sized dataset where the solution require knowledge ANN is more suitable. In such cases ANN can be treated as one of the multivariate nonlinear nonparametric statistical method (White, 1989; Replay, (1993); Cheng *et. al*., 1994). Secondly, even if the sample data contain noisy information, it can generalized the data and can predict future behaviour of the data. Thirdly, it is seen that ANN approximate any continuous function to any desired accuracy. So, it is a universal function approximator (Irie *et. al.,* 1988; Hornik *et. al.,* 1989; Cybenko, 1989; Funahashi, 1989; Hornik, 1991). Any forecasting model assumes that there is a relationship between the past values and the future of a time series or other relevant variable. ANN have a better ability to identify the functional relationship than traditional statistical forecasting models. Finally, ANN are non-linear. In most of the traditional statistical forecasting models such as the Box-Jenkins or ARIMA methods (Box and Jenkins, 1976; Pankratz, 1983) assume that the models are linear. But the models would be totally inappropriate if the system is non linear. In fact real world systems are often nonlinear. (Granger *et. al*., 1993).

The rainfall data are multidimensional, nonlinear and dynamic. In this paper we focus on the multilayer perceptrons (MLP) introduced by Culloch and Pitts (1943). An MLP is typically composed of several layers of nodes. The first or the lowest layer is an input layer where external information are received. The last or the highest layer is an output layer where the problem solution is obtained. The input and output layers are separated by one or more intermediate layers called the hidden layers. The nodes in adjacent layers are usually fully connected by acyclic arcs from a lower layer to a higher layer. Fig 1 gives an example of fully connected MLP with one hidden layer.

For an explanatory forecasting problem the inputs to an ANN are usually the independent or predictor variable. The functional relationship estimates by the ANN can be written as –

$$y = f(x_1, x_2, ..., x_p) \tag{3.3}$$

Where $x_1, x_2, ..., x_p$ are *p* independent variables and y is a dependent variable. In this case the neural network is functionally equivalent to a nonlinear regression model. For an extrapolative time series forecasting problem inputs are typically the past observations of the data series and output is the future value. The ANN performs the following function mapping:

$$y_{t+1} = f(y_t, y_{t-1}, y_{t-2}, ..., y_{t-p}) \tag{3.4}$$

where y_t y_t is the observation at time *t*. In this case the ANN is equivalent to the nonlinear autoregressive model for time series forecasting problem.

Mathematically,

$$y = f\left\{\sum_{i=1}^{n}(w_i x_i + b)\right\} = f\left(W^T X + b\right) f(.) \tag{3.5}$$

where W denotes the vector of weights, X is the vector of inputs, b is the bias and $f(.)$ is the activation function.

A Multilayer Perceptron (MLP) consists the following processing functions.

(i) Receiving the inputs.

(ii) Assigning appropriate weight coefficients of inputs.

(iii) Calculating weighted sum of inputs.

(iv) Comparing this sum with some threshold and finally

(v) Determining an appropriate output value.

Neural Networks are composed of simple elements operating in parallel. A neural network can be trained to perform a particular function by adjusting the values of the connections (weights) between the elements. Commonly neural networks are adjusted or trained so that a particular input leads to a specific target output. Such a situation is shown in Fig 1.

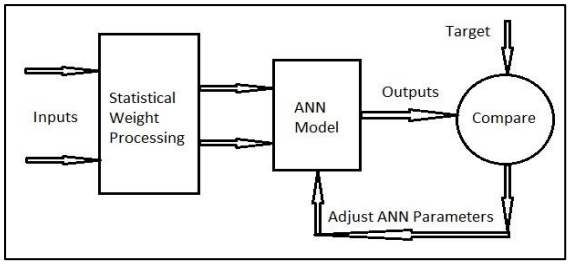

Fig. 3.1 Neural Network Algorithm

Here, based on a comparison of output and targets the network is adjusted, until the sum of square differences between the target and output values becomes the minimum. Typically many such input/target output pairs are used to train a network. Batch training of a network proceeds by making weights and bias changes based on an entire set (batch) of input vectors. Incremental training changes the weight and biases of a network as needed after presentation of each individual input vector.

Basic building blocks of every artificial neural network is artificial neuron, that is a single mathematical model (function). Such model has three simple set of rules: multiplication, summation and activation. At the entrance of artificial neuron the inputs are weighted what means that every input value is multiplies with individual weight. In the middle section of artificial neuron is sum function that sums all weighted inputs and bias. At the exit of artificial neuron the sum of previously weighted inputs and bias is passing through activation function that is also called transfer function.

Types of Activation Function:

An activation function is defined by $f(x)$ and defines the output of a neuron in terms of its input x. There are three types of activation function –

1. Threshold Function:

$$f(x) = \begin{cases} 1, & if\ x \geq 0 \\ 0, & if x < 0 \end{cases}$$

2. Piecewise Linear:

$$f(x) = \begin{cases} 1, & if\ x \geq ½ \\ X, & if\ -½ < x < ½ \\ 0, & if\ x \geq ½ \end{cases}$$

3. Sigmoid Functions:

(i) Logistic Function, whose domain is [0,1]:

$$f(x) = \{1 + \exp(-\alpha x)\}^{-1}$$

(ii) The Hyperbolic Tangent Function, whose domain is [-1,1]:

$$f(x) = \frac{1 - \exp(-\alpha x)}{1 + \exp(-\alpha x)} = \tanh\left(\frac{\alpha x}{2}\right)$$

Performance Measures

To compare the predictive capabilities of the proposed models, Mean Absolute Error (MAE), Mean Squared Error (MSE), and Mean Absolute Percentage Error (MAPE) are employed as performance indicators given as follows.

$$MAE = \frac{1}{n}\sum_{i=0}^{n}|y_E - y_O|$$

$$MSE = \frac{1}{n}\sum_{i=1}^{n}(y_E - y_O)^2$$

$$MAPE = \frac{1}{n}\sum_{i=1}^{n}\left|\frac{y_E - y_O}{y_O}\right| \times 100$$

where y_E is the computed and y_O is the observed value.

Results and discussion

GARCH Modeling

Table 4.11 depicts the ACF, PACF, Q–Statistics and p–values (up to three places of decimal) of the squared error ε^2 of AR(1) fit for the monthly rainfall data under our study.

Table 4.1.1 ACF, PACF, Q-Statistics and p-values of ε^2 of AR(1) Fit

Dibrugarh				
LAG	ACF	PACF	Q-statistics	p-value
1	0.0737	0.0737	7.1403	0.008
2	0.0814	0.0764	15.863	0.000
3	0.0139	0.0253	16.116	0.001
4	0.0633	0.0676	21.3976	0.000
5	0.0895	0.0787	31.9709	0.000
6	0.0825	0.0624	40.9555	0.000
7	0.0489	-0.029	44.1209	0.000
8	0.0338	0.0245	45.6298	0.000

ISSN 2348-0637

9	0.0082	0.0057	45.7187	0.000
10	0.0596	0.0483	50.4268	0.000
11	0.0324	0.0088	51.8172	0.000
12	0.1556	0.1351	83.9622	0.000

Table 4.1.2 shows the estimated parameters of the proposed GARCH (1,1) model by Maximum Likelihood Estimation (MLE) technique.

Table 4.1.2 Estimated Parameters of the GARCH (1,1) Model

α_0	α_1	α_2
4065.55	0.27211	0.17857

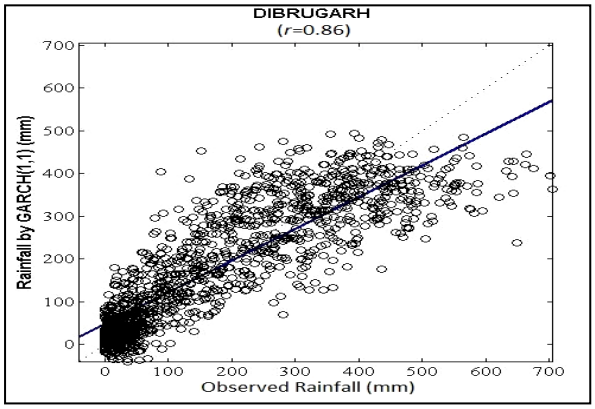

Fig 4.1.1 Scatter Plot Between Observed and Predicted Rainfall by GARCH(1,1) Model with *r* Value for Dibrugarh

Figure 4.1.1 shows the scatter plot between the observed and the predicted rainfall computed by GARCH (1,1) model along with the *r* value between them. High value of *r* indicates the high correlation between the observed and the GARCH predicted rainfall and a very prediction capacity of the proposed GARCH (1,1) model.

Table 4.1.2 MSE, MAE, MAPE and r Values for the GARCH(1,1) Model

MSE	MAE	MAPE	*r*
7076.28	61.45	252.66	0.86

Table 4.1.2 shows the MSE, MAE, MAPE and r Values for GARCH (1,1) model.

ANN Modeling

The rainfall data has been trained using Levenberg-Marquadrt algorithm. In Table 4.2.1Mean Absolute Error, Mean Square Error (MSE) and *r* at different levels of Feedback Delays (Lag) and hidden layers of neuron are shown.

Table 4.2.1 Comparison of ANN Models for Dibrugarh

No. of Neurons	FD : 6			FD : 12			FD : 18		
	MSE	MAE	*r*	MSE	MAE	*r*	MSE	MAE	*r*
10	7036.9	60.07	0.86	5896.6	56.03	0.88	6400.1	56.72	0.88
15	6694.9	58.71	0.87	7210.9	59.45	0.87	6255.5	58.06	0.88
20	6668.6	57.92	0.87	**5799.6**	**55.42**	**0.89**	6150.6	57.35	0.88
25	6500.8	57.06	0.87	6036.7	55.88	0.88	6325.1	59.79	0.88

Table 4.2.2 depicts the lowest MSE, lowest MAE and highest *r* values for the trained neural networks for the monthly rainfall data in Dibrugarh.

Table 4.2.2 Number of Hidden Neurons, Feedback Delays (FD), MSE, MAE, MAPE and R Values for the Best Fitted ANN Models

Neurons	**FD**	**MSE**	**MAE**	**MAPE**	***r***
20	12	5799.6	55.42	248.65	0.89

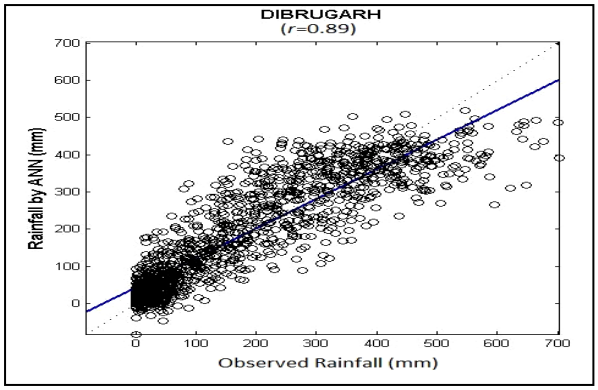

Fig 4.2.1 Scatter Plot Between Observed and Predicted Rainfall by ANN Model with *r* Value for Dibrugarh

Comparison of ANN and GARCH Models

Table 4.3.1 Comparison of GARCH and ANN Models

Models	MSE	MAE	MAPE	*r*
GARCH	7076.28	61.45	252.66	0.86
ANN	5799.60	55.42	248.65	0.89

Table 4.3.1 shows the Mean Squared Error (MSE), Mean Absolute Error (MAE) and Mean Absolute Percentage Error (MAPE) of GARCH and ANN models for the gauge station at Dibrugarh. All the performance functions for GARCH models are greater than those for the ANN models indicating superiority of ANN model over the GARCH model.

Conclusion

In this analysis, it is found that the ANN model is more efficient in predicting monthly rainfall compared to GARCH models. However, if we observe the summary statistics of both these models, the differences between the values of the corresponding summary statistics are very low. Also, the superiority of ANN models over GARCH models is not universally accepted. Hence, it may be concluded that, for the monthly rainfall data in Dibrugarh, although the ANN model is slightly better than the GARCH model, both are competing models.

References

Banik, S., Chanchary, F. H., Rouf, R. A. and Khan, K. (2007). Modeling chaotic behaviour of Dhaka stock market index values using the neuro-fuzzy model. *Proceedings of 10th ICCIT*. 80-85.

Bollerslev, Tim (1986). Generalized Autoregressive Conditional Heteroskedasticity. *Journal of Econometrics*. **31**: 307-327.

Box, G. E. P. and Jenkins, G. M. (1976). Time Series Analysis: Forecasting and Control. Holden-Day, San Francisco, CA.

Charhate, S. B. and Deo, M. C. (2007). Storm surge prediction using NN and GP. Paper Presented the 6th Conference on AI application to Environmental Science AMS Annual Meeting, 20-24 January, New Orleans Louisianna, USA.

Cheng, B. and Titterington, D. M. (1994). Neural networks: A review from a statistical perspective. *Statistical Science*. **9(1)**: 2-54.

Culloch, W. S. and Pitts, W. (1943). A logical calculus of the ideas immanent in nervous activity. *B Math Bioohys*. 115-133.

Cybenko, G. (1989). Approximation by superpositions of a sigmoidal function. Mathematical Control Signals Systems 2. 303-314.

Engle and Robert F. (1982): Autoregressive Conditional Heteroscedasticity with Estimates of the Variance of United Kingdom Inflation. *Econometrica*. **50(4)**: 987-1007.

Funahashi, K. (1989). On the approximate realization of continuous mappings by neural networks. *Neural Networks 2*. 183-192.

Geng, S., Penning de Vries, F. W. T. and Supit, I. (1986). A Simple Method for Generating Daily Rainfall Data. *Agric. For. Meteorol*. **36(4)**: 363-376.

Granger, C. W. J. and Terasvirta, T. (1993). Modelling Nonlinear Economic Relationships. Oxford University Press, Oxford.

ISSN 2348-0637

Hamlin, M. J., and Rees, D. H. (1987). Use of Rainfall Forecasts in the Optimal Management of Smallholder Rice Irrigation, A case study. *Hydrol. Sci. J*. **32**: 15-29.

Hoogenboom, G. (2000). Contribution of Agrometeorology to the Simulation of Crop Production and its Applications. *Agric. Forest Meteorol*. **103**: 137-157.

Hopfield, J. J. (1982). Neural networks and physical systems with emergent collective computational abilities. *Proceedings of the National Academy of the Sciences of the U.S.A*. **79**: 2554-2558.

Hornik, K. (1991). Approximation capabilities of multilayer feed-forward networks. *Neural Networks 4*. 251-257.

Hornik, K., Stinchcombe, M. and White, H. (1989). Multilayer feed-forward networks are universal approximators. *Neural Networks 2*. 359-366.

Irie, B. and Miyake, S. (1988). Capabilities of three-layered perceptrons. *In: Proceedings of the IEEE International Conference on Neural Networks.* **1**: 641-648.

Islam, M. N., Islam, S., Hayashi, T., Terao, T. and Hiroshi, U. (2002). Application of a method to estimate rainfall in Bangladesh using GMS-5 data. *Journal of Natural Disaster Science*. 83-89.

Jang, J. S. R. (1993). ANFIS: Adaptive-network-based fuzzy inference systems. *IEEE Transactions on Systems, Man, and Cybernetics*. 665-685.

Kamruzzaman, J. and Sarker, R. A. (2003). Comparing ANN based models with ARIMA for prediction of forex rates. *ASOR Bulletin*. 1-10.

Kihoro, J. M., Otieno, R. O. and Wafula, C. (2000). Seasonal time series forecasting: A comparative study of ARIMA and ANN models. *African Journal of Science and Technology*. 41-49.

Kohonen, T. (1982). Self-organized formation of topologically correct feature maps. *Biological Cybernetics*. **43**: 59-69.

Kumar, A. and Debroy, T. (2007). Tailoring fillet weld geometry using a genetic algorithm and a neural network trained with convective heat flow calculations. *Welding Journal*. 26-33.

Laux, P., Vogl, S., Qiu, W., Knoche, H. R. and Kunstmann, H. (2011). Copulabased statistical refinement of precipitation in RCM simulations over complex terrain. *Hydrol Earth Syst Sci Discuss*. **8**:3001-3045.

Lee, Y. H., Park, S. K. and Chang, D. E. (2006). Parameter estimation using the genetic algorithm and its impact on quantitative precipitation forecast. *Annales Geophysicae*. 3185-3189.

Mimikou, M. (1983). Forecasting Daily Precipitation Occurrence with Markov Chain of seasonal Order. International Symposium on Hydrometeorology, June 13-17, 1982, Denver, Colorado. *Journal of American Water Resources. As.* 219-224.

Mondol, R. U. and Shahid, D. S. (2004). A neural network approach for the prediction of monthly rainfall. *Jahangirnagar University of Science*. 87-95.

Navone, H. D. and Ceccatto, H. A. (1994). Predicting Indian monsoon rainfall: A neural network approach. Climate Dynamics, 305-312.

Pankratz, A. (1983). Forecasting with Univariate Box-Jenkins Models: Concepts and Cases. John Wiley, New York.

Ripley, B. D. (1993). Statistical aspects of neural networks. In: Barndorff-Nielsen, O. E., Jensen, J. L. and Kendall, W. S. (Eds.), Networks and Chaos-Statistical and Probabilistic Aspects. Chapman and Hall, London. 40-123.

Sen, Z. and Oztopal, A. (2001). Genetic algorithms for the classification and prediction of precipitation occurrence. *Hydrological Sciences*. 255-267.

Sentelhas, P. C., de Faria, R. T., Chaves, M. O., and Hoogenboom, G. (2001). Evaluation of the WGEN and SIMMETEO Weather Generators for the Brazilian Tropics and Subtropics, Using Crop Simulation Models. *Rev. Bras. Agrometeorologia.* **9(2)**: 357-376.

Sharda, R. (1994). Neural networks for the MS/OR analyst: An application bibliography. *Interfaces*. **24(2)**: 116-130.

Wahid, C. M. and Islam, M. N. (1999). Patterns of rainfall in the northern part of Bangladesh. *Journal of Science Research*. 115-120.

Whigham, P. A. and Crapper, P. F. (2001). Modeling rainfall-runoff using genetic programming. Mathematical and Computer Modeling, Canberra, Australia. 707-721.

White, H. (1989). Learning in artificial neural networks: A statistical perspective. *Neural Computation*. **1**: 425-464.

Widrow, B., Rumelhart, D. E. and Lehr, M. A. (1994). Neural networks: Applications in industry, business and science. Communications of the ACM. **37(3)**: 93-105.

Yusof, F. and Kane, I. L. (2013). Volatility modelling of rainfall time series. *Theoretical and Applied Climatology*. **113(1)**: 247-258.

Yusof, F. and Kane, I. L. (2013). Assessment of Risk of Rainfall Events with a Hybrid of ARFIMA-GARCH. *Modern Applied Science*.**7(12)**.

ISSN 2348-0637

PALYNOLOGICAL INVESTIGATION OF UPPER PALAEOCENE—EOCENE OIL BEARING SEDIMENTS OF MORAN OILFIELD IN PART OF UPPER ASSAM SHELF

Reviewed

Thejakielie Meyase
Department of Geology, Kohima Science College (Autonomous) Jotsoma-797002, Nagaland, India
e-mail: thejakieliemeyase@gmail.com

Abstract: The present palynological investigation of Upper Palaeocene-Eocene oil bearing sediments of Moran Oilfieldcomprises mostly of alterations of shales and sandstone with thin beds of limestone. The samples (drill cuttings) of the present study were provided by the Oil India Limited from the Moran oilfield. The reported palynotaxas of the Moran oilfield are a variety of pteridophyte spores, angiosperms pollens, fungal spores and foraminifers indicating warm humid tropical climate and deltaic to shallow marine palaeoenvironment for Upper Palaeocene- Eocene period.

Keywords: Palynology, Palaeoenvironment, Moran Oilfield, Upper Assam Shelf, India.

Introduction

The Upper Assam Tertiary sedimentary basin is the earliest explored and established onshore petroliferous basin in India. It represents the northeastern extremity of the Indian subcontinent encompassing an area of 57,000 sq. km and forms the northeastern part of Assam-Arakan Basin and contains several oil and gas fields. Until late eighties, the main oil producing horizons within Oil India Limited's (OIL) operational areas were within Upper Eocene-Oligocene (Barail) and Miocene (Tipam) reservoirs. The Upper Palaeocene-Lower Eocene sediments of Upper Assam Basin deposited through 58 million years (Cowie, J.W and Basset, M.G. 1989) is gaining importance; since the discovery of commercial oil in the Upper Palaeocene- Lower Eocene clastic reservoirs within the concession areas of OIL lying in the central part of Upper Assam Basin in 1991. The present exploration thrust in the basin is towards the deeper reservoirs (depth>4000m). At present more than 50% of the crude oil production is from the deeper reservoirs (Upper Palaeocene- Lower Eocene).

Several palynological studies of the Upper Palaeocene-Eocene sediments of Moran oilfields has been undertaken to ascertain the depositionalenvironment of the sediments. The first palynological studies in this region was attempted by Sahni as early as in 1947 with the Tertiary sediments of Assam. Subsequent developments in palynological studies in analysing the Tertiary sediments of Upper Assam by Sah and Dutta (1967), Singh and Tewari (1979), Sah *et al.* (1980), Kar *et. al* (1994) have made significant progress on the palynoassemblages of the sediments in this region.

Geological setting

The area under investigation, Moran oilfield lies in the north east corner of India (27°10'56" N and 94°55'3"E) and is part of the Upper Assam Basin. The Assam Basin is located in the alluvial covered foreland shelf zone, known as Upper Assam Valley and contains several oil and gas fields (Fig-1).Geologically the Upper Assam valley is regarded as the Upper Assam shelf bounded by the Brahmaputra valley, Himalayan ranges in the north and Naga hills in southeast, Dhansiri valley in south upto Mishmi hills in the extreme northeast.The Moran oilfield is one of the oldest oilfields in the alluvium covered foreland shelf zone of Upper Assam basin. A few oil and gas fields of Upper Assam are located in the Naga thrust sheets of Assam Arakan fold belt. This part of India is very significant from both geological and commercial perspective, as it represents one of the most representative and thick Cenozoic sections of the North Eastern region andits surrounding present major oil and gas fields and coal fields as well.

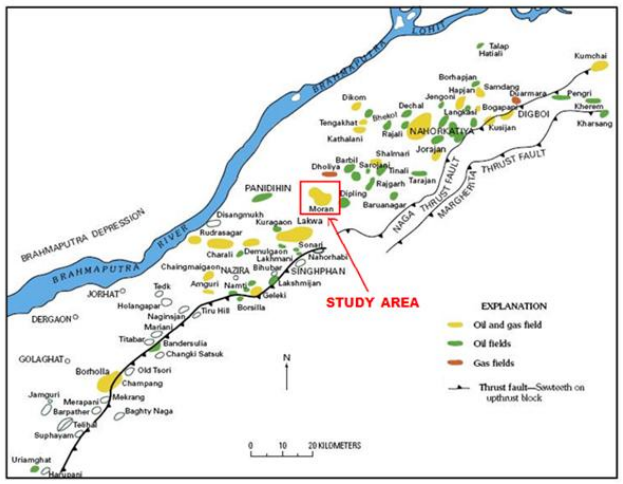

Figure-1: Geological map of Upper Assam and its oil and gas fields (modified from Naidu and Panda 1997, and Mallick 1997)

Objectives

The present investigation on subsurface palynostratigraphy of Upper Paleocene- Eocene oil bearing sediments of Moran oilfield have been undertaken to study the palynomorphs present in the deposits and their taxonomic identification, stratigraphic position, age and palaeoenvironment.

Methodology

The present work has 20 samplesof drill cuttings collected by Oil India Limited were taken for making palynological slidesusing standard palynological techniques of digesting sedimentary rock in hydrochloric acid, hydrofluoric acid, nitric acid and heavy liquid separation with acetic acid followed by 5% solution of KOH. The slides were washed in polyvinyl alcohol and mounted in Canada balsam.The slides were then ready for identifying the grains under LEITZ ORTHOPLAN biological microscope.

Palynofloral composition

The palynotaxa recovered from the oil bearing sediments of Moran oilfield is rich and diversified and the assemblage is dominated by pteridophyte spores and angiosperm pollens. The important palynotaxa of the assemblage are:

- Pteridophyte spores: *Lygodiumsporites sp., Cyathidites sp., Laevigatosporites sp., Polypodiisporites sp., Florschuetzia sp.*
- Angiosperms**:** *Proxapertites sp., Straitipollisbellus, Spinizonocolpites sp., Palmeopollenites sp., Longapertites sp., Polycolpites sp.,Retistephanocolpites sp., Foveotricolporites sp., Longapertites sp., Meyeripollisnaharkotensis, Marginipollis sp., Couperipollis sp.*

In addition to this, fungal remains, especially the representative Phragmothyrites are also good indicators of palaeoclimate. The given samples ranges in depth from 3736m – 4510m (Table-1). The bottom depth i.e. 4510m is at the Langpar Member (Paleocene + Mid. Eocene) and the uppermost depth i.e. (3736m is at the Barail Group (Oligocene). The macerated residue studies of this sandstone, shale and limestone samples also shows presence of microfauna mainly foraminifera and ostracoda. The thin section and macerated residue studies of this sandstone, shale and limestone samples also shows presence of microfauna.

Identification, name of author, depth, description, affinity, occurrence and remarks against the specimens are furnished in the following.

Systematic palynology

Longapertites- Arecaceae

Genus: *Longapertites vaneendenburgi* Van Hoeken-Klinkenberg, 1964

Depth- 3736m

Affinity: Arecaceae

Description: The specimen highlighted is unfortunately not very clear but after comparing with species like *L. proxapertitoides (*Van der Hammen& Garcia de Mutis, 1965),*L. marginatus (*Van Hoeken-Klinkenberg, 1964), and *L. vaneendenburgi*, we can confirm that the present specimen is identified as *L. vaneendenburgi* showing finely perforate walled structure and the distal is curved-shaped.

Occurrence: Campanian-Eocene, Nigeria; Eocene India.

POLLEN

Superdivision POLLENITES Potonie, 1931

ISSN 2348-0637

Genus: *Meyeripollis naharkotensis* Baksi & Venkatachala 1970
Depth- 3850m
Description: Pollen grain broken, triangular, colpi not distinguishable, pores obscured with ornamentation.
Affinity: Uncertain. Similar type of spore have been recorded by Ghosh, Jacob and Lukose (1964) from Assam. Banerjee (1974) stated that this type of spore is possibly related to the family Schizaeaceae (*Lygodium*).
Distribution: Upper Eocene to Upper Miocene of Assam (Meyer 1954, Ghosh et. a1 1964, Baksi and Venkatachala, 1970), more common in the Oligocene, occasional in other horizons (Banerjee 1974).In the present study, it has been recovered from the upper part of the Kopili formation. Therefore the occurrence of this mioflora in the Upper-Palaeocene-Eocene sediments is questionable and may have happened due to contamination in drill cuttings before the samples were even collected.

MONOLETES
Superdivision MONOLETES
Division AZONOMONOLETES
Subdivision LAEVIGATOMONOLETES

ANTETURMA SPORITES
TURMA TRILETES
SUPRASUBTURMA ACAVATITRILETES
SUBTURMA AZONOTRILETES
Infraturma Laevigati

Genus*:* *Laevigatosporites sp. Ibrahim 1933*
Depth- 3760m
Description: Spores oval in shape. Size ranges 40-50µm, bean shaped.
Affinity: Spores of this kind are found commonly in various members of *Polypodiceaeviz, Thylepteris, Asplenium, Athyrium, Aspidium,* etc.
Remarks: Ibrahim (1933) proposed the genus *Laevigatosporites sp.* with the following diagnosis: "Spores with a dehiscence mark and more or less smooth surface". They are bean-shaped spores, straight elongate marks.

Genus-Straitopollisbellus *sp.* Salar & Cheboldaeff 1977
Depth-3886m
Description: Pollen grains tricolporate, oval in equatorial and sub-sircular in polar view.
Remarks: The pollen of *striatopollis bellus* Sah 1976 is tricolpate but the pollen attributed to this species by Salard-Cheboldaeff 1977 is tricolporate and resembles that of striatocolporites.

Genus: *Lygodiumsporites sp.* Sah & Kar 1969
Depth-4174m
Affinity- Schizaeceae
Description: Microspore is roundly triangular trilete where the Y-mark is distinct.
Occurrence: Tropical to Subtropical

Genus: *Palmaepollenites sp.* Potonie 1950
Depth-4030m
Description: Pollen grains oval-elliptical size range 60-70µm.
Affinity: Palmae, Arecacea

Genus: *Polycolpites sp.*
Depth- 4264m
Description: Polycolpate, semicircular, 70µm in diameter.
Remarks: The Polycolpate pollen grains are common in Lower Tertiary sediments of Assam (Sah & Dutta 1966).
Affinity: Utricularia (Lentibulariaceae), fresh water, aquatic, terrestrial mostly in tropics.

Genus: *Marginipollis sp.* Clarke and Frederiksen, 1968
Depth-3620m
Affinity: Lecythidaceae
Description: Pollen grains are isopolar, prolate, spheroidal in equatorial view.

Genus: *Proxapertites sp.* Van der Hammen, 1956
Depth-3760m, 4030m
Affinity: Aracaceae
Remarks– Van der Hammen (1956) considered the pollen of *Proxapertites*as dyads with contiguous apertural faces. Muller (1968) however, found neither an evidence of a membrane covering the so-called 'aperture' nor a double membrane in the fossil grains interpreted as dyads. Observation from the present study has confirmed the opinion of Muller that, there is but a single membrane uniting the two halves of the pollen.
Occurrence- Tropical to temperate.

Genus: *Spinizonocolpites sp.* Muller 1968
Depth- 4102m
Diagnosis: Pollen grains subcircular to oval, size range around 45µm.
Remarks– Species attributed to *Spinizonocolpites* are spheroidal or ovoidal in shape. It also possess an extended sulcus and with a spinose exine.
Age: The genus *spinizonocolpites sp.* may indicate a Paleocene age.

Genus- *Adnatosphaeridium multispinosum*, William & Downie 1966
Depth- 4462m
Description: body is subspherical to spherical in shape.
Dimension: Size of cyst body 40-50µm
Remarks: This species vary in size and development. Older specimens are commonly larger and younger specimens are more commonly smaller and have more delicate process.

Turma TRILETES
Suprasubturma ACAVATITRILETES
Subturma AZONATI

Genus: *Cyathidites sp.* Couper 1953
Depth- 4030m
Description: Spores subtriangular to triangular, size range around 60µm.
Distribution: Cyathea is a common tree fern in Assam and on the precipitous slopes of Himalayas.
Affinity: Cyatheaceae
Occurrence: Tropical to temperate.

Genus: *Couperipollis sp.* Venkatachala & Kar 1969
Depth: 4174m
Remarks: The present pollen grain fall within the specific dimension range recorded so far. Sah & Dutta 1966, who stated after the diagnosis of this species that it possess long spines with bulbous base and rounded tip.
Geologic and geographic distribution: Eocene, Assam (Biswas 1962, Sah & Dutta 1966, Singh 1977)
Horizon: Lower Tertiary (Probably Eocene)

Genus: *Florschuetzia sp.* Germeraad 1968
Depth: 4030m
Description: Pollen grains are subspherical, one lobe distinct, pores circular.

Genus: *Polypodiisporites sp.* Potonie 1934
Depth- 3778m
Description:the Spores are bean shaped, measuring 50-70µm in size.
Affinity: Polypodiaceae

Genus: *Foveotricolporites sp.* Sah 1967
Depth-3748m
Description: Pollen grains spheroidal-oval in equatorial view, tapering on either ends.

Genus: *Retistephanocolporites sp.* Van der Hammen and Wymstra, 1964
Depth- 3748m
Description: Pollen grain circular in polar view.

Genus: *Phragmothyrites* Edwards 1922
Depth: 4264m
Description: Perithecium dark brown, subcircular in shape, outer part ruptured probably.

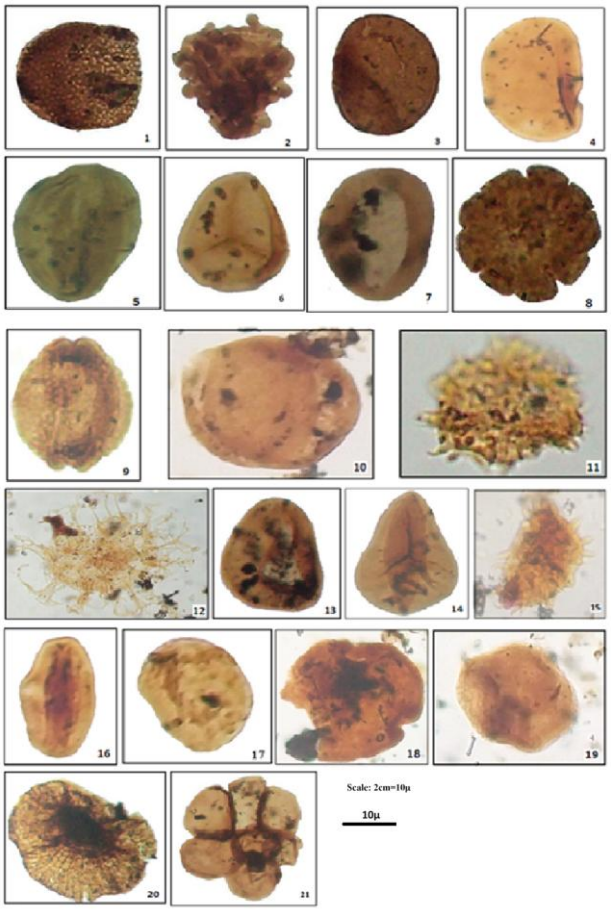

ISSN 2348-0637

Figure 2:
(1) Longapertites sp. (2) Meyeripollisnaharkotensis
(3) Laevagitosporites sp. (4) Laevagitosporites sp.
(5) Straitopollis (6) Lygodiumsporites
(7) Palmaepollenites sp. (8) Polycolpites sp.
(9) Marginipollisconcinnus (10)Proxapertites
(11) Spinizocolpites (12) Adnatosphaeridium sp.
(13 & 14) Cyathidites (15) Couperipollis sp.
(16) Florschuetzia sp. (17) Polypodiisporites sp.
(18) Favitricolporites sp. (19) Retistephanocolpites sp.
((20) Phragmothyrites (21) Microforaminifera(?)

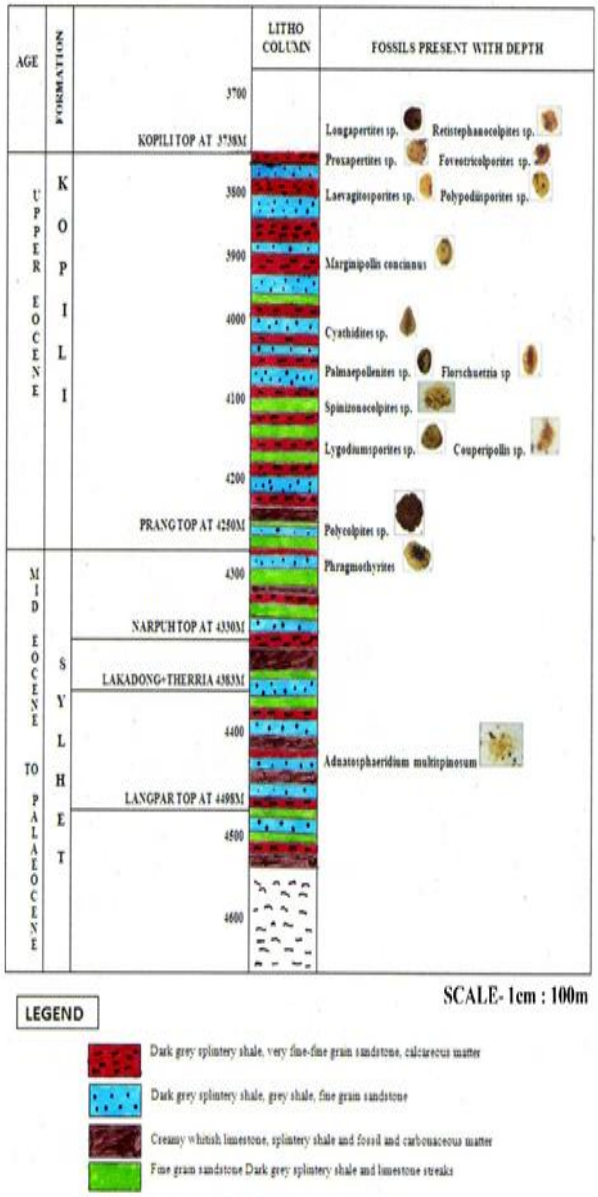

Table 1: Lithological section of a well in Moran of Upper Assam Basin (Prepared from Litholog obtained from OIL).

Palaeoclimate and depositional environment

From the microfloral investigation in Moran, it is evident that the pteridophytic spores along with angiospermous pollen are significantly represented in the assemblage whereas the gymnospermous forms are scarce. Table 1 shows the distribution of Upper Palaeocene to Eocene palyno-assemblage recovered from sediments in a well of Moran oilfield, Upper Assam Basin.

- **Swamp Water Edge Members:** *Laevigatosporites, Polypodiisporites, Lygodiumsporites, Polycolpites*
- **Thick forest members:** *Longapertites, Palmeopollenites*
- **Mangrove and Back Mangrove Members**: *Spinizocolpites*
- **Fresh water influx:** *Polycolpites*
- **Shallow Marine members:** *Adnatosphaeridium multispinosum*

Pollen grains belonging to Arecaceae (Monocolpopollenites, Palmidites) occur near the sea coast and are shore line elements. The palynotaxa of the Moran oilfield indicate that swamp and water edge elements viz. *Polypodiisporites sp., Lygodiumsporites sp.* and *Polycolpites sp.* and dense forest elements such as *Palmeopollenites sp.* and *Longapertites sp.* are found in the assemblage. According to Rull (1997) and Germeraad et al. (1968) the presence of *Laevigatosporites sp.* indicate a swampy fresh water or brackish water environment. The presence of mangrove member e.g *Spinizonocolpites sp.* of the humid tropics in the assemblage is significant as it suggest marine influx in the basin (Herngreen, 1998; Schrank, 1987). The occurrence of a few grains of *Polycolpites sp.* in the assemblage indicate fresh water influence at the time of deposition and thus it collectively indicate deltaic to shallow marine depositional environment.

It is interesting to note that the presence of pollen grains of Palmae (*Palmaepollenites sp.*) in the assemblage and also recorded earlier by Venkatachala & Mathur (1976) testifies to the fact that the basin of deposition was having some sort of coastal communication and the Palmae Province suggests a hot tropical to subtropical climate and the assemblages are interpreted as indicative of a warm and humid climate (Herngreen, 1998). The presence of spores of Schizaceae, Polypodiiceae and Cyatheaceae in the assemblage indicates that a subtropical climate prevailed at the time of

deposition of the Eocene sediments of Moran area. According to literatures, *spinizonocolpites* flourished in back mangrove in coastal areas and with the withdrawal of marine waters, genera like *florschuetzia* flourished. The presence of dinocysts i.e, *Adnatosphaeridium multispinosum* indicates warm shallow marine environment. The presence of microthyriaceous fruiting bodies like *Phragmothyrites* and other fungal spores are typical epiphyllous fungi and their occurrence in the present assemblage indicates the existence of a terrestrial plant ecosystem and represent a warm and humid climate with heavy rainfall.

Conclusion

From the present investigation which confines to Moran oilfield, it maybe concluded that:

1. The Palaeocene-Eocene palynofloral assemblage from the Moran oilfield consists of pteridophytic spores, angiosperm pollens, fungal spores and foraminifers.

2. On the basis of affinity with the modern families, it is suggested that a warm humid tropical climate may have prevailed during the sedimentation of the oil bearing sediments in Moran area.

3. The composition of the palynological assemblage suggests that the sediments were deposited under a fluctuating energy of deltaic to shallow marine water environment.

Acknowledgement

The author would like to thank Dr. Mrs. Kalpana Deka Kalita, Professor, Department of Applied Geology, Dibrugarh University, Dr. G. B. Gilfellon, Chief Geologist Oil India Limited and Mr. N. K. Borah, Senior Palynologist, RGL Sivasagar, ONGC and his colleagues, Palynology Lab, ONGC for their constant support.

References

Atta-Peters, D. and Salami, M. B. (2004). Late Cretaceous To Early Tertiary Pollen Grains From Offshore Tano Basin, Southwestern Ghana. *Revista Española de Micropaleontología*. **36(3)**: 451-465.

Baksi, S. K. and Venkatachala, B. S. (1970). Meyeripollis, a new genus from the Tertiary sediments of Assam. *Journ. Geol. Soc. India*. **11(1)**; 81-83.

Biswas, B. (1962). Stratigraphy of the Mahadeo, Langpar, Cherra and Tura formations, Assam, India. *Bull. geol. min. metall. Soc. India*. **25**: 1-48.

Clarke, R. T. and Frederiksen, N. O. (1968). Some new sporomorphs from the Upper Tertiary of Nigeria: Grana, **8**: 210-223.

Couper, R. A. (1953). Upper Mesozoic and Cainozoic spores and pollen grains from New Zealand. *Bull. N. Z. Geol. Surv. Palaeontol*. 22:1-77.

Cowie, J. W. and Basset, M. G. (1989). Global Stratigraphic Chart. Bureau of International Commission on Stratigraphy.

Edwards, W. N. (1922). An Eocene Microthyriaceous fungus from mull, Scotland: With plate VIII. *Transactions of the British Mycological Society*. **8(1-2)**: 66-72.

Germeraad, J. H. Hopping, C. A. and Muller, J. (1968). Palynology of tertiary Sediments from tropical areas. *Review of Palaeobotany and Palynology*. **6**: 189-348.

Germeraad, J. H.. Hopping, C. A. and Muller, J. (1968). *Review Paleobotany and Palynology*. **6**; 189-348.

Hammen, T. van der (1956a). A palynological systematic nomenclature. *Bol Geol.* **4**: 2-3, Bogotá.

Hammen, T. van der (1956b). Description of some genera and species of fossil pollen and spores. *Bol. Geol*. **4**: 2-3, Bogotá.

Herngreen, G. F. W. (1998). Cretaceous sporomorph provinces and events in the equatorial region. *Zentralblatt fur Geologie und Paläontolgie, 1. 1996 (11/12).* 1313 - 1323.

Kar, R. K., Handique, G. K., Kalita, C. K., Mandal, J., Sarkar, S., Kumar, M. and Gupta, A. (1994): Palynostratigraphical studies on subsurface Tertiary sediments in Upper Assam Basin, India. *The Palaeobotanist*. **42(2)**; 1 83- 198.

Mandaokar, B. D. and Mukherjee, D. (2012). *International Journal of Geology, Earth and Environmental Sciences*. September – December. **2(3)**: 157-175.

Muller, J. (1968). Palynology of the Pedawan and Plateau Sandstone formations (Cretaceous-

ISSN 2348-0637

Eocene) in Sarawak, Malaysia. *Micropaleontology*. **14**: 1-37.

Naidu, B. D. and Panda, B. K. (1997). Regional source rock mapping in upper Assam Shelf, in Proceedings of the Second International Petroleum Conference and Exhibition, PETROTECH-97: New Delhi. **1**: 350–364.

New Zealand fossil spores and pollen: An illustrated catalogue, 1933 Laevigatosporites vulgaris (Ibrahim) Ibrahim. pl. 2, fig. 16. 39.

New Zealand fossil spores and pollen: An illustrated catalogue, 1932 Sporonites vulgaris Ibrahim in Potonie *et al*. pl. 15, fig. 16. 448.

Polypodiisporites Potonié 1934 ex Potonié 1958 View on spore nomenclature. Geol. Mag. 95. 491-496.

Potonie, R., Thomson, P. W. and Thiergart, F. (1950). 2ur Nomenclature und Klassifikationder neogenen Sporomorphae (Pollen sporen). *Ceol. lb*. **65**: 35-70.

Rull, V. (1997). Sequence analysis of Western Venezuelan Cretaceous to Eocene sediments using palynology–Chrono-paleoenvironmental and paleo vegetational approaches. *Palynology*. **21**: 79-70.

Sah, S. C. D. & Dutta, S. K. (1966). Palynostratigraphy of the sedimentary formations of Assam-1. Stratigraphical position of the Cherra Formation. *Palaeobotanist*. **15 (1-2)**: 72-86.

Sah, S. C. D. and Dutta, S. K. (1967). Palynostratigraphy of the Tertiary sedimentary formations of Assam: 2. Stratigraphic significance of spores and pollen in the Tertiary succession of Assam. *The Palaeobotanist.* **16(2)**: 177 -195.

Sah, S. C. D. and Kar, R. K. (1969). Pteridophytic spores from the Laki Series of Kutch, Gujarat, India. *J. Sen. Mem.* Vol. Calcutta. 109–112.

Sah, S. C. D., Singh, R. Y. and Singh, H. P. (1980). Palynological zonation of the Tipam Group in Naharkatiya area of Upper Assam. *IV Int. Palynol. Conf., Lucknow ('1976-1977).* **2**: 635-642.

Schrank, E. (1987). Paleozoic and Mesozoic palynomorphs from northeast Africa (Egypt and Sudan) with special reference to late Cretaceous pollen and dinoflagellates. *Berliner Geowissenschaftliche Abhandlungen Reihe A.* **75(1)**: 249-310.

Singh, R. Y. and Tewari, B. S. (1979): A note on the palynostratigraphy of the Tertiary sediments of Upper Assam. *Bull. Ind. Geol. Assoc*. **12(2)**: l5l-159.

Van der Hammen, T. and Wymstra, T. A. (1964). A palynological study on the Tertiary and Upper Cretaceous of British Guiana. *Mededelingen Rijks Geologische Dienst*. **30**: 183-241.

Van Hoeken-Klinkenberg, P. M. J. (1964). A palynological investigation of some Upper Cretaceous sediments in Nigeria. *Pollen et Spore*. **6(1)**: 209-231.

Van der Hammen, T. and Garcia de Mutis, C. (1965). The Paleocene pollen flora of Colombia. MededelingenRijksGeologischeDienst. **35**: 105-116.

Venkatachala, B. S. and Kar, R. K. (1969). Palynology of the Tertiary sediments of Kutch-1. Spores and pollen from bore-hole no. 14. *Palaeobotanist*, **17 (2)**: 157-178.

Wandrey, C. J. Sylhet- Kopili/Barail-Tipam Composite Total Petroleum System, Assam Geologic Province, India. U.S. Geological Survey Bulletin 2208-D.

Williams G. L. and Downie, C. (1966). Further Dinoflagellates cysts from the London Clay. *Bull. Brit. Musc. Nat. Hist. (Geol.)*, Supplement. **3**: 215-235.

TRADITIONAL KNOWLEDGE OF ZOOTHERAPEUTIC USE AMONG THE ANGAMI TRIBES OF NAGALAND, INDIA

Reviewed

*Vethselo Doulo, Dziesevituo Angami and Kerheingunuo Shüya
Department of Zoology, Kohima Science College, Jotsoma-797002, Nagaland, India
*e-mail: vdoulo4@gmail.com

Abstract: Zootherapeutic use of different animals as whole or body part or by product like blood, urine, bones, organ, honey, skin ,quills, intestine, legs, etc., for the treatment of different kind of ailments including tuberculosis, malaria, asthma, jaundice, blood cancer, stomach disorder, whooping cough, rheumatism, typhoid, diabetics, ear ache, fractured bones, anaemia, etc. among the Angami tribes of Kohima district, Nagaland has been discussed. 45 species of animals were listed (15 invertebrates and 30 vertebrates), which are being used for treating about 38 ailments.

Key words: Zootherapeutic Traditional Knowledge. Angami tribes. Nagaland.

Introduction

Throughout human history, and in practically every human culture which presents a structured medical system, animals have been used as medicinal resources for the treatment and relieve of a wide variety of human health challenges (Costa-Neto, 2005). The use of animals for medicinal purposes is part of a body of traditional knowledge which is increasingly becoming more relevant to discussions on conservation biology, public health policies, sustainable management of natural resources, biological prospection, and patents (Alves and Rosa, 2005). There is a delicate interrelationship between the forest ecosystem, its inherent biodiversity and traditions culture of tribes. Indigenous people, their communities and other local communities have a vital role in environmental management and development because of their knowledge and traditional practices. States should recognize and support their identity, culture and interests and enable their effective participation in the achievement of sustainable development. The traditional knowledge and resource management practices of the indigenous people should be applied in modern development strategies. Hence the knowledge of medicinal or nutritive quality of all animal species becomes the need of the hour (Holennavar, 2015). There are only a few reports available from the region about the use of animals in traditional medicine. Reports on Naga traditional knowledge for the treatment and relieve of various health challenges using animals and animal derived products have been reported by workers such as Kakati and Doulo (2002), Jamir and Lal (2005), Kakati, Bendang and Doulo (2006).

In the present study, an attempt has been made to document this vanishing knowledge of the traditional medicinal properties of animals commonly used by the Angami Nagas. Study of precise status of these animal species in the wild needs to be ascertained, followed by sustainable exploitation of the same for their traditional use in medicine. Traditional knowledge base is fast eroding with the younger generation and therefore strategic plans should be devised to preserve this knowledge for generations to come.

Methods

The study was carried out in various villages of Kohima district. According to the 2011 census Kohima district has a population of 2, 67,988. For the purpose of this study, information was gathered from the Angami community. The Angamis are a major Naga ethnic group native to the state of Nagaland in North East India settled in Kohima district. Information were obtained through field survey by combination of semi-structured interview and open-ended interviews with selected people (informants) to collect information about traditional knowledge regarding use of animals and their products. The selection of informants was based on their recognisation as experts and knowledgeable members concerning folk medicine. The informants were asked to provide the local name of the animal used as remedy, parts used as medicine, conditions treated with the remedy, methods of preparation and administration, whether the animal parts were

ISSN 2348-0637

administered singly or in combination with other ingredients, restrictions of use, adverse effects linked to the use, use of live or dead animals, how animals were obtained, storage conditions, collection sites, gear used to collect the animals, efficacy of the remedies, reliance on animal-based remedies. Informants were also asked the modes of preparation of remedies & how the medicine can be therapeutically efficient in terms of right ingredients and the proper dose. Vernacular names of species were recorded as cited during interviews.

Result and Discussion

Table 1 and 2 summarizes the scientific names of the medicinally used invertebrates and vertebrates, their vernacular names, the part(s) of the animal used, the diseases or ailments the animal derived medicines are thought to be effective for, and the ways the treatments are carried out.

In the present study, 45 species of animals were listed (15 invertebrates and 30 vertebrates), which are being used for treating about 38 ailments. These animals are used as whole or body part or by product like blood, urine, bones, organ, honey, skin ,quills, intestine, legs, etc., for the treatment of different kind of ailments including tuberculosis, malaria, asthma, jaundice, blood cancer, stomach disorder, whooping cough, rheumatism, typhoid, diabetics, ear ache, fractured bones, anaemia, etc. Out of the 45 recorded species, the use of mammals and their parts was highest, constituting about(40%), followed by arthropods (24%), aves (11%), reptiles (9%), annelids (5%), mollusk (5%), pisces (4%) and amphibians (2%). In similar studies carried out, mammals were also recorded the highest use as part of local folk medicines (Kakati, Ao and Doulo, 2006), (Negi and Palyal, 2007), (Das, 2015), (Borah and Prasad, 2016), while in some cases largest numbers of medicinal species used in traditional practice was found to be reptiles followed by mammals (Alves *et. al*, 2010).

Local community's knowledge in the use of animal resources is very important for conservation efforts directed at protecting the wildlife. Folk medicine practitioners tend to have extensive knowledge of the ecology and use of the local flora and fauna. However, as many local cultures are increasingly threatened, the need to document their knowledge of animals for medicinal and other uses becomes more urgent. Since, very little is known about the animal species being used for medicinal and to some extent, in rituals, it is important that such information be collected, collated and measures be taken to provide a framework for the conservation of the same. There are many rare and endangered animal species, which are being exploited, chiefly for their medicinal uses and at the same time, little are known to the outside world (Negi and Palyal, 2007). Knowledge about animals that were used for remedial purposes in the past and are still used as such to the present day is part of traditional and ethnic medicine. The knowledge is relevant to science and human society. Its importance lies in fostering better understanding of this phenomenon from historical, economic, sociological, anthropological, and environmental viewpoints throughout bygone centuries (Lev, 2003). The knowledge on the use of different animals in traditional medicine by different ethnic communities is generally passed orally from one generation to another generation and this knowledge is sometimes lost with the death of the elderly knowledgeable person. Nowadays, traditional knowledge system is fast eroding due to urbanization. So, it is vital to study and document the ethnobiological information regarding the therapeutic use of different animals in traditional medicine among different ethnic communities before the traditional cultures are completely lost (Trivedi, 2002). The findings from the present study reveal a rich traditional knowledge of indigenous people of Kohima district, Nagaland regarding the use of animals and animal derived products used in traditional healthcare system. It is suggested that this kind of traditional knowledge on medicinal use of faunistic resources should be conserved and strategies should be devised to preserve and tap this rich knowledge in a more sustainable way for the benefit of mankind.

Table 1: List of invertebrate animals and animal parts medicinally used, their vernacular names, the diseases or ailments and the ways the treatments are carried out.

Sl. no	Animal Group	Zoological Name	Common Name	Vernacular Name	Part used	Treated disease	Prescription
1	Annelida	*Eisenia fetida*	Redworm	Doshü	Whole body	Antidote for snake bite, cures pneumonia, eye related problems.	Body is crushed and locally applied. Body is orally administered (raw red worm).
2	Annelida	*Hirudo medicinalis*	Leech	Rüva		Blood purification	Leeches are used to suck impure blood from the body.
3	Arthropoda	*Myrmeleon immaculatus*	Ant lion	Puchürü	Whole body	Wart, wounds, removes thorns from skin.	Body is freshly crushed and locally applied over infected area or wound. Helps removal of thorns from skin.
4	Arthropoda	*Apis indica Apis spp*	Bee	Mepfhi	Honey	Deep wound, ulcer, antidote for snake bite, cough.	Honey is locally applied over the wound, ulcer of mouth; honey is locally applied on surrounding area of snake bite. It is taken orally to cure cough.
5	Arthropoda	*Prionoxystus Robiniae*	Carpenter worm	Loungu	Whole body	Rheumatism, muscle cramp, nerve problem.	Boil the worm and apply the water on body. Bathe with the water of worm. Cut open and locally apply.
6	Arthropoda	*Cancer pararus*	Crab	Seguo	Whole body	Urethritis, jaundice, cough, malaria, earache.	For urethritis -whole body is crushed, dissolved in water and orally administered. For malaria and cough- body is cooked and the extracted soup is orally administered.. For earache- body is freshly crushed and 2 drops of the extracted liquid is applied to the ear.
7	Arthropoda	*Scylla serrata*	Black crab	Seguo keteiu	Whole body	Jaundice	Freshly crushed raw black crab juice is orally administered. Good for liver and cures jaundice
8	Arthropoda	*Pseudocantho termes*	Termite	Shülhe	Whole body	Asthma	Roast and orally administered. Protein rich source.

ISSN 2348-0637

9	Arthropoda	*Pediculus sp.*	Wood louse	Lolu	Whole body	Diabetes, bone TB	Boil and soup is orally administered.
10	Arthropoda	*Achaeta*	Cricket	Pfüteo	Whole body	Dysentery	Body is roasted and orally administered.
11	Arthropoda	*Mantis sp.*	Mantis		Whole body	Urinary disorder	Roasted mantis is orally administered.
12	Arthropoda	*Simulium*	Black fly larva	Sonhe	Whole body	Body aches, nerve problem, rheumatism, improves eyesight.	Whole body is cooked and orally administered. Improve eyesight and strengthens weak body.
13	Arthropoda	*Solenopsis geminata*	Red ants	Tsorie	Whole body	Anaemia	Whole body is orally administered. Iron rich source.
14	Mollusa	*Pila globosa*	Snail	Noula	Flesh	Asthma, tuberculosis, stomach disorder, eye problem, wounds and fractured bones.	Flesh is orally administered after cooking as a relief measure for asthma, stomach disorder, eye related problems, and tuberculosis. Rapid healing of wounds and fractured bones. Good for nerves.
15	Mollusca	*Slug*	Garden slug	Noula mhie	Whole body		Slug is eaten for rapid healing of fractured bones

Table 2: List of vertebrate animals and animal parts medicinally used, their vernacular names, the diseases or ailments and the ways the treatments are carried out.

Sl. no	Animal Group	Zoological Name	Common Name	Vernacular name	Part used	Treated disease	prescription
1	Pisces	*Monopterus albus*	Eel	Tinyhü khuo	Blood, whole body	Anaemia, asthma	Fresh blood is orally administered to cure general weakness and to relieve asthma and anaemia.
2	Pisces	*Monopterus cuchia*	Eel	Tinyhü khuo	Blood, whole body	Low blood pressure	Fresh blood is orally administered to cure asthma and anemia, mineral rich source.
3	Amphibian	*Limnonectes limnochari*	Frog	Gorünuo	Skin, flesh, whol	Skin burn, wound, tuberculosis	Skin of frog is applied on burn wounds for rapid healing of

		s, Rana tigrina.			e body		wounds. Flesh of frog is cooked and consumed for rapid healing of wounds. Whole body of frog, *Limnonectes limnocharis* is consumed (alive) to cure tuberculosis.
4	Reptiles	*Mabuya sp.*	Sand lizard	Teilei	Whole body	Whooping cough	Roast the body with warm ash and orally administer.
5	Reptiles	*Python reticulates*	Python	Cienyhü.	Gall bladder, fats	Wounds, rheumatism, body ache, fractured bones and sprained ankle	One grain size of dried gall bladder of python added to one cup of water is a powerful tonic, heals old wound. Fats of python is locally applied to relieve body ache, rheumatism, fats is massaged on fractured bones and sprained ankle for rapid healing.
6	Reptiles	*Hydrophis sp.*	Snake	Tinyhü, dzünyhü	Liver, fats	Diarrhea, dysentery, malaria, typhoid, wounds	A little portion of the liver is orally administered along with water. Fats are locally applied over the wounds.
7	Reptiles	*Calotes sp.*	Lizard	Sokru	Whole body	Pneumonia	The body is roasted and orally administered.
8	Aves	*Aquila sp.*	Eagle	Kekrüra rümou	Feather, flesh	Wound, spleen enlargement, liver enlargement, herpes zoaster	Feather is locally applied over the wound, flesh is cooked and orally administered
9	Aves	Family picidae	Wood pecker	Siedou	Flesh	Gall bladder problems	Orally administered to treat gall bladder problems.
10	Aves	*Upupa epops*	Hoopoe	Kijüneru	Flesh	Gall stone	Flesh is cooked and orally administered.
11	Aves	*Gallus sonnerati*	Jungle fowl	Terhei	Flesh, feet claws	Cough	Roast the flesh and administer orally for breathing problems
12	Aves	*Gallus sp.*	Hen	Vütho, thevü	Gizzard, gall bladder	Stones in body, fever and cough	Dried gizzard is orally administered to remove stones in the body. Gall bladder is cooked

ISSN 2348-0637

							and administered orally to treat fever and cough.
13	Mammal	*Sus crisatus*	Wild boar	Menyi	Flesh, gall bladder	Stomach pain, cough	Flesh is cooked and orally administered.
14	Mammal	*Gazelle bennettii*	Antelope	Thelou	Bone marrow	Nerve problems	Apply bone marrow locally on fractured bones, cure nerve problems.
15	Mammal	*Selenarctos sp.*	Bear	Thega	Gall bladder , fats	Cough, asthma, malaria , fever, typhoid, stomach ache and fractured bones	Dried gall bladder is administered orally to cure cough, whooping cough, fever, typhoid, asthma, malaria, stomach ache and remove stones in the body. Apply fats locally on fractured bones for rapid healing
16	Mammal	*Cervulus sp.*	Barking deer	Chüzhie	Bone marrow	Fractured bones	Massage the bone marrow over the fractured bones for rapid healing
17	Mammal	*Maschus sp.*	Musk deer	Chüzhie	Urine, foetus, womb, foetus leg, hoof	Ear infection, ear ache, labour pain, dysentery, stomach ache	Urine is used as ear drops for healing ear infections. Foetus of deer is dried, boiled and the soup is orally administered to help with labour pain. Womb is orally administered to cure dysentery and nausea. Foetus leg is boiled and orally administered to help in childbirth. Foetus leg is also used to knock child's knees to make the child walk. Hoof scratched to make soup and orally administered.
18	Mammal	*Pteromys sp.*	Flying squirrel		Flesh, urine, intestine,	Cough, constipation	Flesh is cooked and orally administered. Urine is orally administered for constipation. Intestine is eaten as an antidote for general poisoning.

19	Mammal	*Entomias sp.*	Chipmunk	Liepruonuo	Whole body, gall bladder	Cough, tuberculosis, pneumonia, gastric pain	Flesh is cooked and orally administered
20	Mammal	*Funambulus sp.*	Squirrel	Keli	Flesh	Cough	Flesh is cooked and administer orally
21	Mammal	*Lutrinae sp.*	Otter	Khuorha	Legs along with claws		Takes out fish bone lodged in throat. The claws are used to take out fishbone
22	Mammal	*Canis familiaris*	Dog	Tefü	Gall bladder, flesh	Insomnia, tuberculosis, malaria, cough, jaundice, asthma	Flesh soup improves pre and post partum health. Gall bladder orally administered. Flesh is cooked and orally administered
23	Mammal	*Macaca sp.*	Monkey	Tepfi	Gall bladder, flesh	Cough, stomach disorder, general weakness.	Flesh is cooked and administer orally
24	Mammal	*Canis lupus*	Wolf	Socie	Urine	Ear infection	Urine is used as ear drops
25	Mammal	*Felix sp.*	Wild rat	Terha zu	Flesh	Cough , asthma, stomach pain	Flesh is cooked and orally administered
26	Mammal	*Canomys badius*	Bamboo rat	Zuru	Whole body	Diabetics, general weakness, eye problem	Flesh is cooked and orally administered. Improves eyesight, consuming it rejuvenates energy for old people
27	Mammal	*Talpa*	Mole rat	Thekha	Whole body	Blood cancer	Body is cooked and orally administered
28	Mammal	*Rattus sp.*	Rat	Khoshü	Flesh	Epilepsy	Flesh is cooked and administered orally
29	Mammal	*Myotis sp.*	Bat		Flesh	Sleep enuresis/ urinary incontinence/ bed wetting.	Flesh is roasted and administered orally.
30	Mammal	*Hystrix sp.*	Porcupine	Chiekru	Quill / spine , Stomach	Heart disease, wound, burnt skin, fever, gastric pain, malaria.	Quill of porcupine is used as anti tetanus and antiseptic. Roast/ burn the quills and the ash powder are mixed with water. This water is orally administered as an antiseptic and is used for curing heart

ISSN 2348-0637

							disease. Quill/ spine of porcupine are roasted and ash powder is locally applied on wound, burnt skin and cures septic wounds and cuts. The dried and powdered stomach is boiled and orally administered for curing gastric pain, fever and malaria.

References

Alves, R. R. N., Oliveira, M., Barboza, R. and Lopez, L. C. S. (2010). An ethnozoological survey of medicinal animals commercialized in the markets of Campina Grande, NE Brazil. *Human Ecology Review*. **17(1)**.

Alves, R. R. N. and Rosa, I. L. (2005). Why study the use of animal products in traditional medicines? *Journal of Ethnobiology and Ethnomedicine*. **1(5)**.

Alves, R. R. N., Oliveira, T. and Rosa, I. L. (2013). Wild Animals Used as Food Medicine in Brazil. Hindawi Publishing Corporation. *Evidence-Based Complementary and Alternative Medicine*. .

Borah, M. P. and Prasad, S. B. (2016). Ethnozoological remedial uses by the indigenous inhabitants in adjoining areas of the Pobitora Wildlife Sanctuary, Assam, India. *International Journal of Pharmacy and Pharmaceutical Sciences*. ISSN- 0975-1491.

Costa-Neto, E. M. (2005). Animal-based medicines: biological prospection and the sustainable use of zootherapeutic resources. *Anais daAcademia Brasileira de Ciências (Annals of the Brazilian Academy of Sciences)* ISSN 0001-3765. **77(1)**: 33-43.

Das, D. (2015). Ethnozoological practices among tribal inhabitants in Khowai district of Tripura, North-east India. *Journal of Global Biosciences*. **4(9)**: 3364-3372.

Holennavar, P. S. (2015). Use of animal and animal derived products as medicines by the inhabitants of villages in Athani Taluka of Belagavi District (Karnataka). *International Journal of Applied Research*. **1(12)**: 437-440.

Jamir, N. S. and Lal, P. (2005). Ethnozoological practices among Naga tribes. Indian *Journal of Traditional Knowledge*. **4(1)**: 100-104.

Kakati, L. N. and Doulo, V. (2002). Indigenous Knowledge System of Zootherapeutic Use by Chakhesang Tribe of Nagaland, India. *J. Hum. Ecol*. **13(6)**: 419-423.

Kakati, L. N., Ao, B. and Doulo, V. (2006). Indigenous Knowledge of Zootherapeutic Use of Vertebrate Origin by the Ao Tribe of Nagaland. *J. Hum. Ecol*. **19(3)**: 163-167.

Lev, E. (2003). Traditional healing with animals (zootherapy): medieval to present-day Levantine practice. *Journal of Ethnopharmacology*. **85**: 107–118.

Negi, C. S. and Palyal, V. S. (2007). Traditional Uses of Animal and Animal Products in Medicine and Rituals by the Shoka Tribes of District Pithoragarh, Uttaranchal, India. *Ethno-Med*. **1**(**1**): 47-54.

Trivedi, P. C. (2002). Ethnobotany: An overview. In Ethnobotany edited by: Trivedi PC. Jaipur: Aavishkar publisher, Vol. 1.

LEAF LITTER DECOMPOSITION IN A SUBTROPICAL VEGETATION UNDER KOHIMA DISTRICT, NAGALAND, INDIA

Reviewed

*Wenyitso Kapfo and **Neizo Puro
*Department of Botany, Kohima Science College, Jotsoma-797002, Nagaland, India
**Department of Botany, Nagaland University, Lumami- 798627, Nagaland, India
*e-mail: wenitso@gmail.com

Abstract: Leaf litter decomposition was measured in Pulie Badze Wildlife Sanctuary and Jotsoma Community Forest under Kohima District to find out whether its rate differs among different vegetation segments. It was determined that canopy species composition significantly affects the rates of litter decomposition. Two trends of decomposition were recognized whereby, mixed forest stands exhibited higher rate of decomposition than those sites which are dominated by sclerophyllous species such as oaks and *Rhododendron arboreum*.

Key words: Leaf litter, sanctuary, community forest, canopy, sclerophyllous.

Introduction

Litter decomposition represents one of the key biogeochemical processes in an ecosystem (Swift *et al.* 1979) to the extent that the nutrients released through litter decomposition accounts for 69-87% (Waring & Schlesinger 1985) and 70–90% (Vogt *et al.* 1986) of the total annual requirement of essential elements by forest plants. The proportion of nutrient release is accelerated by favourable environmental conditions due to enhancement of faunal and microbial activities (Swift *et al.* 1979). Disturbance in the form of moderate grazing treatment also enhances the rate of litter break- down (Shariff *et al.* 2012).

It is generally accepted that the quality of litter is the chief determinant for the rate of its decomposition under a given climate (Coûteaux *et al.* 1995; Aerts, 1997; Cadish & Giller, 1997; Dearden *et al.* 2006; Zhang *et al.* 2008) and between natural forests and plantations (Pandey *et al.* 2007).

In subtropical North East (N.E.) India, the rate of litter decomposition shows seasonality such that it is highest during the wet summer months and least in dry winter months (Devi & Yadava, 2006) and it is positively correlated to abiotic factors (Kumar *et al.* 2014), relative humidity and mean temperature (Pandey *et al.* 2007).

The rate is not constant during the course of litter break breakdown. In general, leaf litter exhibits a rapid initial loss leaving behind a mass that decomposes at a slower rate (Xu *et al.* 2004; Aponte *et al.* 2012). This trend is more pronounced in litter of deciduous species than that of evergreen species (Aponte *et al.* 2012) and more in typhoon-generated litter than normally senesced leaf litter (Xu *et al.* 2004).

Materials and Methods

The study area lies between 25° 35. 800' to 25° 40. 100' N latitudes and 94°01. 700' to 90° 05. 800' E longitudes, with an altitude range from 1600m m asl to about 2300m asl. Located on the South-West of Kohima town, it is contiguous with the second highest peak in Nagaland, namely Japfu, and phyto-geographically falls within Eastern Himalayas. The study area consists of two physically contiguous sites namely Pulie Badze Wildlife Sanctuary (PWLS) and Jotsoma Community Forest (JCF). Both of these are protected areas and are separated by a physical fencing, collectively covering an area of 50 sq. km.

Leaf litter decomposition was determined using the litter bag technique described by Swift & Anderson (1989). Litter bags of mesh size 1.2 mm were sewn from window screen nylon mesh to 10x10cm size. Freshly fallen leaf litter were collected from the forest floor. During collection, the leaf litter of various species were mixed in the proportion that approximated species composition of the site from which the litter was collected. They were then air-dried in mesh bags and weighed. Each litter bag was filled with pre-weighed air-dried leaf litter ranging from 8 to 10 gm. At the same time, sub-samples of the collected leaf litter were oven dried to determine the difference between air-dried and oven-dried weight.

Nine litter bags with pre-weighed air-dried leaf litter were placed on the surface of the

ISSN 2348-0637

forest floor at twenty different locations spread over four forest stands. Thus altogether 180 litter bags were used. Each of the nine litter bags per site was retrieved in 2-monthly interval during the first 12 months and 4-monthly interval during the remaining 12 months. The sampling interval was doubled during the second year partly because decomposition steadied to an almost constant rate following the first four months of observation (see figure A) and partly because sample collection was very restrictive due to difficult terrain and insurgency activity in the study area during the investigation. The 4-monthly interval data was converted into a 2-monthly representation by working out the average percentage loss in mass from the 13th to 24th month.

Thus, litter decomposition was measured as two-monthly rate and four-monthly rate. Hence, each of the twenty sites was visited nine times during the 24-month period, each time a litter bag was retrieved. In the laboratory, the litter bags were cleaned from the outside with a brush and water and the content was oven dried to constant weight at 105°C and its weight was recorded. The oven-dried weight thus obtained was subtracted from the initial weight (oven dried weight), and the remaining mass was recorded.

Sampling sites were decided through visual inspection of dominant canopy tree species composition and local topography assuming that these factors would influence litter decomposition. Hence the sampling was carried out on four categories of forest stands namely, JCF-North western slopes (JCF-NW), JCF-Hillock/Ridges (JCF-R), JCF-Mixed vegetation (JCF-M) and PWLS. Leaf litter decomposition was assessed for 24 months commencing from May 2013 and culminated in April 2015.

Results

In general, leaf litter decomposition exhibited a rapid initial rate for all sampling sites during the first four months (May-August), which decreased and remained roughly constant during the rest of the assessment period (20 months). This decomposition behaviour gives a reverse J-shaped curve (figure A) for all forest stands. Nonetheless, by the degree of steepness of the curves, two different trends of leaf litter decomposition emerged from amongst the four stands. The first trend, comprising JCF-R and JCF-NW (Blue and Red lines in figure A and B) was distinguished by slower rate of decomposition where the initial rate ranged from 16.64-20.96% mass loss which levelled off after the fourth month to a steady rate of about 5% mass loss against the interval of time specified in the methodology till the 24th month (figure A). In terms of remaining mass (figure B), >30% of the initial litter mass remained undecomposed at the end of the 24th month. Conversely, the second trend represented by JCF-M and PWLS (green and purple lines in figure A and B) showed a comparatively higher initial rate of decomposition, and thus steeper curves, with an initial rate of up to 43% mass loss, while <10% mass remained after the 24th month. Details of litter decomposition at the four forest stands are presented in table 1.

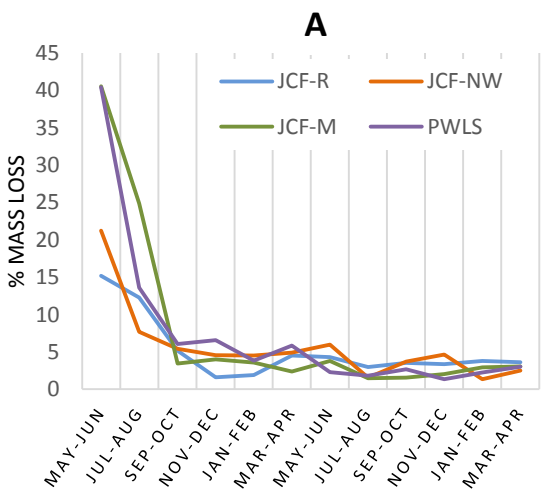

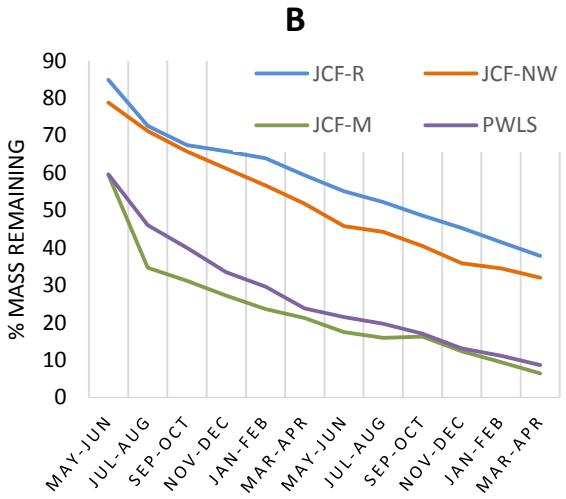

Figure **A**: Rate (in %) of leaf litter decomposition in two-monthly duration (May 2013 to April 2015)
B: Percent of remaining mass of leaf litter during the same time intervals.

Table 1: Litter decomposition during 2013-2015 in four forest stands with sampling site numbers, namely JCF-R (1-4), JCF-NW (5-10), JCF-M (11-14) and PWLS (15-20). * samples damaged or lost in the field.

Veg. Stand	Sites	Initial weight (gm)		Final weight (gm) for 2-month intervals												% mass remaining
				2013				2014				2015				
		Air dried	Oven dried	May to Jun	Jul to Aug	Sep to Oct	Nov to Dec	Jan to Feb	Mar To Apr	May to Jun	Jul to Aug	Sep to Oct	Nov to Dec	Jan to Feb	Mar To Apr	
JCF-R	1	11.03	9.76	8.29												84.93
		13.55	11.99		8.64											72.05
		11.27	9.97			6.74										67.58
		13.72	12.14				7.90									65.80
		10.69	9.76					6.37								65.26
		11.80	10.44						6.22							59.56
		10.00	8.85							5.12						57.85
		10.00	8.85								5.08					57.40
		10.00	8.85									5.04				56.95
		10.00	8.85										5.00			56.50
		10.00	8.85											4.70		53.11
		10.00	8.85												4.40	49.72
	2	10.00	8.50	7.31												86.00
		10.00	8.50		6.21											73.06
		10.00	8.50			6.02										70.82
		10.00	8.50				5.90									70.00
		10.00	8.50					5.48								64.47
		10.00	8.50						5.32							62.59
		10.00	8.50							4.43						52.06
		10.00	8.50								4.15					48.82
		10.00	8.50									3.88				45.59
		10.00	8.50										3.60			42.35
		10.00	8.50											3.40		40.00
		10.00	8.50												3.20	37.65
	3	10.00	8.85	7.67												86.67
		10.00	8.85		6.52											73.67
		10.00	8.85			6.08										68.70
		10.00	8.85				6.00									67.80
		10.00	8.85					5.95								67.23
		10.00	8.85						5.92							66.89
		10.00	8.85							5.55						62.71
		10.00	8.85								5.00					56.50
		10.00	8.85									4.45				50.28

ISSN 2348-0637

		10.00	8.85										3.90			44.75
		10.00	8.85											3.58		40.40
		10.00	8.85												3.25	36.72
	4	10.00	8.85	7.23												81.69
		10.00	8.85		6.32											71.41
		10.00	8.85			5.53										62.49
		10.00	8.85				5.20									59.55
		10.00	8.85					5.18								58.53
		10.00	8.85						4.29							48.47
		10.00	8.85							4.22						47.68
		10.00	8.85								4.05					45.76
		10.00	8.85									3.68				41.53
		10.00	8.85										3.30			37.29
		10.00	8.85											2.85		32.20
		10.00	8.85												2.40	27.12
JCF-NW	**5**	10.00	8.85	6.86												77.51
		10.00	8.85		5.63											63.62
		10.00	8.85			5.52										62.37
		10.00	8.85				5.30									60.23
		10.00	8.85					4.53								51.19
		10.00	8.85						4.46							50.40
		10.00	8.85							4.44						50.17
		10.00	8.85								4.21					47.57
		10.00	8.85									3.46				39.04
		10.00	8.85										2.70			31.30
		10.00	8.85											2.49		28.08
		10.00	8.85												2.27	25.65
	6	10.54	9.33	8.24												88.34
		10.00	8.85		7.24											81.81
		10.00	8.85			6.68										75.48
		13.20	11.68				7.40									63.86
		14.08	12.46					6.77								54.33
		14.03	12.42						5.10							41.07
		16.31	14.43							5.28						36.59
		16.31	14.43								5.20					36.03
		11.38	10.07									4.30				42.70
		11.38	10.07										3.40			34.16
		10.00	8.85											3.03		34.18
		10.00	8.85												2.65	29.94
	7	14.72	13.03	8.22												63.10
		12.53	11.09		6.96											62.76
		17.32	15.33			8.68										56.63
		11.45	10.13				5.60									55.66
		12.43	11.00					5.41								49.18
		16.16	14.30						6.53							45.66

		11.07	9.80							3.21					32.76
		11.07	9.80								3.20				32.66
		14.61	12.93									3.62			28.00
		14.61	12.93										4.04		31.25
		12.84	11.36											3.77	33.19
		12.84	11.36												3.50	30.80
	8	12.84	10.91	9.23												84.57
		10.60	9.01		5.99											66.48
		11.75	9.99			5.41										54.17
		11.75	9.99				5.20									52.37
		12.19	10.36					5.63								54.34
		9.09	7.73						4.05							52.42
		11.87	10.09							4.76						47.18
		11.87	10.09								4.66					46.19
		12.45	10.58									4.63				43.76
		12.45	10.58										4.60			44.22
		13.14	11.17											4.40		39.39
		13.14	11.17												4.20	37.60
	9	10.00	8.85	7.26												82.03
		13.69	12.12		9.88											81.55
		11.54	10.21			8.10										79.31
		12.77	11.45				8.56									74.76
		11.56	10.23					7.42								72.53
		11.71	10.36						6.92							66.77
		10.00	9.85							6.76						68.63
		10.00	9.85								6.33					64.26
		10.66	9.43									5.08				53.82
		10.66	9.43										3.82			40.49
		10.00	8.85											3.56		40.23
		10.00	8.85												3.30	37.29
	10	10.00	8.85	6.83												77.18
		10.00	8.85		6.24											70.51
		10.00	8.85			5.86										66.21
		10.00	8.85				5.30									59.89
		10.00	8.85					5.15								58.19
		10.00	8.85						4.78							54.01
		10.00	8.85							3.46						39.10
		10.00	8.85								3.39					38.31

ISSN 2348-0637

		10.00	8.85									3.15				35.54
		10.00	8.85										2.90			33.45
		10.00	8.85											2.80		31.64
		10.00	8.85												2.70	30.51
JCF-M	11	10.00	8.75	5.69												65.03
		10.00	8.00		3.31											41.38
		20.00	16.00			6.17										38.56
		10.00	8.63				2.82									32.68
		20.00	16.00					4.50								28.13
		10.00	8.44						1.99							23.58
		20.00	16.00							3.10						19.38
		20.00	16.00								2.98					18.63
		10.00	8.32									1.47				17.67
		10.00	8.32										1.22			14.66
		10.00	8.00											0.72		9.00
		10.00	8.00												0.22	2.75
	12	15.26	12.97	7.31												56.36
		15.39	13.08		4.01											30.65
		12.10	10.29			2.93										28.49
		14.15	12.03				3.13									26.02
		12.36	11.80					3.05								25.85
		14.83	12.61						3.21							25.47
		10.00	8.50							1.44						16.94
		10.00	8.50								1.32					15.53
		10.00	8.50									1.20				14.12
		10.00	8.50										1.08			12.71
		10.00	8.50											0.94		11.06
		10.00	8.50												0.80	9.41
	13	10.00	8.50	4.59												54.00
		10.00	8.50		2.75											32.35
		10.00	8.50			2.24										26.35
		10.00	8.50				2.14									25.18
		10.00	8.50					2.04								24.00
		10.00	8.50						1.86							21.88
		10.00	8.50							1.75						20.53
		10.00	8.50								1.69					19.88
		10.00	8.50									1.64				19.24
		10.00	8.50										1.58			18.59
		10.00	8.50											1.24		14.59
		10.00	8.50												0.90	10.59
	14	10.00	7.50	4.68												62.40
		10.00	7.50		2.55											34.00
		10.00	7.50			2.34										31.20
		10.00	7.50				1.85									24.67

		10.00	7.50					1.22								16.27
		10.00	7.50						1.04							13.87
		10.00	7.50							0.96						12.73
		10.00	7.50								0.72					9.60
		10.00	7.50									0.49				6.47
		10.00	7.50										0.25			3.33
		10.00	7.50											0.23		3.00
		10.00	7.50												0.20	2.67
PWLS	**15**	10.90	8.50	4.02												47.29
		13.27	12.56		4.58											36.46
		11.87	10.60			3.55										33.49
		14.42	13.23				3.87									29.25
		10.00	8.50					2.53								29.76
		10.00	8.50						2.24							26.35
		10.00	8.40							1.96						23.33
		10.00	8.40								1.93					22.98
		12.04	11.00									2.13				19.32
		12.04	11.00										2.32			21.09
		10.64	9.50											1.91		20.11
		10.64	9.50												1.50	15.79
	16	10.00	8.50	6.02												70.82
		10.00	8.50		4.21											49.53
		10.00	8.50			4.12										48.47
		10.00	8.50				3.70									43.53
		10.00	8.50					3.35								39.41
		10.00	8.50						2.86							33.65
		10.00	8.50							2.90						34.12
		10.00	8.50								2.59					30.47
		10.00	8.50									2.28				26.82
		10.00	8.50										1.97			23.18
		10.00	8.50											1.59		18.65
		10.00	8.50												1.20	14.12
	17	10.00	7.50	4.37												58.27
		10.00	7.50		4.10											54.67
		10.00	7.50			3.25										43.33
		10.00	7.50				1.47									19.60
		10.00	7.50					1.13								15.07
		10.00	7.50						1.13							15.07
		10.00	7.50							1.12						14.93
		10.00	7.50								0.90					12.00
		10.00	7.50									0.68				9.07
		10.00	7.50										0.46			6.13
		10.00	7.50											0.33		4.40

ISSN 2348-0637

		10.00	7.50												0.20	2.67
	18	10.00	7.50	5.00												66.67
		10.00	7.50		4.15											55.33
		10.00	7.50			2.83										37.73
		10.00	7.50				2.74									36.53
		10.00	7.50					1.86								24.80
		10.00	7.50						1.28							17.07
		10.00	7.50							1.25						16.67
		10.00	7.50								1.12					14.93
		10.00	7.50									0.99				13.20
		10.00	7.50										0.86			11.47
		10.00	7.50											0.68		9.07
		10.00	7.50												0.50	6.67
	19	10.00	8.75	4.81												54.97
		10.00	8.75		3.70											42.29
		11.97	10.20			4.10										40.20
		10.42	8.65				3.40									39.31
		8.99	7.90					3.05								38.61
		10.00	8.75						2.56							29.26
		10.17	8.78							2.01						22.89
		10.17	8.78								1.84					20.96
		11.10	0.00									*				
		11.10	0.00										*			
		10.79	0.00											*		
		10.79	0.00												*	
	20	10.00	8.50	5.05												59.41
		10.00	8.50		3.20											37.65
		10.00	8.50			3.10										36.47
		10.00	8.50				2.73									32.12
		10.00	8.50					2.53								29.76
		10.00	8.50						1.79							21.06
		10.00	8.50							1.43						16.76
		10.00	8.50								1.41					16.59
		10.00	8.50									1.40				16.41
		10.00	8.50										1.38			16.24
		10.00	8.50											1.24		14.59
		10.00	8.85												1.10	12.43

Discussion

This finding in this work is in agreement with previous works in the N.E. India where leaf litter decomposition was correlated to seasonal temperature, rainfall and relative

humidity. Specifically, warm, moist and humid conditions are known to promote rapid rate of decomposition (Devi & Yadava 2006; Kumar *et al.* 2014; Pandey *et al.* 2007).

Further, the initial rate (the first four months) was significantly more rapid than the subsequent period. The differential rate during the course of decomposition observed here is similar to earlier observations (Xu *et al*. 2004; Aponte *et al.* 2012) which is attributable to leaching of readily soluble chemical constituents of leaf litter (Xu *et al.* 2004).

The high initial rate observed in this study might also have been accelerated by the season for commencement of decomposition measurement i.e. during moist and warm months which, along with nutrient availability, is associated with higher rate of decomposition (Jorgensen *et al*. 1975) as these factors encourage greater activity of decomposers (Swift *et al*. 1979). In addition, the leaf litter samples were mostly wind-generated, being collected after the windy season (April). Typhoon-generated leaves are known to break down at a faster rate as compared to naturally senesced leaves because of their immature state with respect to its anatomy and initial chemical concentrations (Schlesinger 1985; Gallardo & Merino 1993). Therefore, a combination of the above factors has likely contributed to the observed rapid initial rate of decomposition.

The two trends of litter breakdown in the study area may be attributed to difference in canopy species composition and local topography. JCF-R comprises ridges on hillocks, where the dominant species is *Rhododendron arboreum* and others including *Ternstroemia gymnanthera, Lyonia ovalifolia, Schima wallichii* and *Exbucklandia populanea*. JCF-NW is dominated by oaks, particularly *Lithocarpus recurvatus* and *Quercus lamellosa.* In general, the dominant canopy species in these two stands, which comprise one decomposition trend, are evergreen and have sclerophyllous leaves. In contrast, JCF-M and PWLS, which comprise the second trend, are dominated by non-sclerophyllous canopy species comprising *Sloanea sterculiaceae, Elaeocarpus lanceifolius, Nyssa javanica, Acer sterculiacea* and *Reevesia wallichii.* That the chief determining factor for differential rates of decomposition is the difference in canopy species composition is affirmed by earlier works (Perez-Harguindeguy *et al.* 2000; Hättenschwiler, 2005).

Conclusion

This work reports that, there are two trends of litter decomposition in the study area, and that this observed difference is a function of the difference in composition of tree canopy species. The influence of local topography on this phenomenon is indirect insofar as it, amongst other factors, determines tree species composition.

Acknowledgement:

The authors would like to acknowledge the government of Nagaland for having granted study leave (to the first author) and the Jotsoma Village Council for their cheerful cooperation to enable this work.

References

Aerts, R. (1997). Climate, leaf litter chemistry and leaf litter decomposition in terrestrial ecosystems: a triangular relationship. *Oikos*. **79**: 439-449.

Aponte, C., García, L. V. and Marañón, T. (2012). Tree Species Effect on Litter Decomposition and Nutrient Release in Mediterranean Oak Forests Changes Over Time. *Ecosystems*. **15(7)**: 1204-1218.

Cadish, G. and Giller, K. E. (1997). Driven by Nature: Plant Litter Quality and Decomposition. *Wallingford: CAB Int.* 432.

Coûteaux, M, M., Bottner, P. and Berg, B. (1995). Litter decomposition, climate and litter quality. *Trends Ecol. Evol.* **10**:63-66.

Dearden, F. M., Dehlin, H., Wardle, D. A. and Nilsson, M. C. (2006). Changes in the ratio of twig to foliage in litterfall with species composition and consequences for decomposition across a long term chronosequence. *Oikos*. **115(3)**: 453-462.

Devi, N. B. and Yadava, P. S. (2006). Seasonal dynamics in soil microbial biomass C, N and P in a mixed Oak forest ecosystem of Manipur, North east India. *Applied soil ecology*. **31**: 220-227.

Gallardo, A. and Merino, J. (1993). Leaf decomposition in two Mediterranean

ISSN 2348-0637

ecosystems of southwest Spain: influence of substrate quality. *Ecology*. **74**: 152-161.

Hättenschwiler, S. (2005). Effects of tree species diversity on litter quality and decomposition. In Scherer- Lorenzen, M., Kirner, C. and Schulze, E. D. (eds.). *Forest Diversity and Function: Temperate and Boreal Systems.* **176**:149- 64.

Jorgensen, J. R., Wells, C. G. and Metz, L. J. (1975). The nutrient cycle. Key to continuous forest production. *J. For.* **73**:400–403.

Kumar, S. and Tewari, L. M. (2014). Pattern of litter fall and litter decomposition in a *Quercus leucotrichophora* Camus forest in Kumaun Himalaya. *Academic Journals.* **6(1)**: 08-114.

Pandey, R. R., Sharma, G., Tripathi, S. K. and Singh, A. K. (2007). Litterfall, litter decomposition and nutrient dynamics in a subtropical natural oak forest and managed plantation in North Eastern India. *Forest Ecology and Management.* **240(1–3)**: 96–104.

Perez-Harguindeguy, N., Diaz, S., Cornelissen, J. H. C., Venramini, F., Cabido, M. and Castellanos, A. (2000). Chemistry and toughness predict leaf litter decomposition rates over a wide spectrum of functional types and taxa in central Argentina. *Plant Soil*. **218**:21-30.

Schlesinger, W. H. (1985). Decomposition of chaparral shrub foliage. *Ecology.* **66**: 1353-1359.

Shariff, A. R., Biondini, M. E. and Grygiel, C. E. (1994). Grazing Intensity Effects on Litter Decomposition and Soil Nitrogen Mineralization. *Journal of Range Management.* **47(6)**: 444-449.

Swift, M. J., Heal, O. W. and Anderson, J. M. (1979). Decomposition in Terrestrial Ecosystems. *University of California Press, Berkeley*. **5**: 167-219.

Waring, R. H. and Schlesinger, W. H. (1985). Forest Ecosystems: Concepts and Management. *Academic Press Inc., Orlando, San Diego.*

Xu, X., Hirata, E., Enoki, T. and Tokashiki, Y. (2004). Leaf Litter Decomposition and Nutrient Dynamics in a Subtropical Forest after Typhoon Disturbance. *Plant Ecology.* **173(2)**: 161-170.

Zhang, D., Hui, D., Luo, Y. and Zhou, G. (2008). Rates of litter decomposition in terrestrial ecosystems: global patterns and controlling patterns. *Journal of Plant Ecology.* **1(2)**: 85–93.

ISSN 2348-0637

INTERROGATIVES OF CHANG (NAGA) LANGUAGE (A COMPARATIVE STUDY)

Reviewed

Keduolhoulie Belho
Department of Tenyidie, Kohima College, Kohima-797001, Nagaland, India
e-mail: keduobelho@gmail.com

Abstract: There are 16 tribes of indigenous Naga Tribes in Nagaland. Nagas are defined by the diversity of languages; each tribe has their own language. The total population of Nagaland, according to 2011 census is 19, 80,602. There are 11 districts and each district administration was headed by a Deputy Commissioner of the district. Tuensang district is the home of Chang tribe. The language spoken by the Chang tribe is called Chang language.

Key Words: Wh-questions and Confirmation seeking questions.

Introduction

The data is collected from both primary and secondary. The primary data is collected from the native speaker of Konya village under Tuensang District. The informants were well educated, Shri Mosha is a social worker who is fully dedicated to the welfare of the society and Shri Chullen is a Government servant. At present, the Chang language is developing and the grammatical development is growing very fast because of many dedicated writers. This write up will be beneficial for the development of Chang language grammar for the upcoming researcher(s).

Wh-Questions were as follows:

1. no **ao** nyenkei
: *nɔ* *ʌ́ɔ* *njʌ̄nkʌ̄*
: your who name
'**What** is your name?'

Ans. ngeibü nyen **John**
: *ŋʌ̄bə* *njʌ̄n* *ʤɔn*
: my name john
'My name is John.'

2. waiyet ka **ai** lotkei
: *wʌijet* *kʌ* *ʌ́i* *lɔtkʌ̄*
: window through what came
'**What** came in through the window?'

Ans. **au** waiyet ka lotkei

: *ʌu* *wʌijet* *kʌ* *lɔtkʌ̄*
: bird window through came
'The bird came in through the window.'

3. nyi **ai** hapbei
: *nji* *ʌ́i* *hʌpbʌ̄*
: you what see
'What did you see?'

Ans. ngei **au** hapbei
: *ŋʌ̄* *ʌ́u* *hʌpbʌ̄*
: I bird saw
'I saw a bird.'

4. no **lanei** kida
: *nu* *lʌnʌ̄* *kidʌ̀*
: you where live
'Where do you live?'

Ans. ngo **kohima** -a kida
: *ŋɔ̀* *kɔhimʌ* - *ʌ* *kidʌ̀*
: I kohima in live
'I live in Kohima.'

5. no chemto **aijiha** ngaila
: *nu* *tʃʌ̄mtɔ* *ʌiʤiʌ* *ŋʌilʌ*
: you home when going
'**When** are you going home?'(time)

Ans. ngo chemtou **chasem jih süma** gailabü
: *ŋɔ* *tʃʌ̄mtɔ* *tʃʌsʌ̄m* *ʤiʔ* *səmʌ̄* *ŋʌilʌbə*
: I home evening time three going back
'I am going home at three o'clock' (time)

6. no chemto **laochalou-a** ngaila
: *nu* *tʃemtɔ* *lʌɔtʃʌlu-ʌ* *ŋʌilʌ*
: you home when (day) going
'**When** are you going home?' (day)

Ans. ngo chemto **chapün** ngailabü

ISSN 2348-0637

: *ŋɔ tʃemtɔ tʃʌpəŋ ŋʌilʌbə*
: I home Sunday going back
'I am going home on Monday'

7. no delhi tou **aila** hauda
: *nu delhi tɔu ʌilʌ hʌudʌ*
: you delhi to why going
'**Why** are you going to Delhi?'

Ans. ngo delhi tou lewala shanga hauda
: *ŋɔ delhi tɔu lewʌlʌ ʃʌŋʌ hʌudʌ*
: I delhi to study for going
'I am going to Delhi for my study.'

8. hao **ao** yingkei
: *hʌɔ ʌɔ jiŋkʌi*
: he who CASE
'Who is he?'
Ans. hao **John** yingkei
: *hʌɔ ʤɔn jiŋkʌi*
: he john CASE
'He is John.'

9. sao **ao** yingkei
: *sʌɔ ʌɔ jiŋkʌi*
: she who CASE
'Whois she?'

Ans. sao **Mary** yingkei
: *sʌɔ meʌi jiŋkʌi*
: she mary CASE
'She is Mary.'

10. haosi **ao** yingkei
: *hʌɔsi ʌɔ jiŋkʌi*
: they(two) who CASE
'Who are they?'

11. haoen **ao** yingkei
: *hʌɔwen ʌɔ jiŋkʌi*
: they (plural) who CASE
'Who are they?'

12. no **ailai** ki
: *nɔ ʌilʌi ki*
: you how CASE
'How are you?'

Ans. ngo **maisho** kia
: *ŋɔ mʌiʃɔ kiʌ*
: I fine have
'I am fine.'

13. nyi ho **ailai** kümbei
: *nji hɔ ʌilʌi kʌmbʌi*
: you this how make
'**How** did you make this?'

Ans. ngei ho **küthangbouei thuiyuko** kümbei
: *ŋʌi hɔ kəthʌŋbuʌi thuijukɔ kʌmbʌi*
: I this my friend help made
'I made this with the help of my friend.'

14. nyi **lading** / **latütbü** hapbei
: *nji lʌdiŋ / lʌtətbə hʌpbʌi*
: you how much get
'How much did you get?' (quantity)

Ans. ngei **hajuche** hapbei
: *ŋʌi hʌʤutʃe hʌpbʌi*
: I this much got
'I've got this much.'

15. nyi **lajuche** hapbei
: *nji lʌʤutʃe hʌpbʌi*
: you how many got
'**How** much did you get?' (number)

Ans. ngei **pümnyi** hapbei
: *ŋi pəmnji hʌpbʌi*
: I two got
'I got two.'

16. lam **lalokche**
: *lʌm lʌlɔktʃe*
: way how long / far
'How long/far is the way?'

17. kaibü jaisina **laobou**
: *kʌibə ʤʌisinʌ lʌɔbʌu*
: your brother which
'Which one is your brother?'

Ans. **nashoubou lounshangbou** kho ngeibü jaisina yingkei
: *nʌʃɔubu lunʃʌŋbu khɔ ŋibə ʤʌisinʌ jiŋkʌi*
: young taller this mine brother CASE

'The taller boy / one is my brother.'

18. kaibü nousina **laobou**
: *kʌibə nɔusinʌ lʌɔbʌu*
: you rsister which
'Which one is your sister?'
19. kaibü pen pümnyi kho **laobou**
: *kʌibə pen pəmnji khɔ lʌɔbʌu*
: your pen two among which
'Which two were your pen?'

Ans: pen pümnyi kho ngeibü
: *pen pəmnji khɔ ŋʌibə*
: pen two these mine
' These two were my pen.'

20. kaibü pen shong **laobou**
: *kʌibə pen ʃɔŋ lʌɔbʌu*
: your pen plural mkr which
'Which were your pen?'

Ans: khübü kho ngeibü pen
: *khəbə khɔ ŋʌibə pen*
: these are my pen
'These are my pen.'

21. lai lamnyu ho tüktebü
: *lʌi lʌmnju hɔ tʌktebə*
: which way this right
'Which way is the right way' (Direction)

Ans: ho lamnyu ho tüktebü
: *hɔ lʌmnju hɔ tʌktebə*
: this way this right
'This is the right way.'

B. Yes / No questions:
1. no kün yoa loudala**o**
: *nu kʌn jɔʌ lʌudʌlʌɔ*
: you us with coming
'Are you coming with us?'

2. no delhi tou haula**o**
: *nu delhi tʌu hʌulʌɔ*
: you delhi to been
'Have you been to Delhi?'
3. nyi kainong jekla**o**
: *nji kʌnlɔŋ ʤeklʌɔ*
: you vehicle buy
'Did you buy a car?'

C. Questions seeking affirmation:
4. nyi kainong jekla**o**
: *nji kʌinɔŋ ʤeklʌɔ*
: you vehicle buy
'Did you buy a car?' (I heard that you bought a car?).

5. no miet lamthena yola**o**
: *nu met lʌmthenʌ jəlʌɔ*
: you yesterday function attend
'Did you attend the function yesterday?' (I heard that you attended the function yesterday?)

D. Tag questions:
6. ngo lewala haumang asüda. **Kheiyinglao**
: *ŋɔ lewʌʌ hʌumʌŋ ʌsədʌ khʌijiŋlʌɔ*
: I study to-go don't like. It isn't
'I don't like to go to school. Do I?'

7. no wethunashou maibü. No **kheiyinglao**
: *nɔ wethunʌʃɔu mʌibə nu khʌijiŋlʌɔ*
: you studentyoung good. You aren't
'You are a good student. Aren't you?'

8. john loulabü. **Kheiyingkaoba**
: *ʤɔn lɔulʌbə khʌijiŋkʌɔbʌ*
: john will come. Isn't It
'John will come. Isn't it?'

E. Alternate questions:
9. john loua si **alou**
: *ʤɔn lɔuʌ si ʌlʌu*
: john come or not come
'Did John come or not?'

Conclusion : Chang language has 13 Wh-question words but there is no question marker of both Wh-questions as well as Confirmation seeking questions.

Wh-question words are :
1. ai /ʌi/ : What
2. lanei /lʌnʌi/ : Where
3. aijiha /ʌiʤiʌ/ : When (time)
4. laochalou-a /lʌɔtʃʌlu-ʌ/ : When (day)
5. aila / ʌilʌ/ : Why
6. ao /ʌɔ/ : Who (any person, name of any person)

ISSN 2348-0637

7. ailai /ʌilʌi/ : How
8. latütbü /lʌtətbə/ : how much (quantity)
9. lading /lʌdiŋ/ : how much (quantity)
10. lajuche /lʌʤutʃe/ : how many (number)
11. lalokche /lʌlɔktʃe/ : how long (length, duration)
12. laobou /lʌɔbɔu/ : Which
13. lai /lʌi/ : which (direction)

References

Bhatia, T. K. (1995). Negation in South Asian Languages. Indian Institute of Language Studies. 101 Passey Road, Civil Lines, Patiala-147001.

Giridhar, P. P. (1980). Angami Grammar (CIIL Grammar Series-6). Mysor: Central Institute of Indian Languages.

Horn, L. R. (2010). *The Expression of Negation.* Walter de Gruyter GmbH & Co. KG, Berlin/New York.

Iyeiri, Y. (2005). Aspects of English Negation. John Benjamin Publishing Company/ Yushodo Press Amsterdam/ Philadelphia/ Tokyo.

Kuolie, D. (2006). Structural Description of Tenyidie, a Tibeto-Burman Language of India. Ura Academy Publication. Kohima: Nagaland.

Kurrik, J. M. (1979). Literature and Negation. Columbia University Press. New York Guildford, Surrey.

Tottie, G. (1991). Negation in English Speech and Writing. Academic Press Limited. Oval Road: London NW 1 7 DX.

Kevichüsa, E. M. (2018). Relative Clause Formation in Tenyidie. Heritage Publishing House. Near DABA Duncan, Dimapur-797113, Nagaland: India.

COUNTING STATISTICAL ANALYSIS AND ESTIMATION OF EFFICIENCY OF GM COUNTER USING STANDARD RADIOACTIVE SOURCES

Reviewed

Dziesetuonuo Mepfhüo, *Chetan Kachhara and Bendangkokba R Jamir
Department of Physics, Kohima Science College, Jotsoma-797002, Nagaland, India
*e-mail: chetankachhara@yahoo.co.in

Abstract: Geiger Müller counter is a tube which uses ionizing particles to detect radiations such as alpha particles, beta particles and gamma rays. It was developed by J.W. Geiger and his student W. Müller in 1928 .[1] The efficiency of GM counter is provided by the manufacturer at the time of procurement. The user has to confirm the counting system responds properly to the radioactivity. The counting efficiency is a one of the major parameter to check the condition of detector. In this paper, we present the efficiency validation of three GM counters procured in our laboratory.

Keywords: GM Counter, efficiency, radiations.

Introduction

GM counter

GM counter is a tube which uses ionizing particles to detect radiations such as alpha particles, beta particles and gamma rays. It was developed by J.W. Geiger in1908. He later came up with an advanced version of the tube with his student W. Müller in 1928 and named as Geiger-Müller counter or GM counter (Tayal, 2008).

Construction

The GM counter consists of a hollow metal tube of cylindrical shape of radius 2 to 3cm and a thin tungsten wire which is stretched along the axis of the cylinder of diameter 0.1mm. The cylindrical surface serves as a cathode and the tungsten wire serves as an anode (Figure 1.1). The cylindrical tube is filled with inert gas neon with trace of a halogen gas like bromine, which is the quenching gas. The two gases are mixed in a ratio 10:1. The total pressure is less than 10cm and the potential difference between the cathode and the anode around ~300 to 400 volts (Ghoshal, 2015).

In some counters argon is mixed with vapour of some compound like ethyl alcohol as the quenching gas. The detector tube has a thin radiation permeable window at one end which is made of mica. This mica prevents the gases inside from escaping and also stops the air from getting into the tube (Ghoshal, 2015). The schematic diagram of GM counter is shown in figure 1.1.

Working of GM counter

When radiations (i.e. from a radioactive source) enter the GM tube through the mica window, it comes in contact with the gas molecules and ionization takes place. Due to this ionization, the gas molecule splits into ions (which are positively charged) and electrons (which are negatively charged). The positive ions are attracted to the cylindrical surface of the tube and the electrons are attracted to the central metal wire of the tube which is maintained at a high positive voltage. Since the electric field between the cathode and the anode is very high (>300volts) the charges will further ionize more number of atoms thereby setting up an avalanche of ions and electrons in the tube (shown in figure 1.2). These large numbers of ionizations sets up a discharge current also called as Geiger discharge, it is where the current causes the voltage between the anode and cathode to drop which the counter detects as signal (Ghoshal, 2015).

Before the counter can detect any more radiations, it needs to be restored to its original state through a process called quenching, which cancels out the effects of Geiger discharge. This is achieved by having a second gas i.e. halogens (quenching gas) inside the tube. This is known as internal quenching. Due to this the ions and electrons are quickly absorbed among billions of gas molecules in the tube so the counter effectively resets itself in a fraction of a second, ready to detect most radiations (Ghoshal, 2015).

ISSN 2348-0637

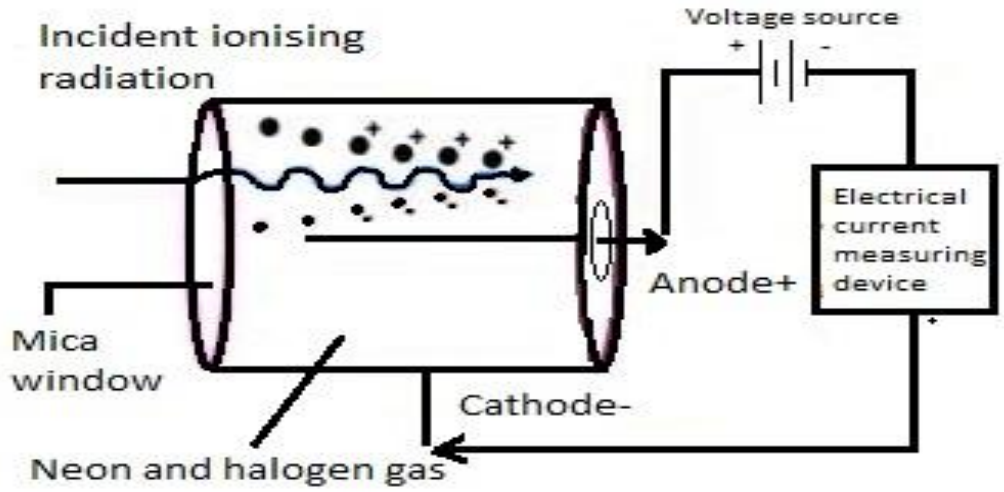

Figure 1.1: The schematic diagram of a GM counte

Characteristic of Plateau curve

The graph between the counts and the voltage which is obtained as a result of the rate of the recorded count as a function of the voltage is called as the characteristic curve for the counter (Ghoshal, 2015). The counter is connected with a device capable of indicating only relatively large pulses but not small ones. So, until the voltage exceeds a certain minimum value known as the threshold voltage or the starting potential, the pulses are called small and do not get detected. When the voltage is low, there is no gas amplification and the electronic circuit will not be able to record and count these pulses. As the voltage is increased, the gas amplification increases and number of pulses rise rapidly to a flat portion of the curve called the plateau region In this region the count rate is nearly independent of the potential difference across the tube. Beyond the plateau, the applied voltage is so high that a continuous discharge takes place in the tube and the count rate increases very rapidly (Tayal, 2008).

Length of plateau = $V_2 - V_1$

Slope of the plateau = $\frac{N_2 - N_1}{N_1} \times \frac{100}{V_2 - V_1} \times 100\%$

Statistical Analysis

Systematic errors control the accuracy of a measurement. Thus, if the systematic errors are small, or if one can mathematically correct them, then one can obtain an accurate estimate of the "true" value. The precision of the experiment, on the other hand, is related to random errors. The precision of a measurement is directly related to the uncertainty in the measurement.

Random errors are the statistical fluctuations during a measurement. If these values are too close to each other, then the random errors are small. But, if the values are not too close, then random errors are large. Thus, random errors are related to the reproducibility of a measurement.

Mean: It is the average value of a set of (n) measurements in an experiment. Mathematically it is defined as

$$\overline{N} = \frac{N_1 + N_2 + N_3 + \cdots + N_n}{n}$$

$$= \frac{1}{n} \sum_{i=1}^{n} Ni$$

Deviation: It is the difference between the actual measured values and the average value. Deviation from the mean, d_i is simply the difference between any data point N_i, and the mean. We define this by $d_i = N_i - \overline{N}$

In some cases the value of the error or the deviation may become zero because, we may have both positive and negative values which get cancelled. Yet an average value of the error will be desirable, since it tells us how good the data is in a quantitative way. Therefore we need a different way to obtain the measure of the

scatter of the data i.e. by Variance (σ^2) and Standard deviation (σ).

$$\sigma^2 = \frac{{d_1}^2 + {d_2}^2 + \cdots + {d_n}^2}{(n-1)} = \frac{1}{(n-1)}\sum_{i=1}^{n} {d_i}^2$$

Standard deviation is a square root of the variance, which is widely used to indicate about the spread of our data.
$\sigma = \sqrt{(\sigma^2)}$.

Methodology

For measuring background radiation

The GM detector registers pulses even when not exposed to radioactive sources. These pulses are caused by natural and man-made radioactive isotopes found in our environment, and also by cosmic radiation. The background radiation varies with time and depends on the local environment, the building material, shielding and the weather. Hence the background count rates (counts per second) are recorded before and after carrying out measurements.

A. To study the background radiations in the laboratory the following procedure is adopted.
The following steps were taken for the experiment:

- GM counter system GC 602A is connected with detector without any radiation source and detector is placed in optical bench.
- System setting the preset time to 10sec and 100 observations were taken.

  The graph between observations and count per second and the frequency distribution for 100 observations is shown in fig 2.1 and fig 2.2.

  For another set, preset time was selected 100 seconds and 10 observations were taken and their graph is shown in fig 2.2.

B. To show that for high number of counts Poisson distribution follows closely normal or Gaussian distribution.
The following steps were taken for the experiment:

- Standard set up was made by connecting G.M. Counting System GC 602A with the detector placed in the optical bench.
- Beta source is placed at 2cm from the end window of the detector.
- Preset time is set to 25sec and 50 readings were recorded.
- Mean, deviation and standard deviation were calculated with the recorded counts.

Plateau Characteristics

To study the characteristics of plateau curve, the following equipments and accessories were used:

a) Electronic unit i.e. the G.M. Counters
b) G.M. Detectors
c) G.M. detector holder, sliding optical bench and source holder
d) Radioactive source

We have 3 G.M. counters out of which one counter is GC601A model and the other two are GC602A model. GC601A type is an economy model. The other two GM counters are GC 602A which are research model. The three counters are shown below in figure 2.1. GC 602A is chosen for this study since it is an advanced system for research works.

In this study, we have used three radioactive source, namely Strontium (Sr^{90}), Thallium (Tl^{204}) and Cesium (Cs^{137}). Strontium and Thallium are beta radioactive source and Cesium is a gamma radioactive source. We used three different G.M. detectors namely GM125, GM120 and GM110. The GM detectors used for this study are shown below in fig 2.2 and experimental setup in fig 2.3. To choose the most appropriate detector for this study, the efficiency of all the detectors were found and are given in table3.2.

ISSN 2348-0637

Figure 2.1: Different models of counters

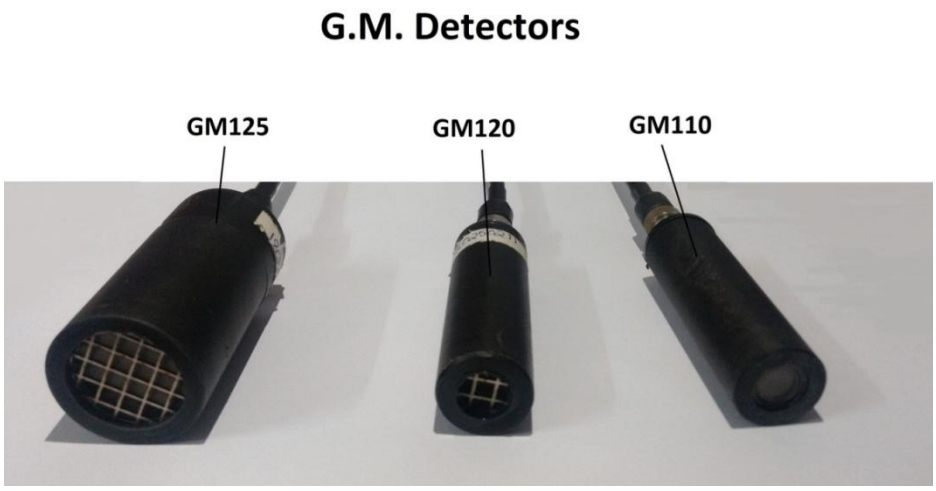

Figure 2.2: Different types of detectors

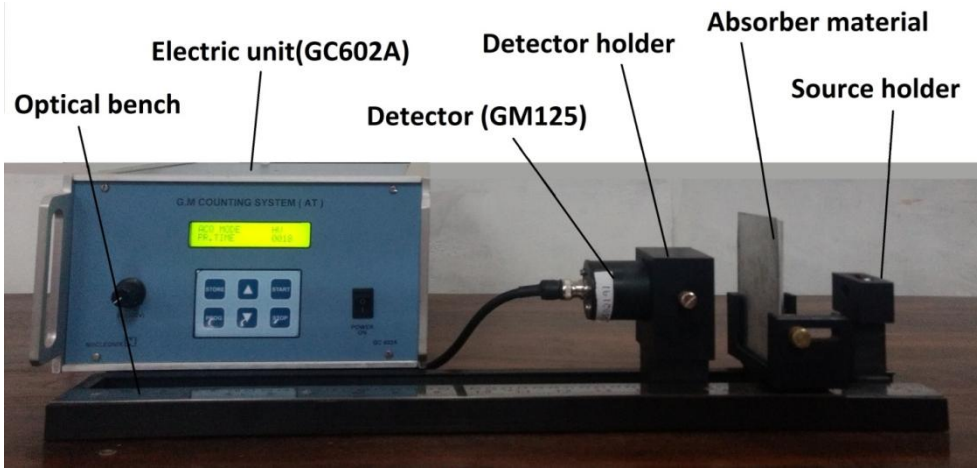

Figure 2.3: Schematic arrangement for experimental setup

Results

Statistical analysis results

The graphs of the measurements of the background radiations and the statistical analysis are shown below-

A. The results for the measurements of the background radiations .

The graph of the no. counts in 10 sec for 100 readings is shown in fig 3.1.

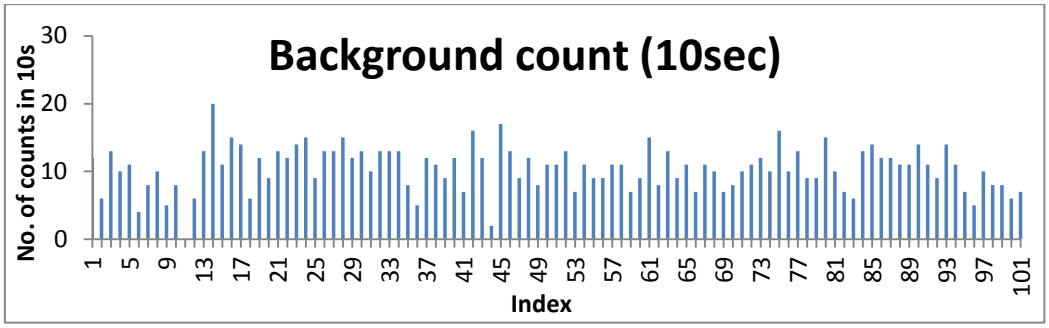

Figure 3.1: Plot of no. of counts in 10s for 100 readings

The frequency distribution for 100 observations is shown in fig 3.2.

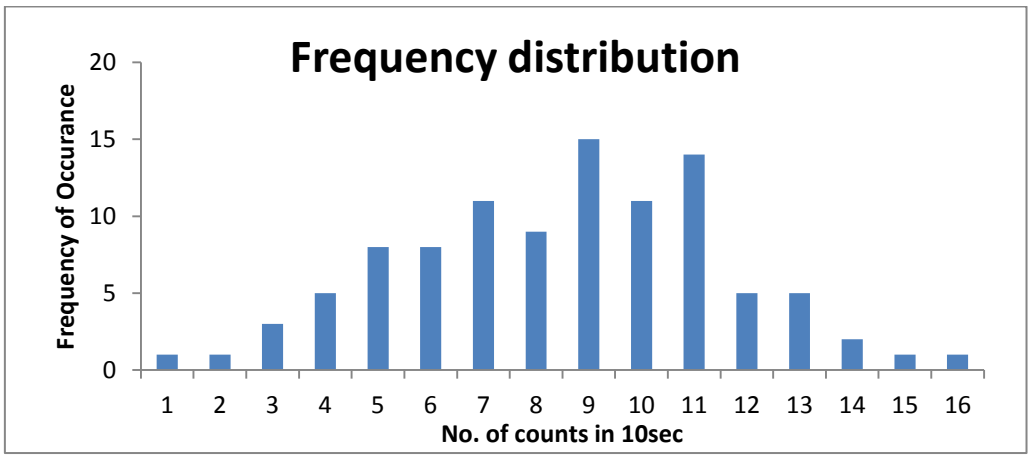

Figure 3.2: Frequency distribution for 100 readings with 10s

ISSN 2348-0637

The graph of the no. of counts in 100 sec for 10 readings is shown in fig 3.3.

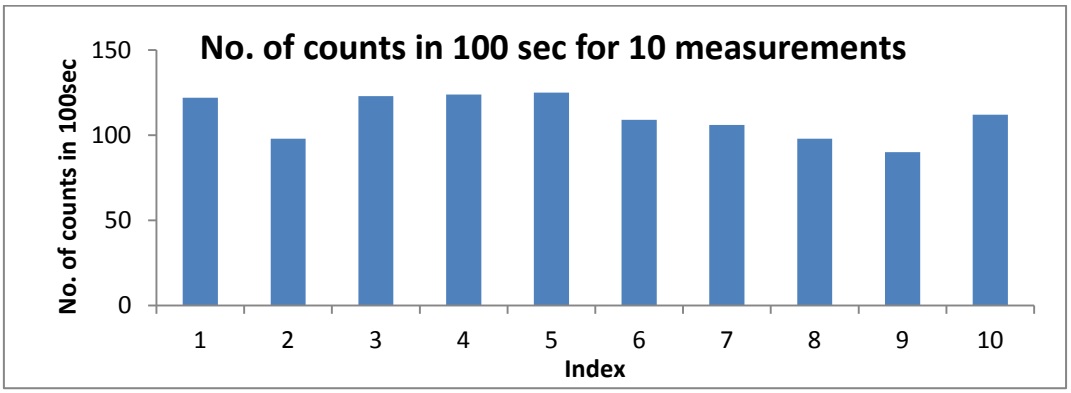

Figure 3.3: Plot of no. of counts in 100 sec for 10 readings

The statistical parameters for the above measurements are found as follows:

Mean Value	: $\bar{N} = 8.7 = 9$
Variance	: $\sigma^2 = 9.1$
Standard Deviation	: $\sigma = 3.01$

From the above results we see that it follow a Poisson distribution on which practically all radioactivity measurements are based. The results show that the mean value N is equal to the variance σ^2; this is characteristic of the Poisson distribution. The variance in any measured number of counts is therefore equal to the mean value of counts.

The square root of variance, the standard deviation is a measure of the scatter of individual counts around the mean value. As a thumb rule we say that approximately 2/3 of the results are within one standard deviation of the mean value i.e., within the interval [(N-σ) and (N+σ), where $\sigma = \sqrt{N}$].

Conversely, given the result from an individual measurement, the unknown 'true' count lies within the interval [$-\sqrt{N}$ and $N + \sqrt{N}$] with a probability of approximately 2/3.

The measured results of mean, variance and standard deviation follow Poisson distribution. Results show that the mean value (N) is almost equal to the variance (σ^2) which is characteristic of the Poisson distribution.

We found that mean value of count is equal to variance, which agrees with the theory.

B. The results of the statistical analysis.
The average count rate for 50 independent measurements is

$$\text{Mean, } \bar{N} = 3904.8$$

The deviation of an individual count from the mean is $(N_i - \bar{\bar{N}})$.

The Standard Deviation, $\sigma = \sqrt{\bar{\bar{N}}} = 62.5$

The graph is shown below

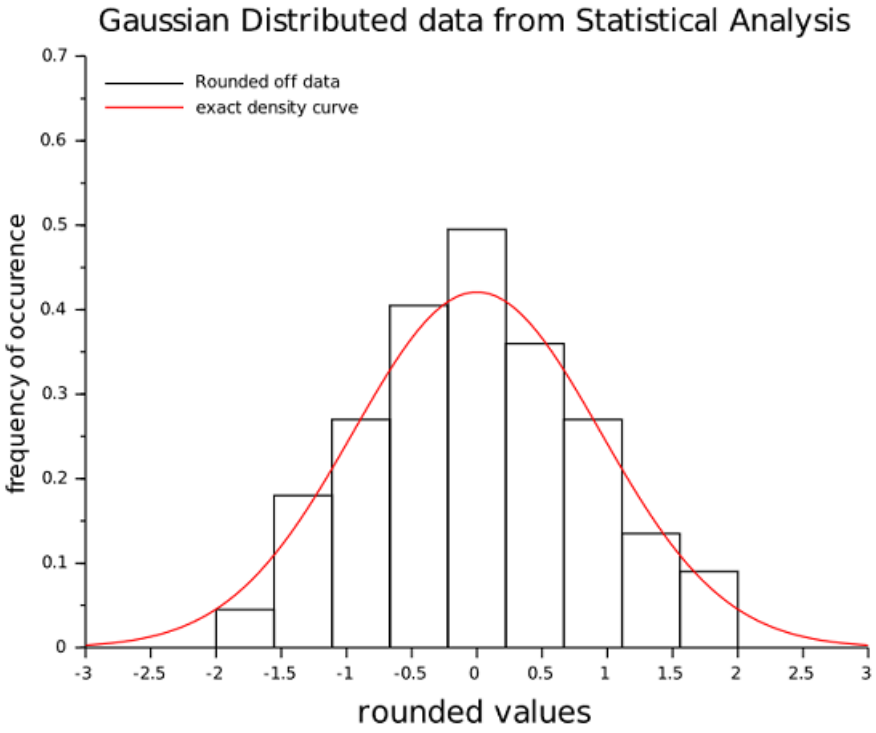

Figure 3.4: Plot of Frequency of occurrence vs rounded off values

The scilab program for plotting the fig 3.4 is shown below-

```
//Gausian Data Generation for a set of data
clc;clear;clf;
m=0;
sd=0.94760708295;
vari=sd^2;
X=[-2,-1.5,-1.5,-1.5,-1.5,-1,-1,-1,-1,-1,-1,-0.5,-
0.5,-0.5,-0.5,-0.5,-0.5,-0.5,-0.5,-0.5,-
0.5,0,0,0,0,0,0,0,0,0,0,0,0.5,0.5,0.5,0.5,0.5,0.5,0.5
,0.5,1,1,1,1,1,1,1.5,1.5,1.5,2,2];
histplot(9,X,style=3);
x=linspace(-3,3);
G=(1/(sqrt(2*%pi*vari)))*exp(-0.5*(x-
m).^2/vari);
plot2d(x,G,strf="000",style=5);
mtlb_axis([-3,3,0,0.7])
xlabel('rounded
values',"fontsize",3,"fontname",3);
ylabel('frequency of
occurence',"fontsize",3,"fontname",3);
title('Gaussian Distributed data from Statistical
Analysis',"fontsize",4,"fontname",5);
legend(["Rounded off data","exact density
curve"],2,%F)
```

To fit the Gaussian curve we calculated the mean, variance and standard deviation from the rounded off values. Mean = 0

Standard deviation = 0.94760708295

Variance = 0.89795918365

We found from figure 3.4 that the distribution is symmetric about the mean value. Since the mean value is large, the adjacent values of the function are not greatly different from each other i.e. the distribution is slowly varying which is the expected behavior of a normal distribution.

Plateau characteristics results

Plateau curves of the 3 sources with the different detectors with counter GC602A is shown below-

ISSN 2348-0637

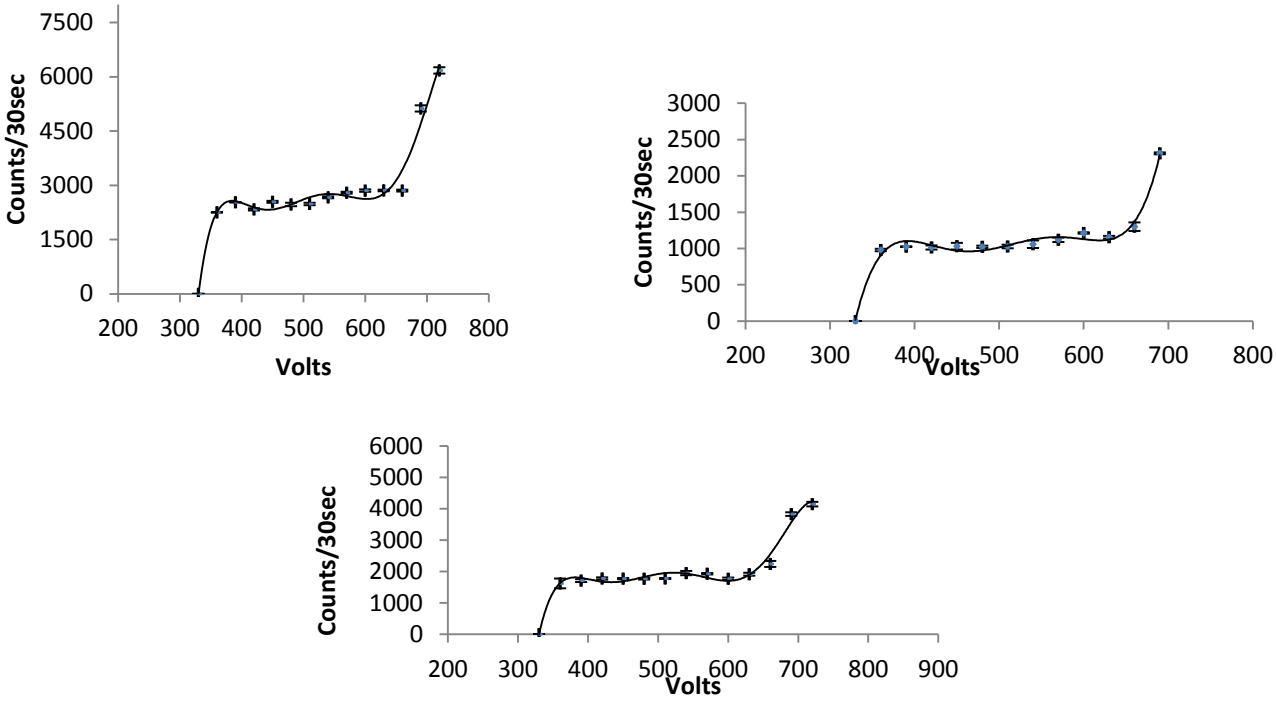

Figure 3.6: Plateau curve of Strontium (Sr^{90}) ,Thallium (Tl^{204}) and Cesium (Cs^{137}) , with GM125

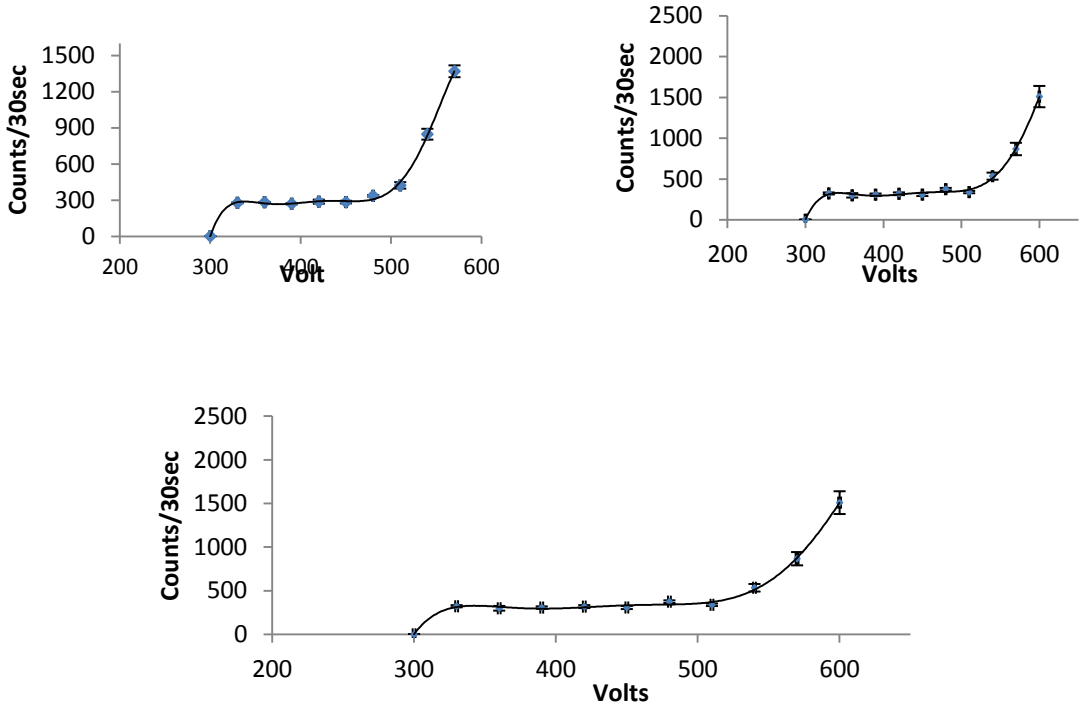

Figure 3.10: Plateau curve of Strontium (Sr^{90}), Thallium (Tl^{204}) and Cesium (Cs^{137}) with GM120

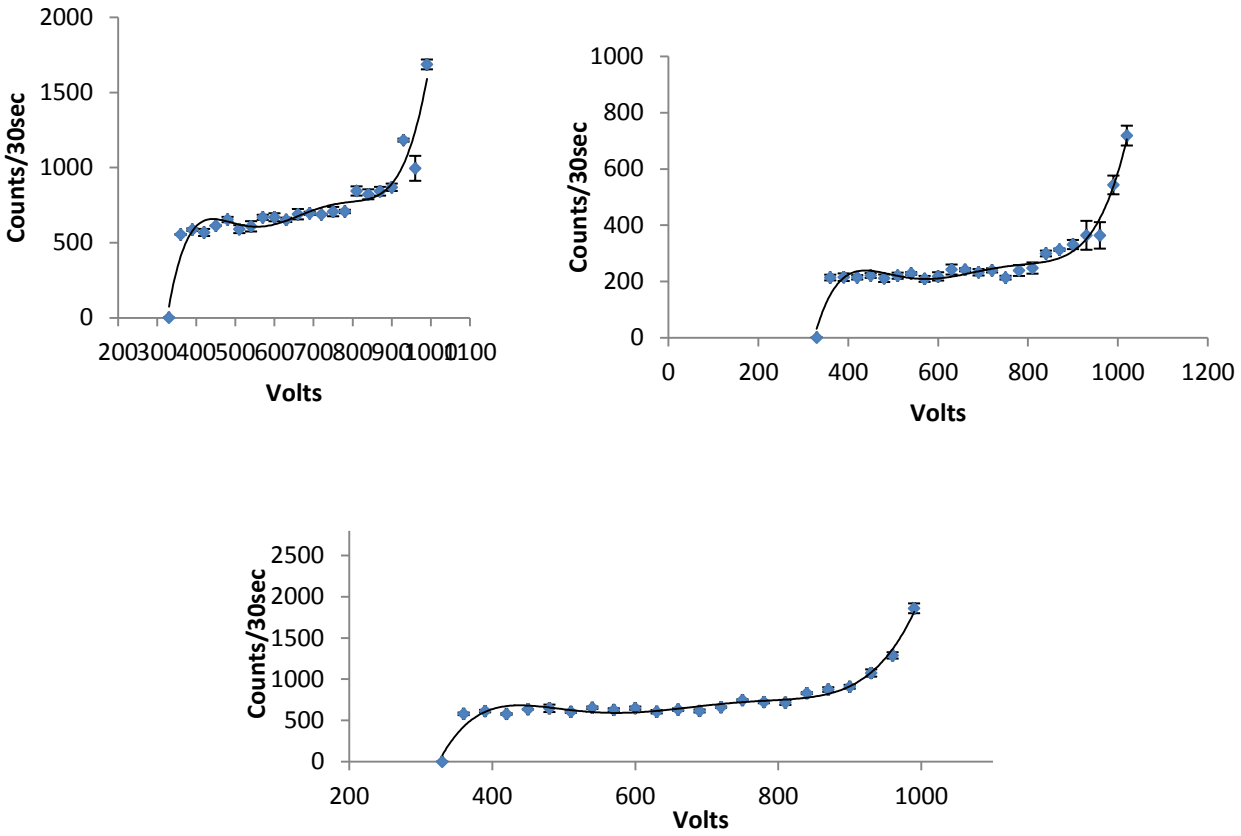

Figure 3.13: Plateau curve of Strontium (Sr^{90}), Thallium (Tl^{204}) andCesium (Cs^{137}) with GM110

The calculated operating voltage for the three detectors GM125, GM120 and GM110 with the three different radioactive sources is shown in table 3.1.

Detector / Source	GM125 (in volt)	GM120 (in volt)	GM110 (in volt)
Strontium (Sr^{90})	510	450	570
Thallium (Tl^{204})	495	450	585
Cesium (Cs^{137})	495	450	585

\\

Table 3.1:
Operating voltages of the three sources with the three detectors

ISSN 2348-0637

The efficiency of three detectors obtained with the three different sources are shown in table 3.2.

Detector / Source	GM125	GM120	GM110
Strontium (Sr^{90})	4.68%	0.78%	1.75%
Thallium (Tl^{204})	1.46%	2.41%	0.54%
Cesium (Cs^{137})	0.013%	0.97%	1.22%

Table 3.2: Efficiency of three source with three detectors

Conclusions

The present study shows that the efficiency of GM125 has the highest efficiency of 4.68% with source ^{90}Sr with fixed distance from seal sources at 6 cm. The overall efficiency found to be much lower than quoted value by manufacturer.The estimation of efficiency depends on many factors such as type, energy and strength of ionizing radiation, distance of source from detector, counting time applied voltages etc. For better, results one needs to study more in detail by vary these parameters which we would like to do in future.

References

Ghoshal, S. N. (2015). Nuclear Physics, Revised Enlarged Edition. S. Chand, ISBN 978-81-219 0413-1. 197-201, 41-59.

Knoll, G. F. (2000). Radiation Detection and measurement, third edition. John Wiley and sons. ISBN 0-471-07338-5.

SI units for ionizing radiation: becquerel. Resolutions of the 15th CGPM (Resolution 8). 1975. Retrieved 22 March 2016.

Tayal, D. C. (2008). Nuclear Physics, Fifth Revised and Enlarged Edition 2008. Himalaya Publishing House. 143-148, 62-84.

ASSESSMENT OF URBAN HEAT ISLAND USING REMOTE SENSING APPLICATION; A CASE STUDY FROM NAGALAND

Reviewed

*Kedovikho Yhoshü and **Petevino Chase
*Department of Geography, Nagaland University, Lumami
**Ura College of Teachers Education, Kohima-797001, Nagaland
**e-mail: petechs@gmail.com

Abstract: The process of urbanization with the increase of population and infrastructural development have created a phenomenon known as urban heat island. This phenomenon has led the land surface temperature to increase owing to anthropogenic interference. The urban heat island in the present study has been estimated based on remote sensing technique, using Landsat 8 satellite imageries. The parameters considered for this estimation consisted of settlement, vegetation, water bodies and bare soil. Further, a comparison of this phenomenon has been done in urban centres of the study area. The areas under settlement and bare soil showed higher land temperature than the other parameters. Lower density settlement has shown lesser temperature compared to its counterpart.

Keywords: Landsat8, Land surface temperature, NDVI, Urban heat island

Introduction

Urbanization is rapidly sweeping the state of Nagaland, be it the commercial hub of Nagaland-Dimapur; or the Capital of Nagaland-Kohima. Urbanization causes expansion both vertically as well as horizontally. Urbanization also causes a rise in land surface temperature known as Urban heat island (UHI), this is characterized by higher temperature rise in the human settlement due to high thermal capacity of construction materials; anthropogenic heat, reduced vegetation cover, etc. (Gago *et al.,* 2013). Factors like urban configuration along with anthropogenic heat source, atmospheric pollution, geographic location and climate of the area also influence UHI (Nakayama and Hashimoto, 2011). The main contribution to thermal difference is thermal properties of the radiating surfaces and a reduced rate of evapotranspiration especially in urban settlement (Streutker, 2002). The application of urban heat however, also depends on the temperature itself. High temperature region known as urban hot spots (UHS) within UHI is mainly due to the development of extreme heat stress developed due to man-made activities in a UHI zone (Chen *et al.,* 2006 and Guha *et al.,* 2018). One of the main factors for UHI is landuse change caused by urbanization (Du *et al.,* 2016).

The use of space technology such as remote sensing has in a huge way impacted the study of earth's resources and its management. The use of remote sensing technique allows a larger spatial coverage with better uniformity sampling than *in-situ* sampling technique. A more practical and approachable way to study UHI is to study the land surface temperature emitted from the surface which can be measured from the thermal band of multispectral satellite imageries (Abutaleb *et al.,* 2015).

Landsat series has been providing multispectral imageries since the 1970's. Landsat 8 is the latest mission launched successfully on 11th February 2013. Landsat 8 mission has two instruments known as Operational Land Imager (OLI) and Thermal Infrared Sensor (TIRS) from which 11 bands are generated. 9 bands (Band1-9) are covered under OLI and 2 bands (band 10 and band 11) under TIRS. The spatial resolution of OLI except band 8 (15 m) which is panchromatic, is 30 m. The band under TIRS comes under 100 m spatial resolution (USGS, 2019; Acharya and Yang, 2015).

This study is about the determination of urban heat island in Nagaland; how parameters such as vegetation, settlement, bare soil and water bodies respond in regard to land surface temperature. Urban heat island and anthropogenic activity reaction too has been studied for better understanding of temperature change in response to anthropogenic effect mainly through landuse changes.

Study area

Nagaland, located in the northeastern part of India is undergoing drastic landuse changes

ISSN 2348-0637

mainly through infrastructure developmental activities. For this study, three districts have been covered *viz*, Kohima, Dimapur and Wokha (Figure 1). The study area extends from 93°32'23"E to 94°23'27"E and 26°33'41"N to 25°31'5"N. The three districts have been considered basing on parameters such as Kohima-The State Capital, Dimapur - Economic hub, Wokha-Doyang hydel power. These primary factors besides certain other factor such as population concentration, area density etc. have been considered for the study.

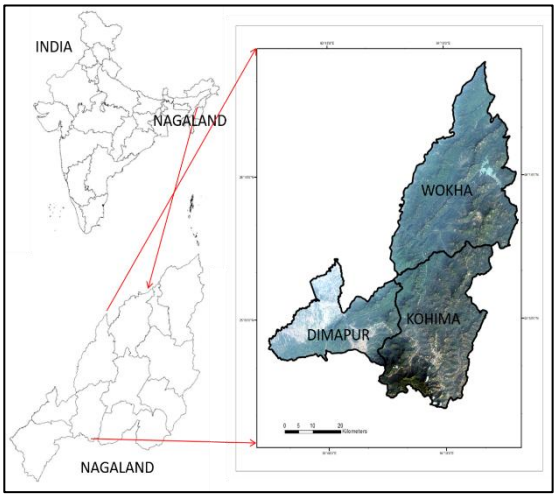

Figure 1: Location map of the study area

The total population of the study area was 7,80,331 (2001 census) and 8,13,142 (2011 census) as shown in table 1. Urban population of Dimapur district was 1,97,277(2011 census) and 1,14,600(2001 census). Wokha district urban population was 37,636 (2001 census) and 35,004 (2011 census). Kohima district urban population consist of 1,21,088 (2011 census) and 77,030 (2001 census) illustrated through Figure 2.

Table 1: Total Population and Urban population of the study area

Districts	**Population**		**Urban population**	
	2001	**2011**	**2001**	**2011**
Dimapur	3,09,024	3,78,811	1,14,600	1,97,869
Kohima	3,10,084	2,67,988	77,030	1,21,088
Wokha	1,61,223	1,66,343	37,636	35,004
Total	7,80,331	8,13,142	229,266	353961

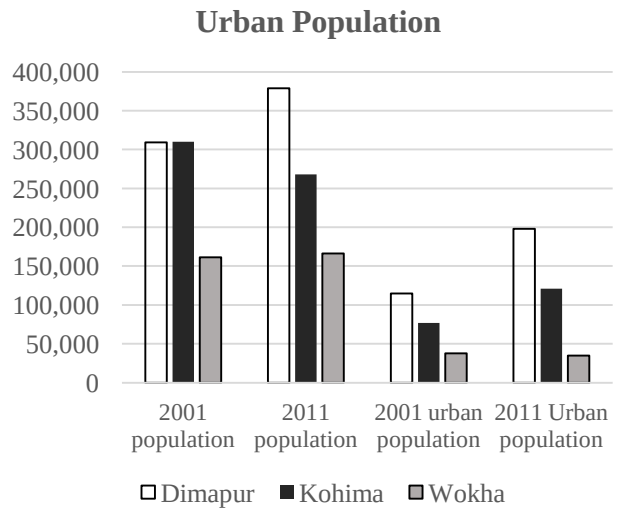

Figure 2: Population distribution of the study area showing urban population and total population.

Methodology

Three multi-date scenes from Landsat 8 OLI and TIRS datasets were assessed for estimation of UHI. The three satellite imagery sets acquired was of winter season dated16th March 2014, 21st December 2017 and 25th January 2019 respectively from the United States Geological Survey (USGS) website, details regarding the imageries have been shown in Table 2. The flowchart of the methodology adopted is shown in Figure 3. The following process was followed to convert the digital number into land surface temperature.

Table 2: Characteristics of the satellite imageries

Sl. o	Date	Path/ Row	Sensor ID	Resolution
1.	16-03-2014	135/42	OLI and TIRS	30 m
2.	25-04-2017			
3.	2019-01-25			

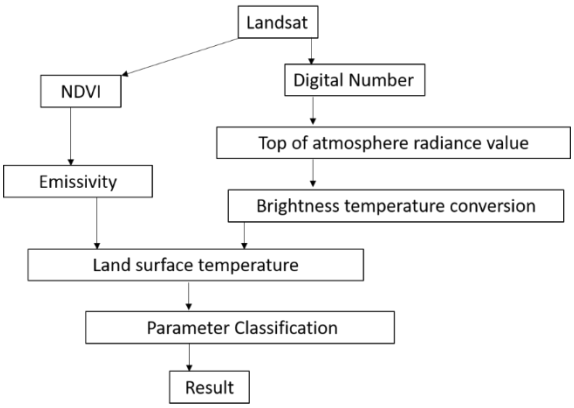

Figure 3: Flow chart of the methodology.

Digital number to top of atmosphere radiance values

Each satellite image is made up of numerous rows and columns known as pixel, each of these pixels are characterized by its digital number. The radiance was calculated based on the following equation-

$L_\lambda = (M_L + Q_{Cal}) + A_L$

Where,

L_λ =Top of atmosphere spectral radiance

M_L=Band specific multiplicative rescaling factor

A_L= Band specific additive rescaling factor

Q_{Cal} = Quantized and calibrated standard product pixel value

Top of atmosphere to brightness temperature conversion

$$T = K_2/(Ln\left(\frac{K_1}{L_\lambda}+1\right))$$

Where,

T = TOA brightness temperature

L_λ= TOA spectral radiance

K_1= band specific thermal conversion constant

K_2= band specific thermal conversion constant

Normalized Difference Vegetation Index (NDVI)

NDVI is used to extract the vegetation richness of an area. The higher the vegetation content, greater is its NDVI value. It is represented by Near Infrared and red band in the band combination to bring out the vegetation differences. The equation for NDVI is as follows-

$$NDVI = (Near\ Infra\ red - Red)/(Near\ Infra\ red + Red)$$

Land Surface Emissivity

Land surface emissivity is the average emissivity of a surface emitted from the Earth's surface; it is derived from the NDVI value. The equation for land emissivity is represented by-

$$PV = (\frac{NDVI-NDVImin}{NDVImax+NDVImin})^2$$

Where,

$PV = Proportion\ of\ vegetation$

$NDVI = DN\ value\ from\ NDVI$

$NDVImin$= Minimum DN from NDVI

$DVImax$= Maximum DN from NDVI

$$Emissivity = 0.004 \times PV + 0.986$$

Land Surface Temperature

Land surface temperature (LST) is the radiative temperature from the surface derived through top of atmosphere, wavelength of emitted radiance and emissivity.

$$LST = \left(\frac{BT}{1}\right) + W \times \left(\frac{BT}{14380}\right) \times Ln(emissivity)$$

Where,

BT = top of atmosphere brightness temperature

W= wavelength of emitted radiance

Results and Discussion

The results obtained from the study are discussed under the following heads.

NDVI

The NDVI values observed for the year 2014 range from -0.056 at the lower extremes and 0.499 at the higher extremes. The minimum and maximum values for NDVI for the year 2017 was -0.074 and 0.560 and for the year 2019 was -0.094 and 0.516 respectively as shown in Figure 4. Low NDVI value is observed in the settlement and areas with bare soil, mostly towards the south western part of the study area. The area under rich vegetation growth depicts a higher NDVI value.

Emissivity

Emissivity holds higher value for areas under vegetation cover. Water bodies, bare soil and settlement region represents area under low emissivity. The minimum and maximum emissivity value for the year 2014 was 0.984

ISSN 2348-0637

and 0.993. For the year 2017, minimum emissivity was 0.985 and 0.991 for maximum emissivity. The emissivity value for 2019 range was 0.991for the minimum extreme and 0.984 for maximum extreme.

Land surface temperature

The land surface temperature represents the heat released from the surface. Land surface temperature depends on location and climatic condition besides others. Land surface temperature is different from atmospheric temperature. From the study it was observed that the year 2014 land surface temperature range was -1.822 for the lower temperature extreme and 37.278 for higher temperature extreme. Land surface temperature for 2017 was 3.250 for minimum temperature and 22.841 for maximum temperature. Both the temperature extremes have increased for 2019 with its value ranging from 1.756 for lower temperature and 26.585 for the higher temperature. Lower temperature is observed towards the south i.e. Dzükou valley located in Japfü mountain range. The higher rate of human settlement tends to increase the temperature in and around the area.

For better understanding of land surface temperature distribution, various parameter/class such as water bodies, settlement, vegetation and bare soil has been taken for comparative study. Under settlement class, urban class was studied based on Kohima, Dimapur and Wokha municipal. It was observed that a settlement nearer to the Highway displayed higher land surface temperature.

Table 3: Parameter classification showing maximum and minimum land surface temperature.

Parameter	2014		2017		2019	
	Min.	Max.	Min.	Max.	Min.	Max.
Bare soil	28.067	30.861	19.104	20.520	19.643	21.192
NDVI bare soil	0.083	0.164	0.143	0.328	0.127	0.215
Water	2.907	20.427	17.660	18.671	16.711	18.688
NDVI water	-0.052	0.049	-0.064	-0.048	-0.090	0.149
Vegetation	10.010	24.783	9.398	19.135	10.671	19.945
NDVI vegetation	0.106	0.447	0.242	0.491	0.220	0.479
Land surface temperature	9.204	29.380	9.245	20.294	11.215	20.824

The highest land surface temperature for bare soil, vegetation and water bodies classification was observed in bare soil class, infact under bare soil it showed maximum land surface temperature with 30.861°C (2014) and lowest was observed in water bodies with 18.671°C (2017). Maximum value for minimum land surface temperature value was shown by bare soil with 28.067 °C (2014) and minimum value for land surface temperature was shown by water bodies with temperature 2.907°C (2014).

As observed in Figure 4 and Figure 6 (LST and NDVI) there is negative correlation between settlement and vegetation. The higher the values for LST, lower is its NDVI value shows that vegetation can check the effects of UHI, hence, lower the emissivity of heat, resulting in a cooler environment.

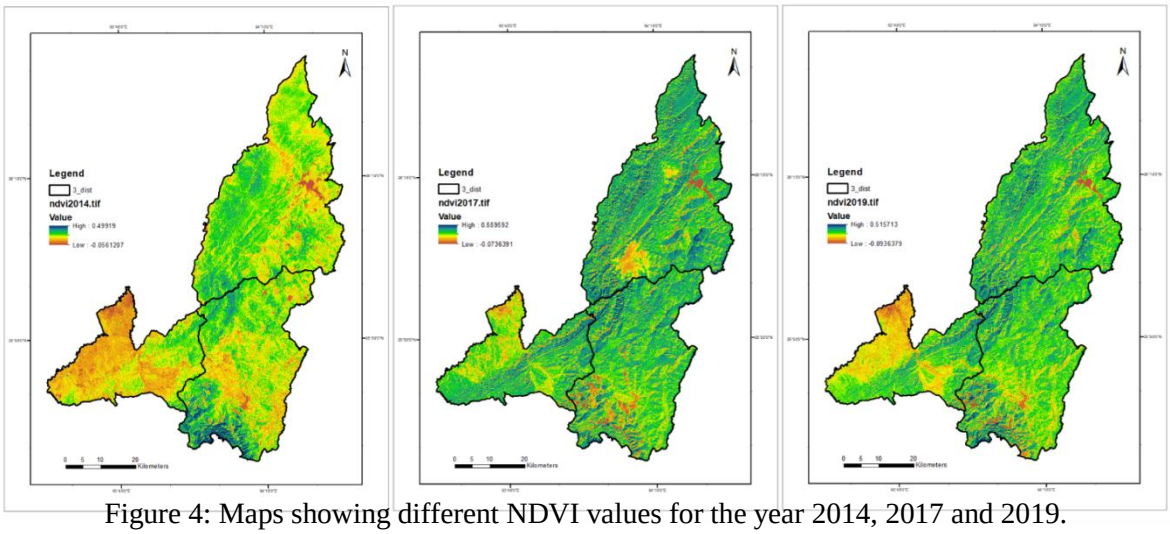

Figure 4: Maps showing different NDVI values for the year 2014, 2017 and 2019.

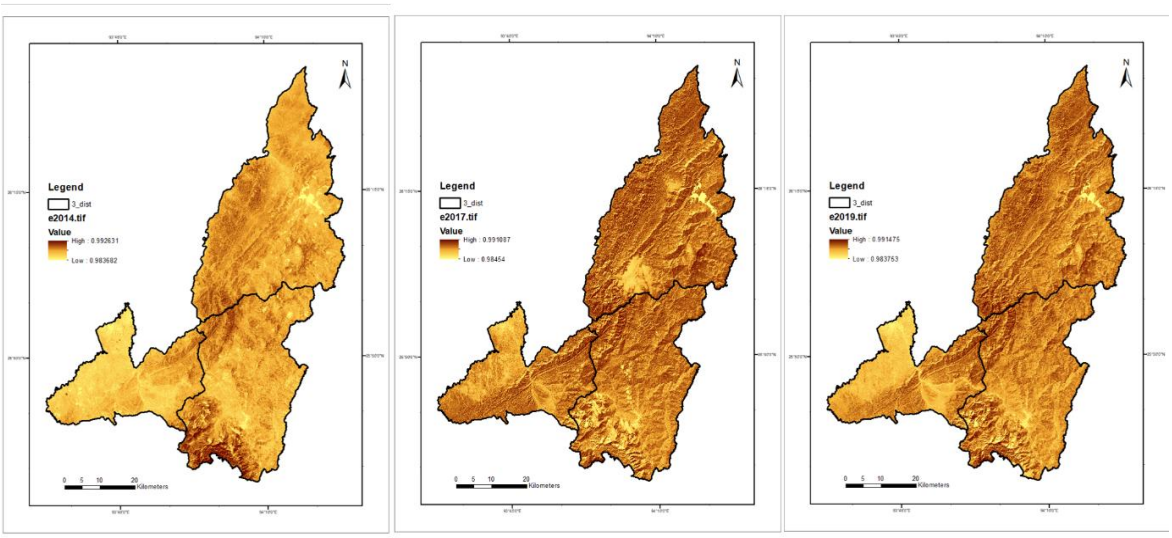

Figure 5: Maps showing Emissivity of the study area for the year 2014, 2017 and 2019.

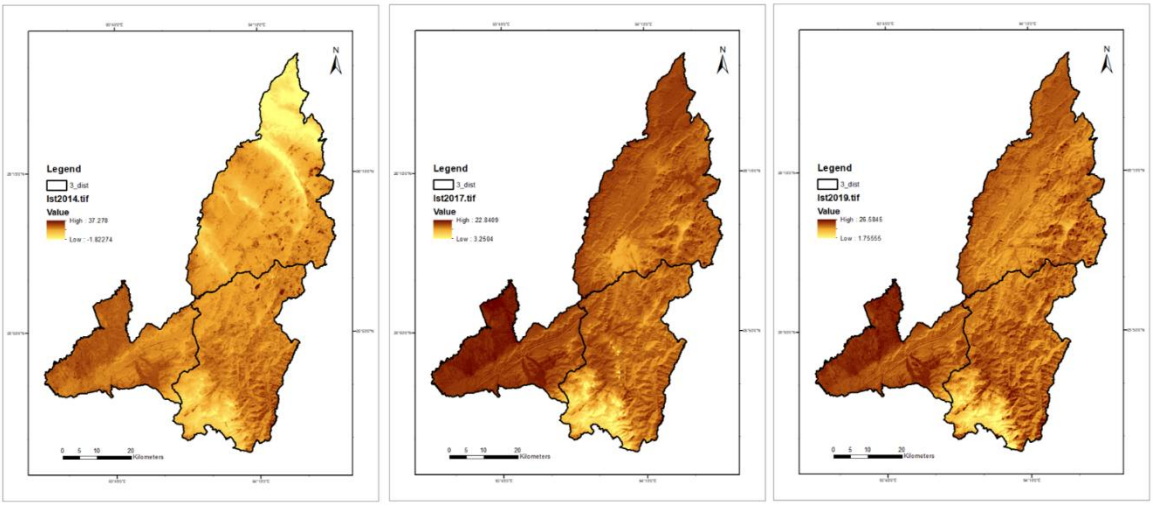

Figure 6: Maps showing Land surface temperature for the study area showing year 2014, 2017 and 2019.

ISSN 2348-0637

Table 4: Table showing land surface temperature of urban settlement

Urban Centre	2014		2017		2019	
	Min.	Max.	Min.	Max.	Min.	Max.
Wokha	23.699	27.082	15.804	18.983	17.153	20.6
Dimapur	26.996	29.366	20.33	22.656	19.923	22.024
Kohima	23.434	28.67	14.2598	20.978	16.017	22.835
NDVI	0.088	0.336	0.068	0.454	0.084	0.399
Vegetation	10.010	24.783	9.398	19.135	10.671	19.945

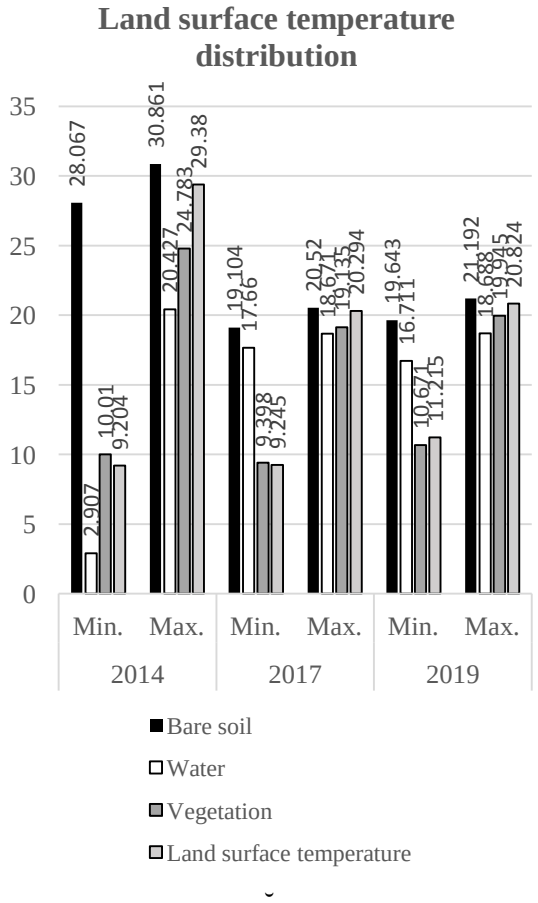

Figure 7: Graph showing land surface temperature of various parameters.

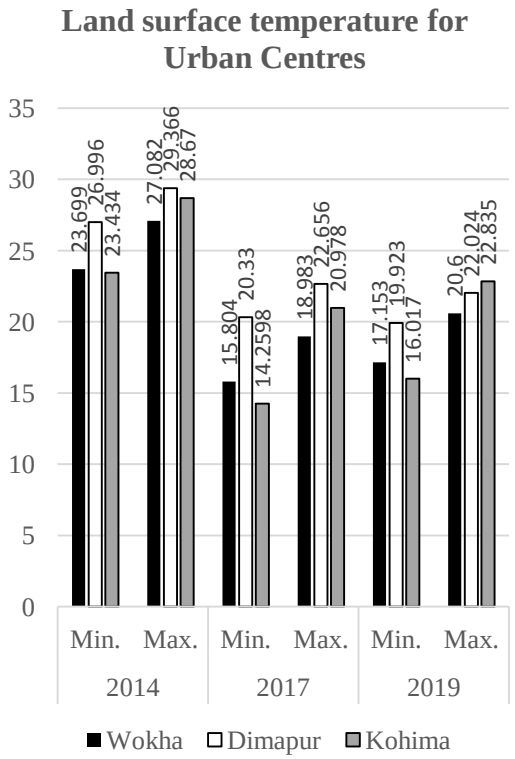

Figure 8: Urban settlement showing respective land surface temperature

Conclusion

There is no denial that urbanization is inevitable, it is part and parcel of infrastructural development. However, as seen from the study, there is a possibility of temperature increase in places where urbanization is more rapid. Landuse land cover is a major contributor to UHI phenomenon due to anthropogenic activities. The relation between the LST and NDVI is inversely related which indicates that green cover will go a long way to reduce surface temperature. Various factors also further escalate the urban heat island temperature such as roofing materials, low vegetation cover, exposed ground surfaces, urban structure, reflective glass in building materials etc. Proper mitigation and planning in the form of green spaces, green architectural design etc. within the urban setups will play a significant role in reducing UHI thereby creating a healthy environment.

References

Abutaleb, K., Ngie, A., Darwish, A., Ahmed, M., Arafat, S. and Ahmed, F. (2015). Asessment of urban heat island using remote sensed imagery over greater Cairo, Egypt. *Advances in remote Sensing*. **4**: 35-47.

Acharya, T. D. and Yang, I. (2015). Exploring Landsat 8. International journal of IT. *Engineering and Applied sciences research*. **4(4)**: 4-10.

Chen, X. C., Zhao, H. M., Li, P. X. and Yin, Z. Y. (2006). Remote sensing image- based analysis of the relationship between urban heat island and land use/cover changes. *Remote sensing of Environment*. **104(2)**: 133-146.

Du, H., Wang, D., Wang, Y., Zhao, X., Qin, F., Jiang, H. and Cai, Y. (2016). Influences of land cover types, meteorological conditions, anthropogenic heat and urban area on surface urban heat island in the Yangtze river delta urban agglomeration. *Sci. Total environ*. **571**: 461-470.

Gago, E. J., Roldan, J., Pacheco-Torres R. and Ordonez, J. (2013). The city and urban heat islands: a review of strategies to mitigate adverse effects. *Renew sustain energy Rev*. **25**: 749-758.

Guha, S., Govil, H., Dey, A. and Gill, N. (2018). Analytical study of land surface temperature with NDVI and NDBI using Landsat 8 OLI and TIRS data in Florence and Naples city, Italy. *European journal of remote sensing.* **51(1)**: 667-678.

Nakayama, T. and Hashimoto, S. (2011). Analysis of the ability of water resources to reduce the urban heat island in the Tokyo megalopolis. *Environ. Pollution*. **159**: 2164-2173.

Streutker, D. R. (2002). A remote sensing study of the urban heat island of Houston, Texas. *International journal of remote sensing*. **23**: 2595-2608.

USGS (2019). Landsat8 (L8) Data Users handbook. LSDS-1574, Version 4.0. 1-103.

Address for correspondence:
Principal
Kohima Science College (Autonomous),
Jotsoma- 797002
Nagaland, India

Rüsie: A Journal of Contemporary Scientific, Academic and Social Issues
Vol. 6, 2019
ISSN 2348-0637

The journal (Rüsie) is published annually.

The views and opinions expressed by the authors are their own statement. They do not reflect the opinion of the college authority and editorial board. The college will assume no responsibility for the statement of the contributors.

RÜSIE

Translation: 'A movement for a cause' is the literal translation of the Tenyidie word **'Rüsie'**. It is a movement of united action and efforts by a group or a community for a specific purpose.

The name 'Rüsie' befits the journal which is also a movement for a cause- of Science and Social issues. A forum to disseminate ideas and knowledge through united and collective efforts.

Name of the journal proposed by Dr Shürhozelie Liezietsu, President, Ura Academy.

FORMAT GUIDELINES

1. Length of the article- maximum 8 pages (A4 size paper), with a font size of 11 and a line spacing of 1.0 (single) in two columns (max. 1500 words).
2. Font style: Times New Roman (preferably typed in Microsoft Word)
3. Headings:
   i) Title
   ii) Abstract (max. 50 words)
   iii) Introduction
   iv) Objectives
   v) Methodology
   vi) Results (preferably with figures and tables in science section)
   vii) Conclusion
   viii) Acknowledgement
   ix) References
   x) Brief bio-data of the author(s)
4. Articles to be submitted in soft copy to the Chief Editor (mhathungy@gmail.com)